

CUMULONIMBUS CONVECTION  
AND LARGE-SCALE SHOWER RAINFALL

by

Stephen Michael Grove

Atmospheric Physics Group  
Department of Physics  
Imperial College  
London SW7

A thesis submitted for the degree of  
Doctor of Philosophy  
in the University of London

September 1977

---

CUMULONIMBUS CONVECTION  
AND LARGE-SCALE SHOWER RAINFALL

Stephen Michael Grove

ABSTRACT

The first part of this thesis is concerned with the ways in which cumulonimbus convection is influenced by the large-scale meteorological flow. Various data are examined, and atmospheric stratifications typical of widespread showers over land and sea are established. The vertical component of relative vorticity is used as an indicator of large-scale vertical motion, and is related to 24-hour, mean areal rainfall values. The ways in which surface topography determines the distribution and intensity of showers is discussed.

The concept of a stationary severe cumulonimbus is introduced, and consideration of past examples of large localized falls of rain leads to some general characteristics. Two broad types of stationary (or slow-moving) storm emerge: one is compatible with a quasi two dimensional mid-latitude storm circulation, with the environmental wind close to zero at the 'steering level'. The other is usually associated with larger values of a mean Richardson number and involves a three-dimensional circulation.

A detailed observational study of a stationary storm over north London (the Hampstead storm) is presented, making use of both routine and voluntary observations. The synoptic conditions leading to the storm are described, and the localization of the storm by meso-scale convergence and the large urban 'heat island' is considered. The study is combined with the results of a numerical simulation, and produces a distinctive model of the storm dynamics, featuring an impulsive yet quasi-stationary system of cumulonimbus which contributed successively to the rainfall over a limited area. The model emphasises the dominant role of the downdraught outflow, which establishes and maintains the storm through its interaction with the low-level flow and the prevailing wind shear. The model's applicability to other stationary storms is considered, and dynamical points arising from the study suggest aspects of cumulonimbus which require further investigation.

CONTENTS

	<u>Page</u>
CHAPTER I : INTRODUCTION	2
CHAPTER II : LARGE-SCALE SHOWER RAINFALL	17
2.1 Mean layer stratifications over land and sea	17
2.2 Quantitative aspects of shower rainfall	31
2.3 Topographic influences on showers	39
CHAPTER III : STATIONARY CUMULONIMBUS	58
3.1 Stationary 'mid-latitude' cumulonimbus	60
3.2 Other stationary storms	63
3.3 Urban influences on cumulonimbus	74
CHAPTER IV : THE HAMPSTEAD STORM - OBSERVATIONAL STUDY	84
4.1 Observational description of the storm	85
4.2 The storm environment	90
4.3 Dwindraught observations	105
4.4 The role of topography	110
4.5 Summary	112
CHAPTER V : THE HAMPSTEAD STORM - NUMERICAL STUDY	114
5.1 The numerical model	114
5.2 The simulation	120
5.3 The Hampstead storm model	128
5.4 Modelling implications	132
CHAPTER VI : DISCUSSION AND GENERALIZATION OF THE HAMPSTEAD MODEL	134
6.1 Precipitation efficiency and impulsiveness	134
6.2 The Mill Hill storm	140
6.3 Vector wind shear	157
CHAPTER VII : SUMMARY AND CONCLUDING REMARKS	168
References	174
Acknowledgements	181

CHAPTER I : INTRODUCTION

In common with many meteorological phenomena, cumulonimbus convection encompasses a great range of space scales, from the synoptic down to the microscopic, and it is the interactions between these different scales of motion which complicate any study, be it observational or theoretical.

Solar energy absorbed at the Earth's surface is transferred by cumulus (or small-scale) convection to the lower troposphere, partly as sensible heat, and partly as the latent heat of evaporated water. Larger scales of convection continue the transfer into the upper troposphere, where the energy is eventually re-radiated into space. In tropical latitudes the transfer is effected by cumulonimbus convection; thunderstorms are widespread and frequent, and are an essential component of the general circulation. Their location and intensity are often subject to topography and motions on a scale larger than themselves, and they may become organized into systems such as tropical cyclones; nevertheless, over a large enough area and a sufficiently long time interval, the rate of rainfall is equivalent to the rate of release of latent heat of evaporation (that is the excess of solar radiation absorbed at the surface over the net upward long-wave radiation). Since the solar flux in the tropics varies little with the time of year, one could reasonably predict a monthly or even weekly rainfall over a large area.

### Mid-latitude rainfall

In middle latitudes large-scale slope convection is dominant, and transfers energy polewards as well as upwards. Cumulonimbus convection is also present, but, compared with the slope convection, probably contributes little to the transport of energy. Early studies on the relative amounts of mid-latitude rainfall from frontal zones and from showers were published by Goldie (1931 and 1936). His examination of autographic records for a three-year period indicates considerable geographical variations; for islands off north-west Scotland about 10% of the rainfall was attributed to showers, whereas this figure rose to 43% in south-east England. It appears that frontal rains are locally intensified by orographic effects over the hills of Scotland; in south-east England, however, shower rainfall results more often from solar heating of the ground (Goldie states that, in summer 51% of the total rainfall is "not obviously associated with a discontinuity").

Such studies as these are necessarily laborious, and, what is more, the results of analyses at particular stations may not be representative of larger areas. (In addition, Tucker (1961) suggests that total precipitation is less over the ocean than over islands or coasts with on-shore prevailing winds; this difference increases southwards, and in south-western Europe there is a considerable discontinuity in rainfall near the coastline.) The most recent work of this kind is by Shaw (1962) who analyzed autographic and synoptic data covering five years (1956 - 1960) for seven stations in northern England. Some geographical features are apparent when comparing results from different locations, but the

relative amounts of frontal and shower rainfall show little variation from station to station. If the rainfall from polar lows (about 10% of the total) is not attributed to cumulonimbus, then over the whole region shower rainfall represents about one quarter of the total precipitation.

#### Objectives of cumulonimbus study

'Ordinary' mid-latitude cumulonimbus convection is generally sporadic in character; showers may form in cool maritime airstreams or as a result of local solar heating of the ground, and persist for  $\frac{1}{2}$  hour or so, evolving through the familiar life-cycle of 'cumulus', 'mature' and 'dissipation' stages. Sometimes, however, in favourable large-scale situations, the convection becomes persistent and more intense. A suitable wind shear, while tending to suppress cumulus convection, may organize the cumulonimbus circulation so that the drag and evaporative cooling associated with the precipitation no longer interferes with the updraught, and the storm is able to retain its identity for several hours. In this form cumulonimbus are one of the most damaging of all meteorological phenomena, especially when accompanied by large hail, violent squalls or tornadoes, so that the two major incentives to their study (apart from natural curiosity) are prediction and possible modification.

Even after many years of experiments, as well as recent advances in the microphysical theory of clouds, the latter goal is still surrounded by considerable controversy. Most recent modification experiments have attempted to inhibit the growth of large hail by 'seeding' in the main

updraught of cumulonimbus, in order to provide extra nuclei which will compete for the available cloud water. Browning and Foote (1976) suggest, however, that such action may actually increase the amount of hail, at least in 'supercell' storms. In general there seems to be a risk of unintentionally affecting more than one parameter, and Borland and Snyder (1974) argue that, in parts of the USA, the financial benefit resulting from a 20% reduction in damaging hail could be completely offset by a reduction of only 5% in rainfall during the early growing season. Seeding experiments remain inconclusive because the natural variability of hailfalls (and their rarity) mean that the 'control' experiment is difficult to define, and convincing statistical data must necessarily cover a long period.

Any attempt at prediction requires the answers to many ostensibly naive questions, such as those posed by Ludlam (1976): where do cumulonimbus clouds form?, will any become intense?, how will they travel?, what combination of large and smaller scale motions are required?

The formation of precipitation in cumulonimbus clouds is always preceded by the generation of precipitation in cumulus clouds whose tops have reached some critical level in the troposphere. (This fact was recognized by Bergeron (1935), although his assumption that the critical level was associated with a cloud temperature low enough for 'large' concentrations of ice nuclei to be present is now considered incorrect, and the critical cloud thickness is more readily associated with the time required to grow raindrops, given appropriate initial conditions.) While the critical depth

required for shower formation appears to be reasonably constant in a given meteorological situation, it is determined by a complex interaction between large-scale motions, topographic features, surface moisture and previous convection.

### Severe Cumulonimbus

Many early observational studies related the occurrence of severe travelling storms to strong winds aloft; a comprehensive review of such work was made by Ludlam (1963). Later theoretical and observational investigations confirmed the importance of vertical wind shear in maintaining persistent convection, and a form of bulk Richardson number ( $Ri$ ) which relates the shear to the potential energy available for convection, has been shown to be a useful parameter of the large-scale motion. Moncrieff and Green (1972) showed that two-dimensional convection can be steady (in the range  $\frac{1}{4} > Ri \geq -1$ ) if the convective system moves with a propagation speed close to that of the flow at some height in the troposphere (the system has a 'steering-level'), but only if the interface between updraught and downdraught slopes down shear. This result conflicts with the model which emerged from the intensive analysis of the Wokingham storm, by Browning and Ludlam (1962). They inferred a quasi two-dimensional circulation with the updraught sloping backwards over the downdraught. This orientation ensured that rain fell directly into the downdraught, which it maintained by evaporative cooling, and also accounted for the recirculation and development of large hail. It appears that the required transfer and evaporation of precipitation can only take place if the



updraught and downdraught assume a three-dimensional configuration; this may develop even if the original environment contains a two-dimensional wind field. The three-dimensional structure of severe local storms is clearly important, and is consistent with the observational evidence that many such cumulonimbus travel with an appreciable component of motion to the right of the mean wind.

Intense cumulonimbus convection usually requires the storage of a large amount of potential energy in a relatively shallow layer near the surface, and some initiating mechanism (perhaps a local maximum of surface potential temperature, or vertical motion associated with some large-scale feature). Favourable conditions are usually described in terms of the parcel theory, in which a small volume of air is assumed to rise adiabatically through an undisturbed environment. When condensation occurs, ascent continues for as long as the parcel is buoyant, while cooling at the saturated-adiabatic lapse rate. Despite the drastic assumptions of the theory, observation shows that the mean lapse rate over a cumulonimbus layer is very close to the wet-adiabatic value (although it cannot be assumed that the air ascends without mixing significantly with the environment). Accordingly, an amount of energy available for convection is represented by the average value of the wet-bulb potential temperature ( $\theta_w$ ), in a layer (usually about 1 km thick) near the surface, being in excess of the saturation wet-bulb potential temperature ( $\theta_s$ ) in the middle and upper troposphere. Abnormally high values of low-level  $\theta_w$  may be achieved if a stable layer exists near the surface, so that the small-scale convection is confined

to the lowest 1 to 2 km of the atmosphere. The magnitude of the rise in  $\theta_w$  (for a given amount of solar energy input at the surface) clearly depends on the depth of the layer, and the fraction of the energy which appears as sensible heat; if the latter is too great then the dry-bulb potential temperature ( $\theta$ ) may rise and destroy the stable layer before  $\theta_w$  can increase sufficiently.

An early attempt to relate thunderstorms in Britain to the synoptic conditions was made by Douglas and Moorhead (1946). They examined records from three stations for the summer months of a five year period (1941 - 1945) in order to relate the direction of the wind at 700 and 500 mb to the incidence of thundery rain. It was found that with middle-level south-easterly winds, between 89% and 97% of the rainfall was associated with thunderstorms. (It is interesting that these authors mentioned the importance of vertical wind shear in cases of prolonged convective storms, but were unable to provide any reason for the connection.)

Carlson and Ludlam (1968) used isentropic relative-flow analysis to examine the synoptic-scale weather situations associated with selected severe local storms over Britain and the USA. They found that the storms occurred ahead of major troughs in the vicinity of confluence lines (recognized as cold fronts at the surface), where the organization and intensification of cumulonimbus were favoured by an increase of wind speed with height. Local convection over France was confined to a shallow layer by a plume of warm air moving north from Spain, while air with a relatively

low value of  $\theta_s$  arrived in the mid-troposphere from the Sahara. One of the case studies examined a similar synoptic situation from which no severe storm developed; on this occasion the surface of western France was unusually dry, so that values of  $\theta$  rose quickly and convection penetrated the stable layer before values of  $\theta_w$  at low levels were sufficiently high for deep cumulonimbus convection.

Forecasters in the USA made considerable advances in the prediction of severe local storms by relating their occurrence to particular synoptic weather patterns. Fawbush and Miller (1954) analyzed nearly 300 representative soundings and were able to distinguish three main types of air mass in which tornadic storms were likely to occur. The most common of these types featured a strong inversion near 800 mb, a moist lower layer, and winds increasing with altitude. Miller (1959) subsequently identified five tornado-producing synoptic patterns, which, for forecasting purposes, were intended to be used in conjunction with the air mass types. The patterns exhibited a middle-level jet, and a westerly or south-westerly current of dry air up to about 700 mb, west of a low-level influx of moisture from the south. Considerable convergence of air at the boundary between moist and dry air (the so-called 'dry line') was also required to promote severe storms.

#### Studies of 'ordinary' convection

Most studies of cumulonimbus have, understandably, tended to concentrate on the more severe storms. In Britain, however, these are rather rare, and most of the shower rain-

fall is associated with ordinary cumulonimbus, which, because of their impulsive nature, are very difficult to forecast, at least on a local basis. Saunders (1966 and 1967) has examined the success of eight different forecasting techniques (mostly instability parameters) over the summers of 1965 and 1966. While identifying the most successful of the stability indices, he concluded that better results over small areas inland were obtained by 'general practice' (when the forecaster was free to use any method of prediction), and that in most cases the skill and judgement of the forecaster himself was an important factor.

In a series of articles, Lowndes (1965, 1966a and b) considered the forecasting of shower activity over different regions of Britain in summer. He correlated the frequency and intensity of showers in north-westerly airstreams with such features as the position of the associated depression, the curvature of the surface isobars, and several instability indices. The forecasting 'skill scores' (which range from zero for no success to unity for complete accuracy) were highest for south-east England, and lower for south-west and north-west England respectively, where the relative proximity of the windward coasts had an effect on the distribution of showers. Turning to showery airstreams in winter (Lowndes, 1966c), he found that from November to February, widespread showers were unlikely in the absence of a surface trough, but that no single predictor provides a useful indication of shower activity. Finally he applied predictors to rain in southerly airstreams over south-east England in summer, but concluded that in general they were of little use in forecasting rain or thunder (Lowndes 1967).

Other studies of shower activity in Britain have been made by Briggs and Johns (1960) at Acklington, Northumberland, and by Sims (1960) at St. Mawgan, Cornwall. Briggs and Johns found a maximum shower frequency with south-westerly winds, and a secondary maximum with north-west to northerly winds; during the night, however, the maximum frequency occurred with the latter. Sims tabulated 'shower-hours' according to surface wind direction, and found a minimum in the frequency of showers with on-shore winds from March to July, and a maximum from November to February. In off-shore winds the shower activity varied little between summer and winter.

Both the previous authors referred to the influence of local topography, and distinguished between showers in airflows arriving from the sea and those from the land. This led Summersby (1967) to consider data from the Ocean Weather Ships I and J, both well away from the influence of land. He examined hourly observations made over a four-year period and concluded that a clear maximum of shower frequency occurred in the winter months, and a minimum in July. Most showers were associated with winds from the west and north-west, and there was only a slight diurnal variation in their frequency.

Most modern forecasts are based to some extent on the results of computer simulations, and Wickham (1974) has presented some examples of rainfall forecasts produced by the Meteorological Office 10-level model. Shower rainfall is 'produced' in the process of convective adjustment, in which the thicknesses of each successive pair of layers above a grid point are mutually adjusted to ensure that no

'unreasonable' static instability develops. 'Dynamic rain' arises whenever the air at some level above a grid point becomes supersaturated due to the convergence of moisture. The author shows that the model has considerable value in the forecasting of general synoptic patterns, but it is clear that predictions on the scale of one grid length (100 km) are much less reliable. The location of forecast rain areas was often in error by one or two grid lengths, and the quantity of rain forecast was only about half of the actual values. These deficiencies are partly attributable to the somewhat unrealistic parameterizations of physical processes, and the poor representation of topography in the model.

#### Thesis outline

Few of the above studies mention the quantitative aspects of shower rainfall. On the scale of individual clouds it is unrealistic to expect more than some estimate of the intensity of convection, since the rate of rainfall at the ground is the product of many interacting small-scale processes, such as the rate at which particles grow and aggregate within the cloud, and also their trajectories, which are in turn determined by the airflow configuration.

Many practical problems in engineering hydrology are concerned with the rainfall total appropriate to a given area of catchment, rather than the amount of precipitation recorded at a particular point. Statistical studies (see NERC, 1975) use an empirically-determined areal reduction factor (ARF) which depends on the size of the area and the duration of the rainfall event; when multiplied by the representative value for a point rainfall event, it yields

the magnitude of the areal rainfall event with the same duration and return period.

We shall attempt some quantitative studies of showers by considering 24 hour rainfall data expressed as a mean value over an area of 100 x 100 km<sup>2</sup>. On this scale we might expect large-scale atmospheric motions to be dominant in determining the amount of rainfall, although topographic effects are also likely to be important. The preparation of mean areal rainfall values by the Meteorological Office is described by Shearman and Salter (1975). Daily rainfall totals (the 'rainfall day' is that 24 hour period beginning at 0900 GMT) are collected, quality controlled and plotted on a 1 : 625000 scale map. The daily totals are then interpolated from the irregularly spaced raingauge network to a regular array of grid points. The grid length was chosen as 5 km; this gives 10,000 grid points in the United Kingdom compared with about 7,000 raingauges. In mountainous regions, where data are sparse, the field of topography is used to assist the analysis and interpolation of rainfall totals. Shearman and Salter acknowledge that there is no reliable formula expressing the relationship between rainfall and topography, so rainfall totals are expressed as percentages of annual average rainfall before interpolation. The rainfall pattern is smoothed, and "the interpolation at grid points reflects more accurately the variations with topography". The average 24 hour rainfall value for a 100 km x 100 km grid square is then simply the arithmetic mean of the grid point rainfall values within the appropriate area.

It is instructive to estimate the mean areal rainfall arising from different hypothetical 'showery' situations.

- (i) Isolated showers, each producing an average rainfall of 5 mm over an area of 25 km<sup>2</sup>. If the showers are about 20 km apart there will be approximately 25 showers within a 100 km square. Assuming that after interpolation the rainfall from each shower is recorded at only one grid point, the mean areal rainfall will be

$$R = \frac{5 \text{ mm} \times 25 \text{ grid points}}{400 \text{ grid points (in a 100 km square)}} = 0.31 \text{ mm}$$

- (ii) A travelling storm, producing an average of 20 mm of rainfall in a band 20 km wide parallel to one side of a 100 km square. The mean areal rainfall is then

$$R = \frac{20 \text{ mm} \times (100 \times 4) \text{ grid points}}{400 \text{ grid points}} = 4.0 \text{ mm}$$

- (iii) A stationary local storm giving 100 mm of rain over an area of 100 km<sup>2</sup>. In this case R is clearly 1.0 mm.

We can see that the areal rainfall is unlikely ever to exceed a few mm, at least in showery conditions, although unrepresentative or misleading results might be obtained when a 100 km square lies mostly over the sea and includes only a small area of land.

In chapter II we shall consider large and intermediate-scale influences on shower rainfall. Mean layer stratifications associated with showers over land and sea are discussed; the



vertical component of vorticity is suggested as an indicator of large-scale vertical motion, and this is related to mean rainfall totals. Topographic influences on the distribution of showers are then investigated in some detail.

Chapter III introduces the concept of the stationary, severe cumulonimbus. A number of incidences of exceptionally large local rainfall totals are discussed, and we infer some general characteristics of these storms, and note the possible significance of a local heat source or prominent topographical feature.

Chapter IV contains a detailed observational study of the Hampstead storm of 14th August 1975 (described as a quasi-stationary, severe cumulonimbus). Atmospheric processes on several scales are shown to have played important parts in determining the location of the storm, and the possibility of topographic and urban influences are also considered. Routine and voluntary observations are combined, and a three-dimensional airflow is suggested.

Chapter V presents the results of a three-dimensional numerical simulation of the storm, using the primitive equation model developed by Miller (1972). Observational and numerical models compare remarkably well, in terms of both airflow configuration and the rainfall pattern at the ground, and combine to emphasize the existence of several cumulonimbus cells exhibiting similar and consecutive life cycles. One of the most important features arising from the study is the interaction between the downdraught outflow and the ambient wind field, which ensures regeneration of the storm.

The discussion in chapter VI attempts to generalize the results of the Hampstead storm study to other incidences of stationary cumulonimbus, in particular that which occurred near Mill Hill (north-west London) in 1963 for which photographic data is available. Several dynamical points which arise from the model are considered, and a number of aspects of cumulonimbus study which require further investigation are suggested, particularly those concerned with 'steadiness' of convection and its relation to efficiency of production of precipitation.

CHAPTER II : LARGE-SCALE SHOWER RAINFALL

In this chapter we examine various aspects of ordinary cumulonimbus convection over land and sea, without becoming concerned with processes on the scale of the clouds themselves. We seek some simple parameters of the large-scale motion of the atmosphere which may be related to mean areal rainfall values.

2.1 MEAN LAYER STRATIFICATIONS OVER LAND AND SEA

Basic differences exist in the nature of convection over land and sea. Over land the fundamental parameter is the flux of energy in sensible and latent form from the surface, which in turn determines the temperature profile at low levels. Water, on the other hand, has a large thermal capacity compared with land, and contrasts between the surface and the air above it are determined by the rate of advection of cold air over relatively warm sea. In this case, therefore, the temperature profile is determined by the synoptic-scale atmospheric motions (including vertical motions), and the energy flux from the surface will adjust to fit the stratification.

A general stratification characteristic of cumulus convection over land has long been established as a result of many observational investigations. Its main features are listed. (1) The surface layer, from the ground to screen level, over which potential temperature ( $\theta$ ) and mixing ratio ( $r$ ) both decrease by several deg C and  $g\ kg^{-1}$  respectively. (2) The superadiabatic layer extends from screen level up to levels as high as 300 m above the surface.

$\theta$  decreases by 1 to 3 deg C and  $r$  by a few  $\text{g kg}^{-1}$ . (3) The adiabatic layer, usually 1 or 2 km deep, extends to cloud base underneath growing cumulus. The stratification here is slightly stable ( $\theta$  increases by up to 1 deg C) and  $r$  also is nearly constant, decreasing by less than  $1 \text{ g kg}^{-1}$ .

(4) Away from clouds is a transition layer which occupies the 200 to 300 m below the level of cloud base. Over this shallow layer  $\theta$  increases by about 1 deg C, and  $r$  decreases by up to  $3 \text{ g kg}^{-1}$ . (5) In the cumulus layer the lapse rate is at first between the dry-adiabatic and wet-adiabatic, but eventually becomes less than the wet-adiabatic. The tops of cumulus usually do not grow beyond the level at which the lapse rate becomes less than the wet-adiabatic.

Because cumulonimbus convection is intermittent, it is more difficult to identify a characteristic stratification in the same way as for cumulus convection. Mean summer soundings from tropical regions, however, do indicate certain features, notably a deep cumulus layer (up to about 550 mb) with a lapse rate close to the saturated-adiabatic. In the upper troposphere the mean lapse rate is just less than the saturated-adiabatic. As mentioned in chapter I, the mean lapse rate over the whole cumulonimbus layer is close to the saturated-adiabatic, with  $\theta_s$  in the cloud tops having nearly the same value found in the cloud base. It is to be remembered, however, that the pseudo-saturated reference process which defines  $\theta_s$  takes no account of the ice phase; if it did, the corresponding value of  $\theta_s$  in the upper troposphere would be several degrees higher than is assumed.

Showers over the sea

The stratification typically associated with cumulonimbus convection over the sea has been examined by means of meteorological aircraft soundings, made over the north-east Atlantic between September 1956 and April 1958. The aircraft observers recorded dry-bulb and dew-point temperatures at altitudes of 200 ft and 1500 ft above the sea, and at pressure levels at 50 mb intervals. The pilots were instructed not to avoid clouds, but to fly at a level immediately below the cloud bases, so that only "tenuous wisps" of cloud were encountered; the level and temperature of cloud bases were thus specified, and the observer also noted whether or not showers were present. From a total of over 260 soundings, almost 100 have been selected which were considered representative of showery conditions. For each sounding the following were evaluated:  $\theta$  and  $\theta_w$  at 200 ft,  $\theta$  and  $\theta_s$  at cloud base,  $\theta_s$  at 800 mb and 700 mb.

The sub-cloud layer is considered by calculating the following parameters, which essentially represent mean lapse rates:

(i)  $\Delta\theta$  (200 - CB)  $\equiv$   $\theta$  (200 ft) -  $\theta$  (cloud base)

(ii)  $\Delta\theta_s$  (200 - CB)  $\equiv$   $\theta_w$  (200 ft) -  $\theta_s$  (cloud base)

Figure 2.1 shows histograms of the percentage frequency of occasions on which the values of  $\Delta\theta$  and  $\Delta\theta_s$  lay within ranges of 1 deg C. The graph of values for  $\Delta\theta$  confirms that the 'adiabatic' layer is slightly stable, with over half of the soundings having  $\Delta\theta$  in the range 0 to -2 deg C. The extreme values of +4 deg C may be accounted for by the presence of a deep superadiabatic layer, and the rather large negative

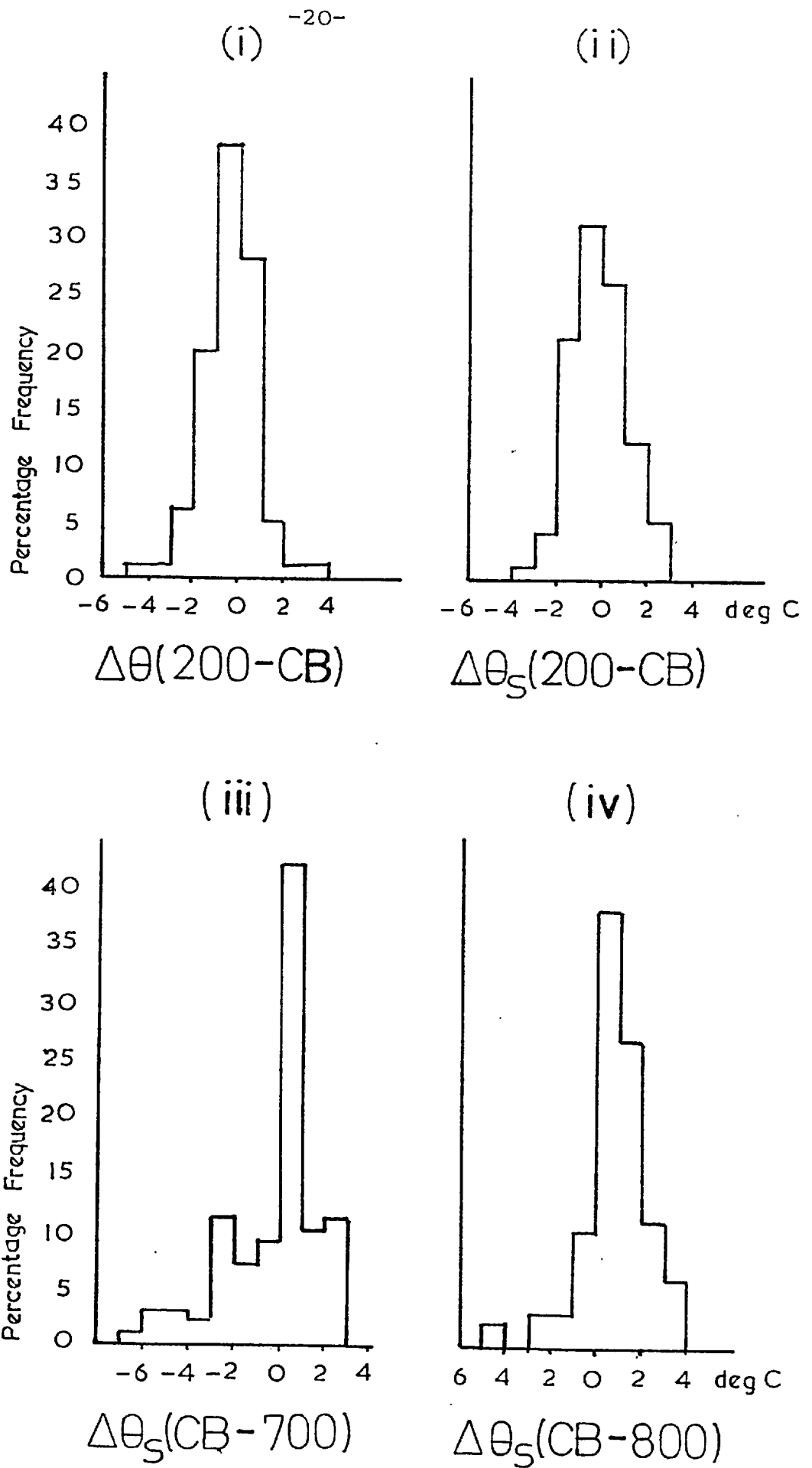


FIG. 2.1

Histograms showing mean lapse rates on occasions of showers over the ocean.

$\Delta\theta$  and  $\Delta\theta_S$  are defined in the text.

values by some uncertainty in the location of cloud base. Statistically these extremes are not very significant, since only 10% of all the values lie outside the range -2 to +2 deg C. The graph of  $\Delta\theta_s$  is only slightly less well-defined in its maximum, with 57% of all soundings lying in the range  $\pm 1$  deg C.

For the cumulonimbus layer itself we consider two more parameters:

$$(iii) \quad \Delta\theta_s \text{ (CB - 700)} \equiv \theta_s \text{ (cloud base)} - \theta_s \text{ (700 mb)}$$

$$(iv) \quad \Delta\theta_s \text{ (CB - 800)} \equiv \theta_s \text{ (cloud base)} - \theta_s \text{ (800 mb)}$$

As can be seen from figure 2.1(iii), the lapse rate in the cloud layer is generally slightly greater than the wet-adiabatic (63% of the soundings having  $\Delta\theta_s$  greater than 0 deg C). On a rather significant number of occasions, however,  $\Delta\theta_s$  is negative; in these cases it is evident that the convection did not reach as high as the 700 mb level. Figure 2.1(iv), on the other hand, shows that the atmosphere between cloud base and 800 mb is almost always slightly unstable; only 18% of the soundings gave negative values for  $\Delta\theta_s$ .

We now extend this type of analysis to employ routine meteorological data. As has already been remarked, the development of precipitation from cumulus demands a minimum cloud thickness, which, over the oceans, is usually about 2 km. (This value is remarkably constant because the microphysical characteristics of low-level air over the ocean are subject to little variation.) If cloud base is at about the usual height of 500 m, then cloud tops must

reach some level between 800 and 700 mb before showers develop, and in these conditions we expect the screen-level value of  $\theta_w$  to be close to the value of  $\theta_s$  aloft, as suggested by the aircraft soundings. There may also be a characteristic value of the difference between  $\theta_w$  at screen level and  $\theta_s$  at the surface (assuming that air in contact with the sea surface is saturated); this would be desirable from the point of view of shower forecasting, since the sea surface temperature is probably easier to predict than that of the air above it.

Data from Ocean Weather Ships I and J covering the period from October 1973 to April 1974 were selected, and classified as either 'showery' or 'dry'. An occasion was deemed 'showery' if the past weather observation indicated showers or thunderstorms in the six hour period before and after the time of observation, and 'dry' if no type of rain was reported. For 100 'showery' and 100 'dry' occasions at both weather ships the following parameters have been calculated to compare their relative values as indicators of 'showers' or 'no showers':

- (i)  $\Delta\theta_s$  (S - 5)  $\equiv$   $\theta_s$  (sea surface) -  $\theta_s$  (500 mb)
- (ii)  $\Delta\theta_s$  (D - 5)  $\equiv$   $\theta_w$  (deck level) -  $\theta_s$  (500 mb)
- (iii)  $\Delta\theta_s$  (S - 7)  $\equiv$   $\theta_s$  (sea surface) -  $\theta_s$  (700 mb)
- (iv)  $\Delta\theta_s$  (D - 7)  $\equiv$   $\theta_w$  (deck level) -  $\theta_s$  (700 mb)

Figure 2.2 shows histograms of the number of occasions on which  $\Delta\theta_s$  lay within ranges of 1 deg C, and also cumulative histograms. Several interesting features emerge from these diagrams.



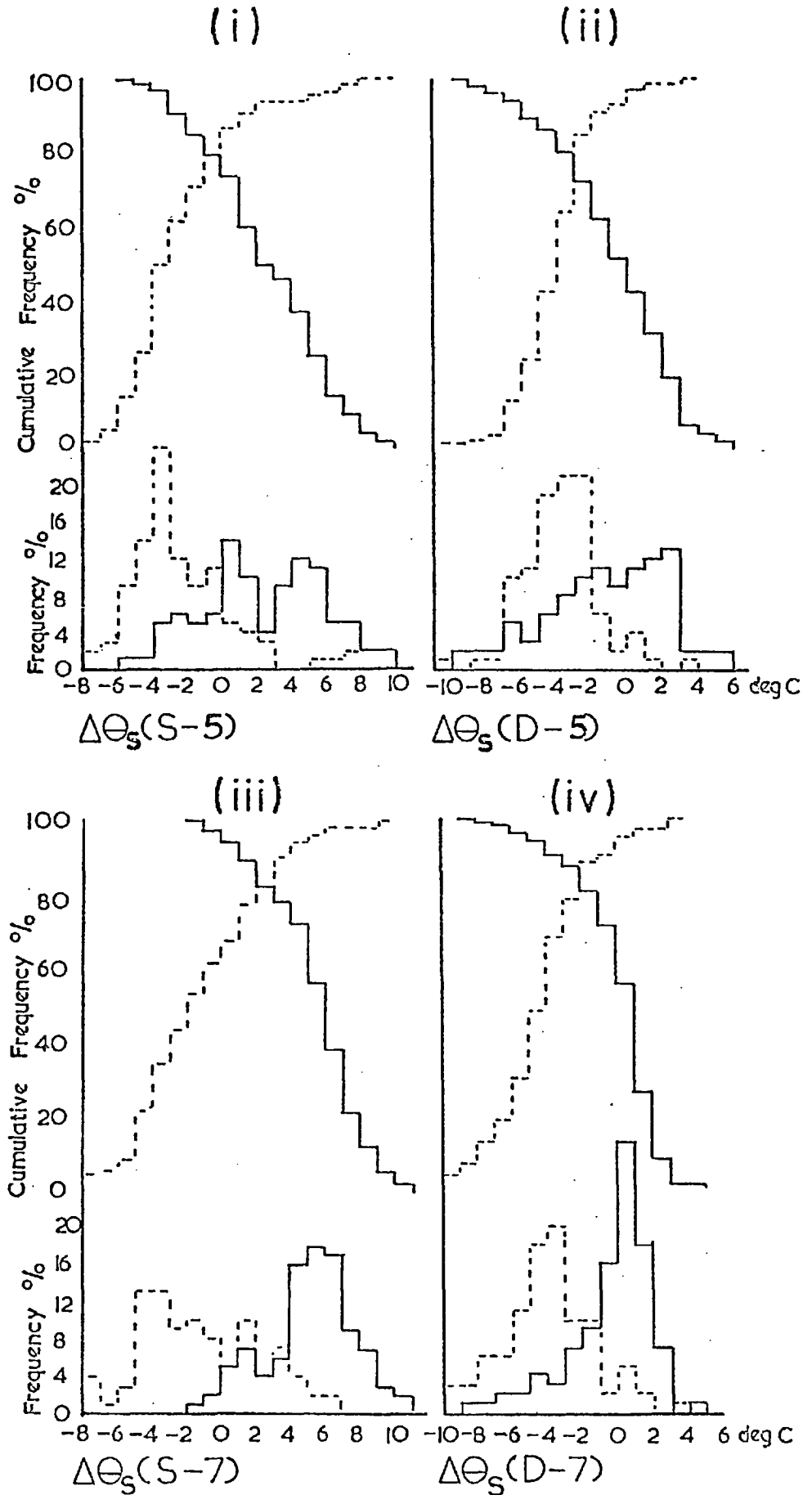


FIG. 2.2

As fig. 2.1 for occasions of 'showers' and 'no showers' (pecked lines). Derived from routine aerological data for OWS I and J.

It is surprising that  $\Delta\theta_s$  (S - 5) reaches such high values as 9 to 10 deg C, but presumably this indicates a large difference between the sea surface temperature and the air temperature at deck level. It is apparent from graphs (i) and (ii) that there is relatively little difference between the stability over a 500 mb layer in showery and in dry conditions; graph (ii) indicates that over half of all showers occurred with  $\Delta\theta_s$  (D - 5) less than -2 deg C. This strengthens the view that clouds need reach only the 700 mb level to produce precipitation, and it is evident that temperatures at the 500 mb level can provide little information relevant to the problem of forecasting showers over the ocean.

Graphs (iii) and (iv), on the other hand, show a much sharper discrimination between 'showers' and 'no showers', particularly the latter, which uses  $\theta_w$  at deck level. Of the occasions examined, about 70% of all showers occurred when  $\Delta\theta_s$  (D - 7) exceeded -1 deg C, consistent with a mean lapse rate close to the wet-adiabatic. It should also be noted that showers were reported with rather large negative values of  $\Delta\theta_s$ ; on these occasions we assume that the convection did not reach the 700 mb level. It may be that data for the 800 mb level would provide an even better discrimination of showery conditions, but this has the disadvantage of being a non-standard level. Clearly the most powerful forecasting criterion is provided by graph (iv); 80% of all showers have  $\Delta\theta_s$  greater than -2 deg C, and 80% of all dry occasions have  $\Delta\theta_s$  less than -2 deg C.

### Stratifications over land

The total concentration of aerosol particles is low in maritime air, but after more than a day in contact with land sources of nuclei the air becomes more polluted, and is classed as 'continental'. As a result there is an increase in both the height of cloud base and the minimum cloud thickness associated with the formation of showers, the latter reaching values as high as 4 or 5 km in stagnant air masses.

As before, we examine the relevance of a simple stability parameter to the incidence of convective rainfall. We have taken data for Crawley, in south-east England, and plotted surface values of  $\theta_w$  together with values of  $\theta_s$  at higher levels in the troposphere. It was decided to compare the summer months (when most of the rainfall is convective) of two contrasting years, 1959 and 1976. Table 2.1 summarizes the main characteristics of the months used in the analysis. Values of  $\theta_s$  aloft were obtained for the 500 mb level (not shown) and the 700 mb level (see figures 2.3 and 2.4).

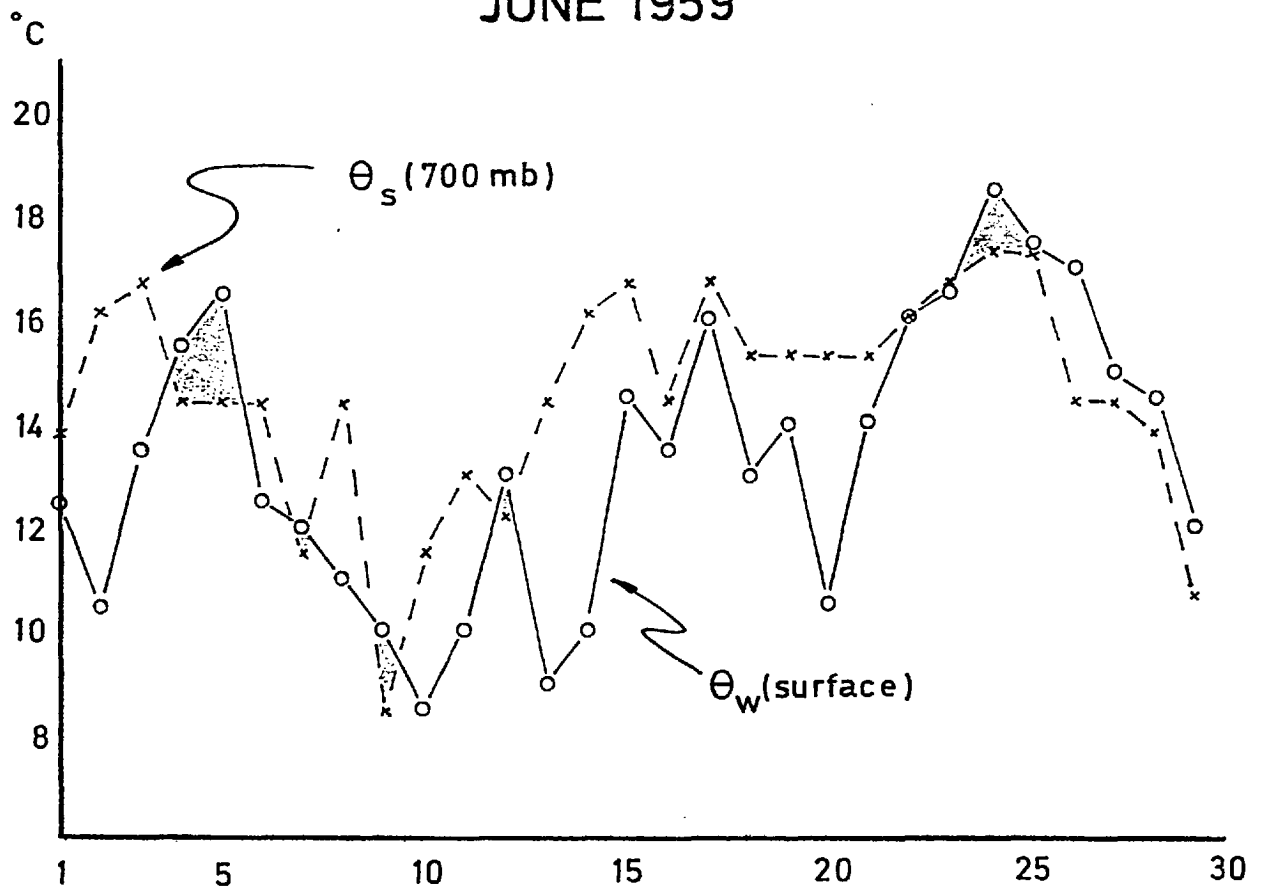
In general as one might expect, the occurrence of thundery rainfall is closely correlated with those periods when the surface value of  $\theta_w$  exceeds that of  $\theta_s$  at upper levels. As in the previous studies, it was found that the atmosphere is rather more unstable over the lowest 300 mb than 500 mb, although the differences are less pronounced over land because here deep convection is more common. Most striking is the comparison between the months of June; there is remarkably little difference between the two graphs, yet June 1976 was almost entirely without showers over the whole of south-east England. An indication of the crucial

TABLE 2.1

	<u>1959</u>		<u>1976</u>	
<u>JUNE</u>	1st-4th	slight rain	1st-2nd	unsettled, some rain
	5th	widespread R's		Generally dry until ...
	6th	'dry' cold front	19th	cyclonic rain
	7th	some rain in cool SW'ly		Dry, sunny, hot ...
		Generally dry until ...		(22nd/23rd R's over SE coast)
	21st-26th	R's	29th-30th	cooler NE'ly
	27th-29th	Occasional R's		
	Total rainfall:	Kew 15 mm Gatwick/Crawley 25 mm		8 mm 11 mm
	Thunder reported:	4 days		0 days
	<u>JULY</u>	1st-3rd	moist SW'ly	1st-8th
4th		sunny, dry	9th	'dry' front
5th		some R's	10th-12th	warm, sunny
6th-8th		sunny, warm	13th-15th	W'ly (little rain)
9th-10th		widespread R's	16th	R's
11th		frontal depression		Generally dry ...
12th		R's		(20th/21st few R's)
13th-25th		generally dry	30th-31st	cool N'ly
26th-30th		R's		
Total rainfall:		Kew 40 mm Gatwick/Crawley 31 mm		25 mm 57 mm*
Thunder reported:	5 days		5 days	

\* includes one fall of 35 mm  
on July 15th

### JUNE 1959



### JUNE 1976

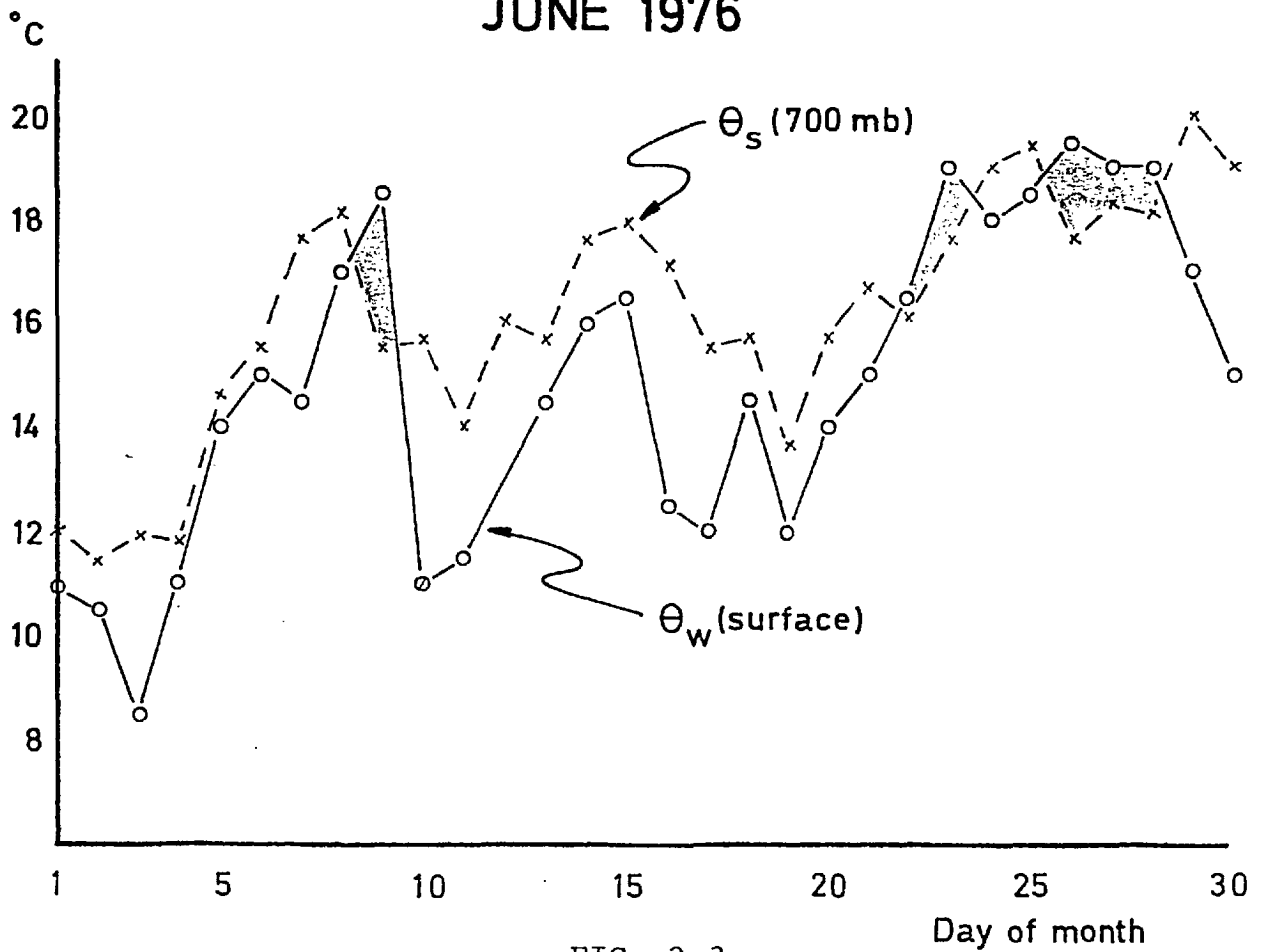


FIG. 2.3

Daily variation of  $\theta_s$  at 700 mb and  $\theta_w$  at screen-level.

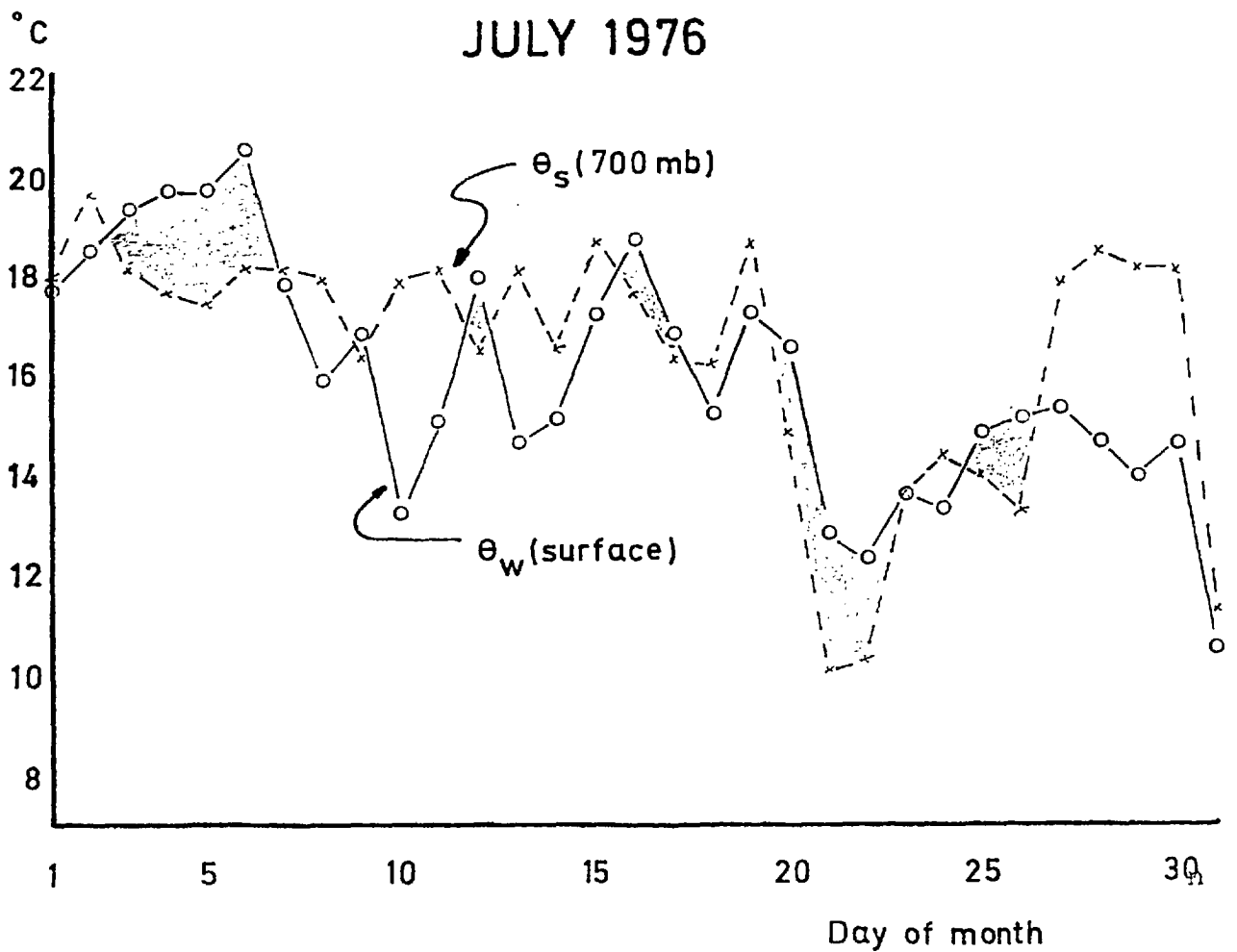
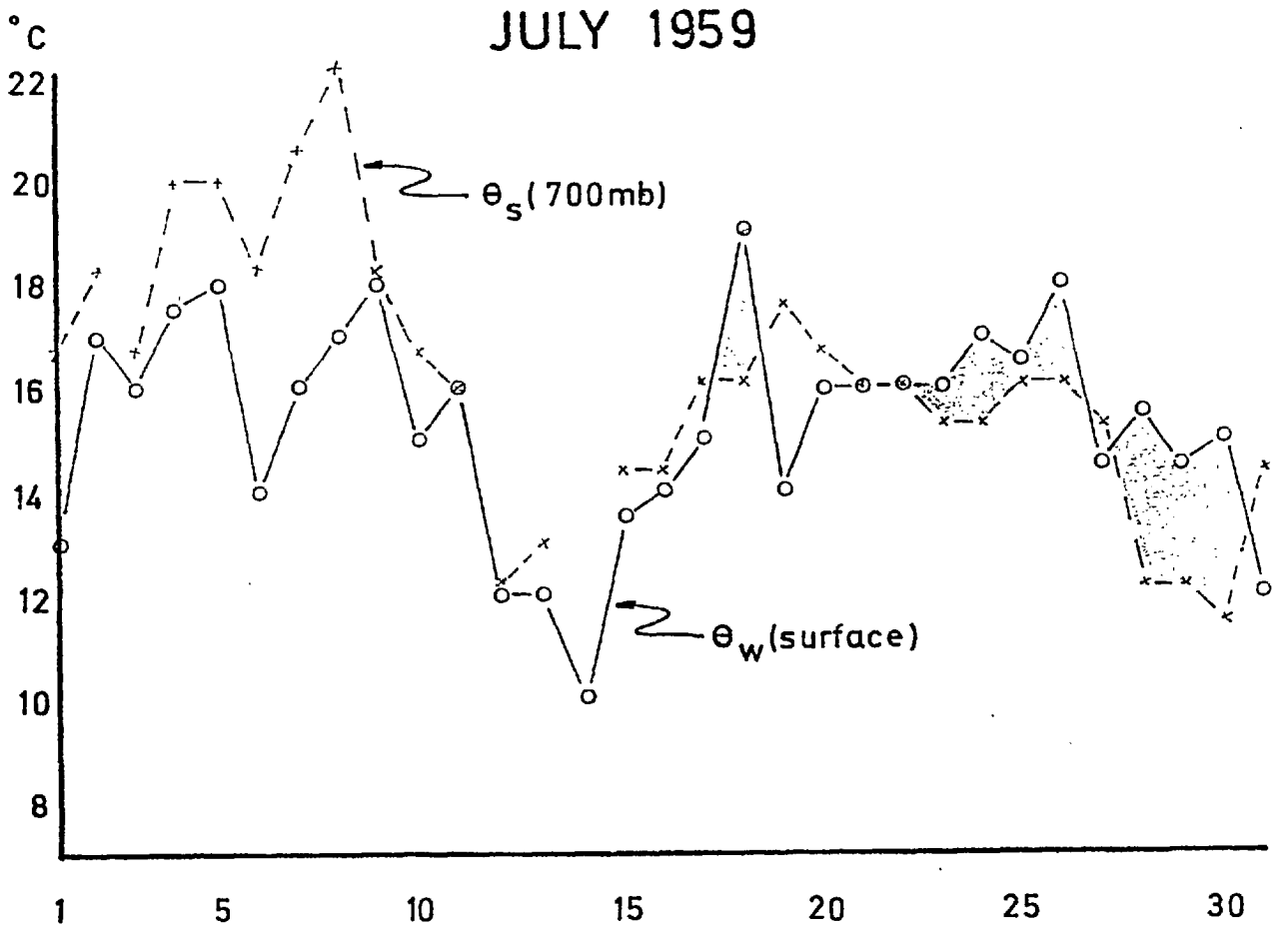


FIG. 2.4

Daily variation of  $\theta_s$  and  $\theta_w$ , as fig. 2.3.

difference, however, is given by the monthly mean values of the parameters; the average value of  $\theta_s$  (500 mb) -  $\theta_w$  (surface) was +2.2 deg C in June 1959, compared with +1.7 deg C for June 1976. Mean values of  $\theta_w$  and  $\theta_s$  aloft were both higher in 1976 than in 1959, by 0.9 deg C and over 3 deg C respectively. It appears that the exceptional dryness of June 1976 was a result of relatively high temperatures at upper levels, which may be associated with unusually strong descent in the prevailing anticyclone. Despite many days of sunshine and very high values of  $\theta$ , the boundary layer rarely became sufficiently moist for deep convection. As suggested in chapter I, this may have resulted from several factors, one of which is likely to have been the exceptional dryness of the months preceding June 1976. Very little moisture was available for evaporation from the surface, so that many days of sunshine resulted in very large values of  $\theta$  near the surface, while  $\theta_w$  remained only slightly above the values typical of June 1959.

A significant feature of figure 2.4, which suggests the forecasting limitations of these simple stability parameters, is the situation at the beginning of July 1976, when  $\theta_w$  at the surface became 2 or 3 deg C greater than  $\theta_s$  aloft in the middle of a dry period. Only by examination of the detailed temperature sounding, shown in figure 2.5, does it become clear that the dryness of the air above about 950 mb makes the surface (screen-level) value of  $\theta_w$  unrepresentative of the boundary layer as a whole, and that the temperature lapse rate at low levels is significantly less than the dry-adiabatic, thus making convection improbable.

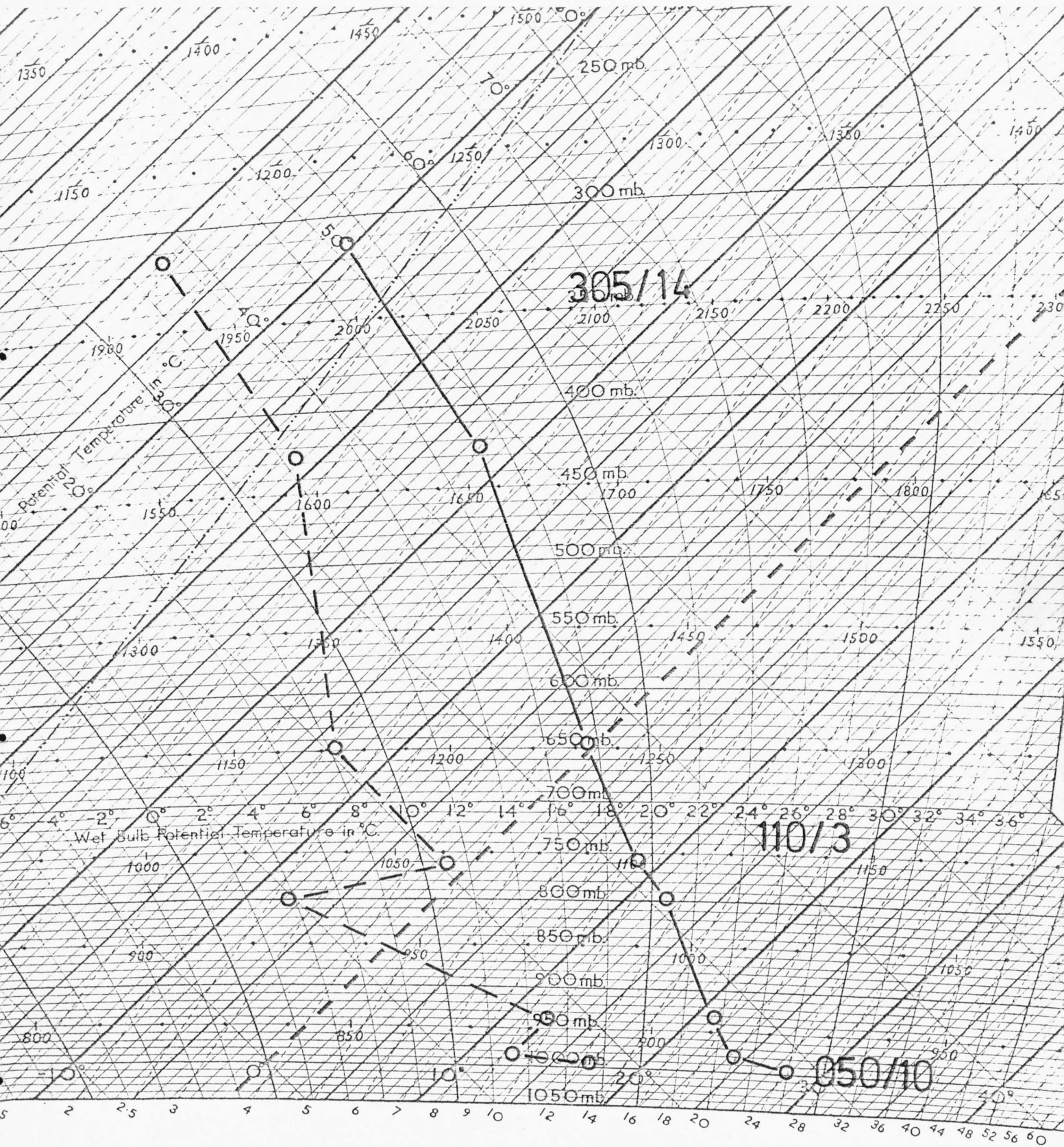


FIG. 2.5

Midday sounding from Crawley, 6 July 1976, plotted on a tephigram, with wind direction in degrees and speed in knots.



## 2.2 QUANTITATIVE ASPECTS OF SHOWER RAINFALL

We have seen that cumulus and cumulonimbus convection are often accompanied by a characteristic atmospheric stratification. The stratification, however, is not itself fundamental, since it is sensitive to large-scale atmospheric flow patterns, particularly vertical motions. Clearly, upward vertical motion leads to adiabatic cooling and destabilization of a layer of air, while large-scale descent warms and stabilizes the air, reducing the probability of widespread convection. When the cloud layer is deepened by upward vertical motion, the rate and persistence of rainfall from individual clouds is likely to be increased, but so also is the spacing between clouds, and it is not obvious that a 24 hour, mean areal rainfall will be substantially greater than some threshold value simply because the clouds are deeper. However, the large-scale vertical motion is likely to be related to the upward mass flux of water in clouds, and hence to a mean areal rate of precipitation.

Over moist surfaces, mean upward motion is probably manifest in a lowering of cloud base, and also in a decrease in the value of the dew point depression ( $T - T_D$ ) near the surface. An attempt was made, therefore, to correlate the mean areal rainfall values (the calculation of which is explained in chapter I) with screen-level values of  $T - T_D$ , for occasions of showery, maritime airstreams. The results (which are not presented here) were very discouraging, perhaps partly because of a large natural variability in  $T - T_D$  which made it almost impossible to select a value representative of a particular area. It was then decided

that a more fundamental parameter of the large-scale motion might yield better results.

#### Estimations of vertical motion

Probably the most satisfactory method of determining vertical motion on a large scale is the technique of isentropic analysis (see, for example, the original paper by Rossby et al., 1937, and some case studies by McIlveen, 1966), which uses the assumption that air trajectories remain on surfaces of constant potential temperature (allowance can be made for radiational cooling). One of its main disadvantages, however, is that isentropic charts are not prepared routinely, so that the use of the technique is normally confined to diagnoses rather than prognoses.

The most straightforward method is known as the 'kinematic method', which essentially consists of computing the divergence directly from the observed wind; integration of the continuity equation leads directly to the vertical velocity, using the boundary condition that  $w = 0$  at the surface. The advantages of the method are that it is based on the definition of divergence, assuming nothing about the processes involved, and the divergence is obtained from instantaneous conditions. Its application is severely limited, however, by the need for extreme accuracy in the wind observations.

The method we shall employ uses the vertical component of relative vorticity ( $\zeta$ ), which is related to vertical motion in the following manner. By differentiating and adding the two horizontal components of the momentum equation, we obtain (neglecting terms which are small on the synoptic

scale):

$$f \left( \frac{\partial u}{\partial x} + \frac{\partial v}{\partial y} \right) + v \frac{\partial f}{\partial y} + \frac{D}{Dt} \left( \frac{\partial v}{\partial x} - \frac{\partial u}{\partial y} \right) = 0 \quad (2.1)$$

where the operator  $\frac{D}{Dt}$  (the substantial derivative) is defined in two dimensions as

$$\frac{D}{Dt} \equiv u \frac{\partial}{\partial x} + v \frac{\partial}{\partial y} + \frac{\partial}{\partial t}$$

and represents the rate of change of a variable following the motion of a parcel of air.

If the scale of the motion field under consideration is such that the variation with latitude of  $f$  (the Coriolis parameter) is small, we have

$$\frac{D}{Dt} \left( \frac{\partial v}{\partial x} - \frac{\partial u}{\partial y} \right) \equiv \frac{D\zeta}{Dt} \approx -f \left( \frac{\partial u}{\partial x} + \frac{\partial v}{\partial y} \right) \quad (2.2)$$

In other words the change in the vertical component of vorticity following the motion of an air parcel is proportional to the horizontal divergence, which, as before, is related by integration to the vertical velocity.

In practice the method can be very laborious: not only has vorticity to be computed from routine data, but charts several hours apart must be compared in order to evaluate the local change of vorticity. Again, the main uses of the full method are usually confined to diagnostic studies.

Some useful information may be obtained from the vorticity alone. Equation (2.2) with the continuity equation, associates positive (cyclonic) relative vorticity at low

levels with recent convergence and consequent upward vertical motion; similarly, anticyclonic relative vorticity implies that there has been large-scale descent of the air. This relation was examined by Petterssen et al. (1945). In a comprehensive study of cumulus and cumulonimbus clouds, the authors considered the correlation between the occurrence of convection and the (qualitative) vorticity of the flow at the 750 mb level, and found the association to be rather low. However, when the cases of convection were divided into 'shallow' (with cloud tops at or below 800 mb), 'deep' (cloud tops up to or above 600 mb) and 'very deep' (when cloud tops reached or exceeded the 400 mb level), the correlations were more striking. There was a slight preference for anticyclonic vorticity aloft when the convection was shallow, but the authors concluded categorically that "deep and very deep convection should not be forecast unless the upper air charts show indication of cyclonic vorticity". Forecasters in the USA, concerned with the problem of predicting cloud-top heights, showed that the 700 mb vorticity, as obtained from routine synoptic charts, was a useful tool. Crutcher et al. (1950) found a high degree of correlation between a 'vorticity index' and observed cumulus cloud tops (the maximum time difference between observation and computation was  $\pm 6$  hours) for over 450 occasions covering an eleven month period. The relationships derived from these original data were then tested against 210 subsequent observations, with a similar degree of success.

As we have seen from section 2.1, the most significant 'standard' level regarding the development of showers is

probably 700 mb, since in maritime airstreams this level must usually be reached by clouds which are to produce precipitation. Thirteen occasions of showery maritime airstreams entering the British Isles were selected from the period October 1974 to July 1976, and values of the 24 hour rainfall, expressed as mean over 100 km x 100 km squares, were provided by the Meteorological Office. A measure of the vertical vorticity of the flow (upwind of the British Isles) was obtained from the German 700 mb charts\* for 00 GMT on each of the rainfall days, using a finite difference method on a grid of approximately 400 km (see figure 2.6). (The German charts are published in a very small format, so it was found necessary to make a transparency of each and project the image onto a plotting surface.)

Normally the vertical vorticity is computed either directly from the reported winds, or from the observations of the pressure field; assuming that the wind is in geostrophic balance, we have the 'geostrophic vorticity'

$$\zeta_g = \frac{\partial v_g}{\partial x} - \frac{\partial u_g}{\partial y} = \frac{1}{\rho f} \left( \frac{\partial^2 p}{\partial x^2} + \frac{\partial^2 p}{\partial y^2} \right) = \frac{g}{f} \nabla_p^2 h$$

where h refers to the height of a pressure level, and the variation with latitude of the Coriolis parameter has again been neglected. At the 700 mb level the wind is almost always in geostrophic balance, so that  $\zeta_g = \zeta$ .

\* these charts appear in the "Täglicher Wetterbericht" of the *Deutscher Wetterdienst*.

The vertical component of relative vorticity is given by

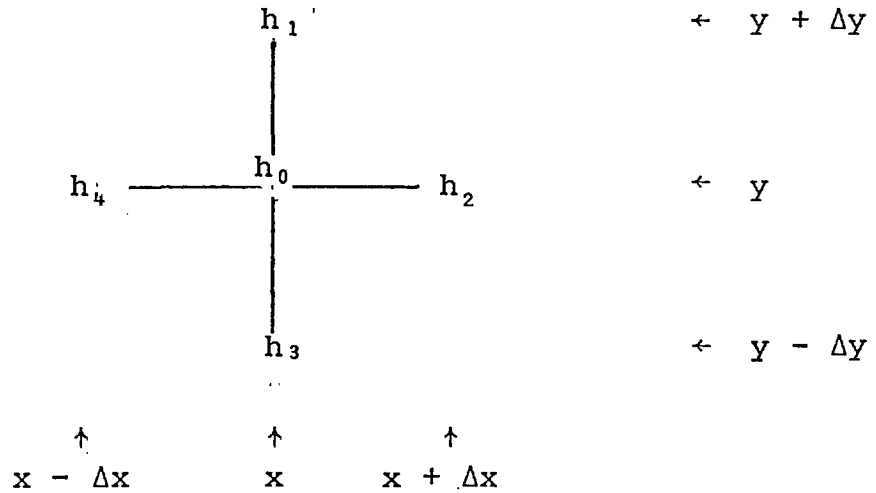
$$\zeta = \frac{g}{f} \nabla^2 h = \frac{g}{f} \left( \frac{\partial^2 h}{\partial x^2} + \frac{\partial^2 h}{\partial y^2} \right) \quad \text{where } h = h(x, y)$$

In finite difference form

$$\frac{\partial^2 h}{\partial x^2} \approx \frac{h(x + \Delta x, y) + h(x - \Delta x, y) - 2h(x, y)}{(\Delta x)^2}$$

and 
$$\frac{\partial^2 h}{\partial y^2} \approx \frac{h(x, y + \Delta y) + h(x, y - \Delta y) - 2h(x, y)}{(\Delta y)^2}$$

So on the grid



where  $\Delta x = \Delta y = \delta$ , say, we have

$$\zeta \approx \frac{g}{f} \frac{1}{\delta^2} (h_1 + h_2 + h_3 + h_4 - 4h_0)$$

FIG. 2.6

### Errors in computation

In terms of accuracy of computation, it is, in theory, preferable to use reported winds, since the vorticity is obtained after only one differentiation, but in practice observations of the wind are often unrepresentative. Although the pressure or height field must be differentiated twice, these charts are more easily obtained than those of wind reports, and in practice it is more convenient to read off directly the height of a pressure surface than to calculate wind components from a given speed and direction.

It was estimated that, with care, the values of  $h$  could be read with a maximum error of  $\pm 3$  m, so that the extreme values of  $\nabla^2 h$  would be within  $\pm 24$  m of the 'true' value, because of the finite difference scheme employed. In effect, then, we have 24 sources of error, each contributing a possible  $+1$  or  $-1$  to the 'true' value, and the standard deviation is simply  $\sigma = \sqrt{24} \approx 5$ . If the errors are distributed normally, then 95% of the computed values of  $\nabla^2 h$  will lie within two standard deviations of the 'true' value, that is  $\pm 10$  m.

### Correlation with areal rainfall

Because the vertical vorticity 'index' ( $\nabla^2 h$ ) is appropriate to a sub-synoptic motion scale ( $\sim 800$  km), it was not possible to relate it to individual values of the 100 km square rainfall. Instead, the maximum value anywhere in the vicinity of the windward coast was recorded (later figures show examples of areal rainfall values). In figure 2.7 we have plotted the maximum recorded areal rainfall against the vorticity index ( $\nabla^2 h$ ) for all 13 occasions (the

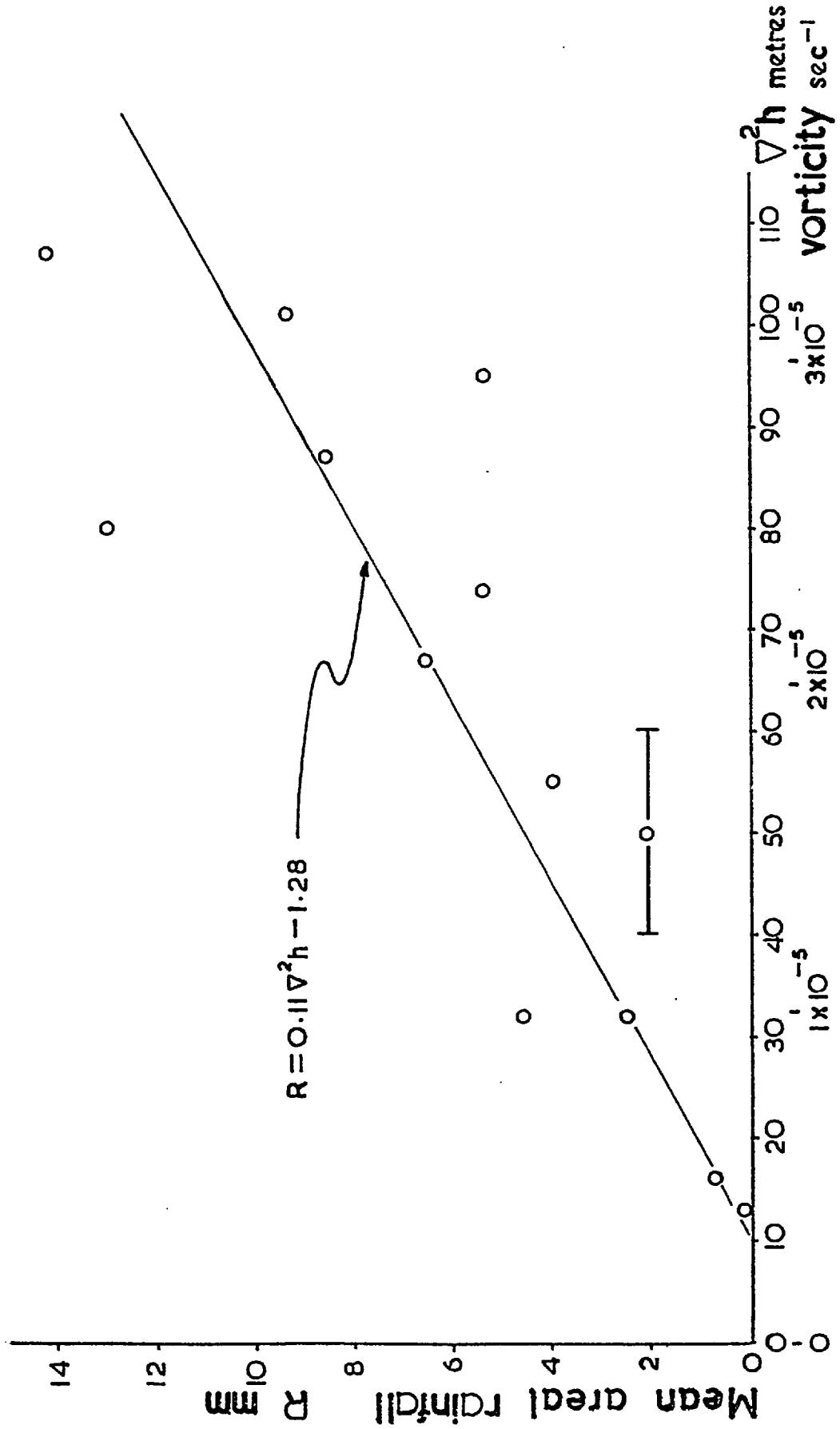


FIG. 2.7

Variation of maximum 24 hour, 100 km square rainfall total with vertical vorticity. Error bar covers two standard deviations (see text).



error bar covers  $\pm$  two standard deviations, as estimated in the previous paragraph). The degree of correlation is encouraging; despite the considerable variability at higher values of vorticity, the coefficient of linear correlation is  $r = 0.84$ ; we have also indicated the 'best straight line', the equation of which is  $R = 0.11V^2h - 1.28$ , with  $R$  in mm and  $V^2h$  in metres. This result justifies the suggestion that vertical vorticity may be used as an indicator of vertical motion, and may prove to have some forecasting value, since we have related the flow at 700 mb to the subsequent 24 hour rainfall. It does, however, only suggest a maximum rainfall; we shall now consider the distribution and intensity of showers on a smaller scale, where the most important influence is topography.

### 2.3 TOPOGRAPHIC INFLUENCES ON SHOWERS

It is common experience that high ground is a preferred region for the development of convection. On many days cumulus clouds, and later showers, are seen to be localized near hills, while the surrounding terrain may remain dry. We shall consider three classes of topographic influence on the distribution of rainfall:- the mechanical lifting effect of hills or mountains blocking the large-scale air flow; altitude and slope effects which give rise to inhomogeneities of potential temperature near the surface; and intermediate scale circulations (such as land and sea-breezes) produced by local variations of topography. Features typical of the British Isles will be considered here, ranging from isolated hills a hundred metres or so in height, to mountain ridges (such as the Pennines) having a vertical extent of about 1 km and a horizontal extent of

up to hundreds of km. Rainfall data will be examined to determine whether topographic effects are detectable in routine meteorological observations, and whether there is any influence on the mean 100 km x 100 km square rainfall values.

### Orographic lifting

An airstream encountering an isolated obstacle will, almost always, tend to flow around it rather than over it. When the obstruction is in the form of a ridge, however, such that its horizontal dimension (across the flow) is many times greater than its vertical extent, significant ascent will occur over the upwind slope, together with descent in the lee of the obstacle. In a situation where there are no showers well up-wind of the hills, the top of the cumulus layer will be lifted and cooled by its passage over the ridge. The level of cloud base, on the other hand, is unlikely to change significantly; Braham and Draginis (1960) and Orville (1965) found that cumulus bases were higher over mountain ridges, although the variation was less than 20% of the variation in the level of the topography. Furthermore the mountains in these studies were up to  $2\frac{1}{2}$  km above sea level, more than twice the size of features typical of Britain. Other work, however, has suggested that there is little consistent relationship between the raising of cloud base and height of the ground; in fact observations made in Sweden (Ludlam and Saunders, 1956) found cloud base up to 300 m lower over high ground.

The net effect of a mountain ridge barrier is thus a

deepening of the layer occupied by cloud, and perhaps additional cloud growth in the clear air between the clouds. Hence, on occasions when convection upwind just fails to attain the critical thickness necessary for shower production, we may expect rainfall to be localized over the hill slopes. In addition, increased cloud cover will reduce the effects of mixing and evaporation, and will favour the presence of larger droplets.

Interesting examples of the influence of mountains on maritime cumulus are provided by studies in Hawaii (Squires and Warner, 1957) and in Tenerife (Garcia-Prieto et al., 1960). Near Hawaii the trade wind inversion is at a height of about 2 km, so that the depth of maritime cumulus is fairly close to that required for the development of precipitation. Orographic lifting over the eastern mountain slopes produces dense, unbroken cloud, extending 20 or 30 miles inland. Measurements in this cloud indicated fewer and larger drops than were found in seaward cumulus; rain over the mountains is remarkably fine but dense and persistent, giving over 300 inches per year in some areas. Tenerife, like Hawaii, is situated in north-easterly trade winds, but at a different latitude, and here strong subsidence near the Azores anti-cyclone places the inversion at about 800 m above sea level. The northern slopes of the island are often engulfed by massed trade wind cumulus, but these clouds only produce significant rain (in total about 30 inches annually) when invasions of polar maritime air raise the inversion above about  $1\frac{1}{2}$  km. Thus the effect of an orographic barrier is most pronounced when the depth of the cumulus layer to windward is insufficient to produce showers; on occasions

of deep cumulonimbus convection the orographic influence may be less well defined.

When the flow near the surface of a ridge follows the shape of the obstacle ('aerodynamic' flow), the displacement of the streamlines fades rapidly with height; according to Scorer (1953a) small ridges produce little or no vertical displacement above the surface adiabatic layer. When the hill influences the flow at levels where the air is stably stratified, the air is often set into large vertical oscillations (lee waves) which may persist for several tens of kilometres downwind of the ridge. These oscillations amplify with height, and reach a maximum amplitude somewhere in mid-troposphere; the horizontal wavelength is typically between 6 and 16 km, and vertical velocities associated with these waves may occasionally reach  $10 \text{ ms}^{-1}$  (Booker, 1963). Hosler et al. (1963) point out that a large wind shear is favourable for the formation of both severe thunderstorms and lee waves. After a study of precipitation maps they conclude that the effect of the oscillations is detectable in rainfall patterns, since convection is likely to be enhanced in the ascending phase of a lee wave, and suppressed in regions of descent.

Other types of interaction between hill or mountain ridges and showers may be suggested, one of which is the effect of sloping terrain on the cool outflow from cumulonimbus. A sufficiently steep slope could even reverse the direction of the downdraught outflow; this would have a profound effect on the subsequent motion of the storm, either constraining it to remain near the hill, or perhaps

resulting in its dissipation by cutting off the supply of warm air. A further possible reason for larger amounts of rainfall over hills is that since cloud base is nearer the surface over high ground (although at about the same level in the atmosphere), falling raindrops will have less time in which to evaporate. A similar point was made by Dennis et al. (1973) in relation to a persistent storm (or series of storms) which produced 15 inches of rain over the Black Hills in South Dakota, USA. The apparently stationary nature of the storm system was attributed to an absence of downdraughts, which the authors explained by the fact that the cloud bases in the rain area were actually on the ground; with moist air aloft there was no opportunity for evaporative cooling to take place anywhere in the storm system.

#### Altitude and slope (thermal) effects

Given similar conditions of radiative exchange, the surface temperature over high ground will be virtually the same as that over neighbouring low ground. Hence air near the surface of a hill will be characterized by a higher potential temperature than air at a lower altitude and at the same level well away from the hill (when there is an appreciable lapse rate of temperature in the atmosphere). Ludlam and Scorer (1953) identified a good thermal source as one from which bubbles of warm air can ascend for longer without a break than in the neighbourhood; thus high ground is a good source since heat is released into the atmosphere at a higher level. It is difficult to estimate the magnitude of the effect except in idealized conditions because surface temperature is sensitive to many influences, but, if the surface temperature is assumed constant,  $\theta$  would

increase by about 1 deg C for every 100 m above the 1000 mb level.

The higher potential temperature of hill surfaces may also be due to the greater radiation per unit area received by a slope in comparison with more nearly horizontal terrain. The magnitude of this effect depends on the elevation of the sun, and will be most significant at sunrise or sunset. For very high solar elevations some steep slopes may actually receive less radiation than flat ground, but this situation is unlikely to be particularly common in middle-latitudes.

No mention has yet been made of the moisture content of the air near hills. This is of considerable importance since, in considering convective motions, we normally consider  $\theta_w$  at low levels rather than  $\theta$ . The problem of the level of cloud base has already been referred to; increasing  $\theta$  will raise cloud base, but increasing moisture near the surface will lower it. Low-level humidity, like temperature, is sensitive to many influences such as rainfall, drainage and vegetation, and it is unlikely that any general rule can be established.

#### Intermediate-scale circulations

The differential heating arising from the hill/plain system often gives rise to a circulation known as the anabatic wind. As air of high potential temperature rises from the sun-facing hillslope, it is replaced by cooler air from the surrounding plain. The anabatic wind draws off the superadiabatic layer from the neighbouring low-lying countryside where convection may not yet have started, and forced ascent up the slope causes this air to become

more unstable. In contrast to the ascent over the hillside, weaker compensatory descent occurs over the plain and tends to stabilize the air there. A reverse circulation is sometimes present at night, when the air close to the surface of the hillside cools more rapidly than air further away at the same level. The descending current, known as the katabatic wind, may be responsible for convergence well away from the hill, and explain the presence of nocturnal thunderstorms over plains and valleys. Anabatic and katabatic winds are thus responsible for the observed 'ring' of low precipitation which Fujita (1967) found surrounding the San Francisco Mountains at a radius of about 5 to 10 miles; during the day showers are most common over the hills, whilst at night the rainfall is a maximum well away from the high ground. On a larger scale Bleeker and Andre (1951) used similar arguments to explain the diurnal distribution of shower rainfall over the central plains and mid-west USA, involving a large-scale circulation system east of the Rocky Mountains.

Another commonly experienced air motion arising from differential heating is the sea-breeze circulation, which may have an important influence in determining the location of cumulonimbus. The sea-breeze is most pronounced when the large-scale wind is light and off-shore; the circulation begins early in the day near the coast and subsequently deepens and spreads inland, reaching its maximum intensity at about the time of maximum surface temperature. The low-level flow may attain speeds of up to  $10 \text{ ms}^{-1}$  and occasionally penetrate over 100 km inland from the coast (Simpson et al., 1977). The land-breeze which develops overnight is a much

less intense circulation, but, in favourable locations, it may be responsible for the development of offshore cumulus or cumulonimbus (Neumann, 1951). The sea-breeze front, which usually moves inland at about half the speed of the air behind it, is often marked by a belt of large cumulus or cumulonimbus, while elsewhere there are only small scattered clouds, or none at all. The effects of the sea-breeze are likely to be more pronounced where there are hills near the coast (such as the South Downs in Sussex) which increase the horizontal potential temperature gradient, and also in regions where sea-breezes can converge from different coasts; Florida, USA, is an example of the latter, and the topographically-induced circulations there have been modelled by Pielke (1974). Britain has a number of peninsulas which might be expected to exhibit similar features; London occasionally receives sea-breezes from the south and east coasts. By studying hourly charts, Findlater (1964) identified three separate sea-breeze systems, originating from the coast at Sussex, Essex/Suffolk and north Norfolk. Three separate thunderstorms occurred by mid-afternoon when the sea-breeze front closely approached a pre-existing convergence zone. Under similar conditions Eastwood and Rider (1961) were able to identify and track two independent sea-breeze fronts using 23 cm radar.

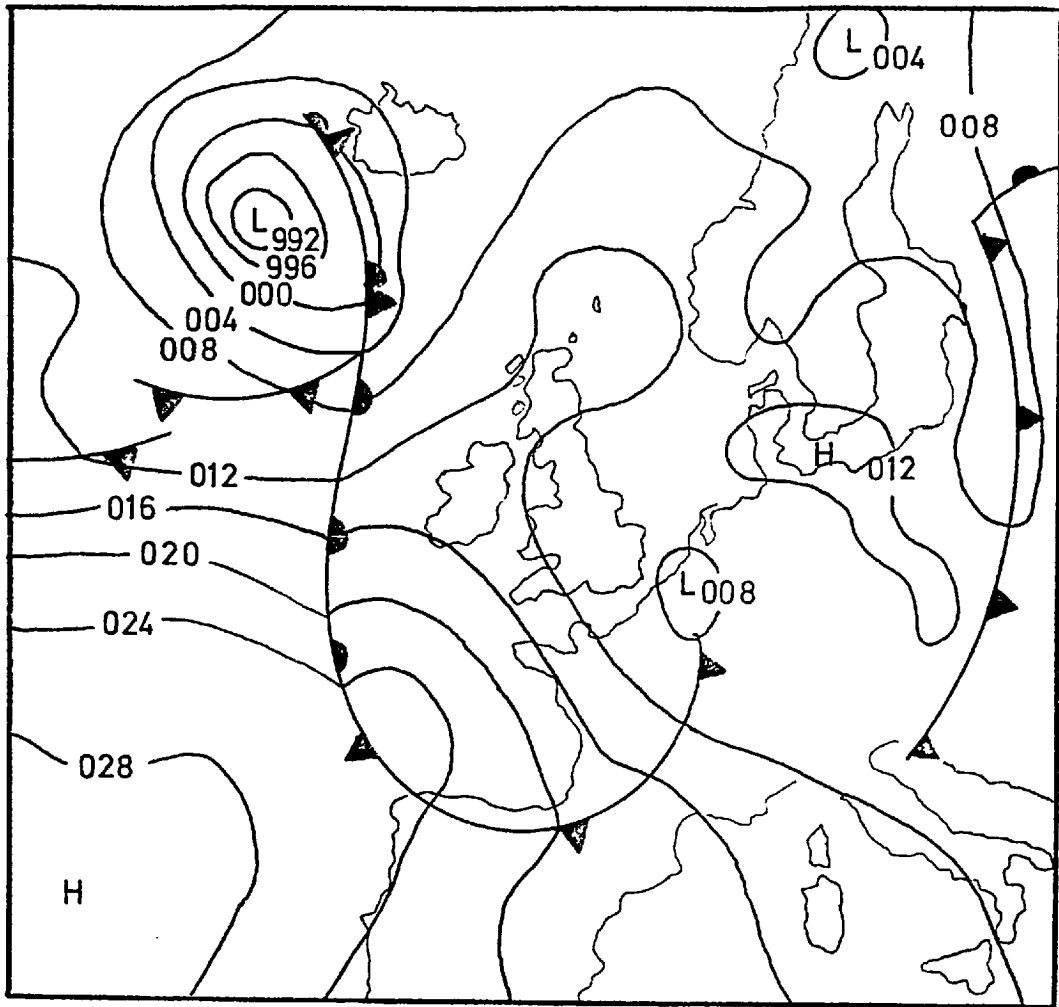
We now present brief case studies of showers over Britain, which illustrate some of the points made above.

17th June, 1975

While much of Britain lay under a weak ridge of high pressure, south-east England was affected by a small



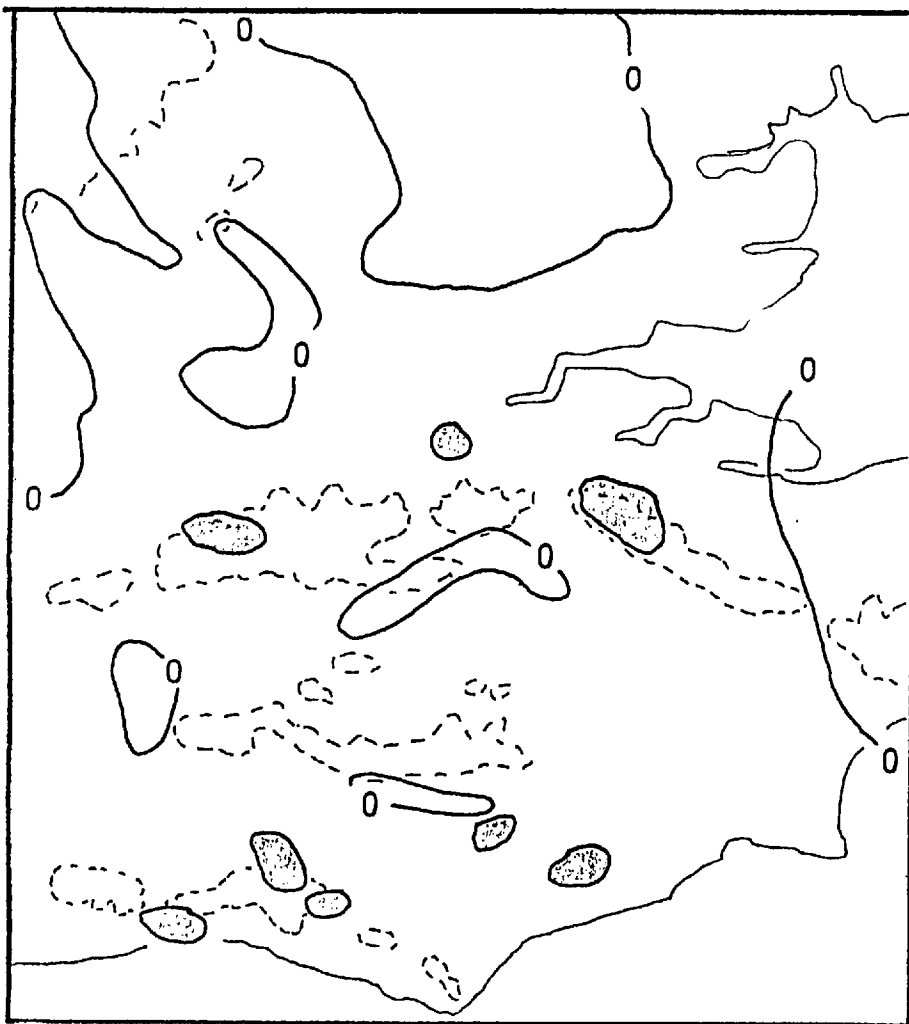
depression over Belgium (figure 2.8). Surface observations from Gatwick (about 50 km south of London) indicate that although one slight shower occurred around midday, the convection did not deepen until mid-afternoon, and showers had completely died out by 2100 GMT. Figure 2.9 shows the 24 hour rainfall totals for south-east England, with isopleths sketched for 0 and 10 mm, and land over 400 ft above sea level also indicated. In general the heavier falls appear to be localized near high ground, and there is also the suggestion of three distinct shower-free regions in the lee of the hills (winds were north-westerly throughout the troposphere). The upper air sounding from Crawley for midday on 17th June (figure 2.10) is consistent with the surface report of cumulus cloud base at just over 1 km, spreading out as stratocumulus at about 1800 m. A few cumulus tops may have been able to reach the small isothermal layer near 650 mb in the morning, but with cloud base only a little below 850 mb this is unlikely to be high enough to produce showers. The midnight sounding on 17th/18th June might be expected to give a better indication of the nature of the previous day's convection, and this is also shown in figure 2.10. The situation may be complicated by the approach of a frontal system from the west, but the troposphere has evidently been warmed by the day's convection. Figure 2.9 also shows the 24 hour mean areal rainfall values, and it can be seen that south-east England was the only part of the country where significant amounts of shower rainfall were recorded; the rather higher values in north-west Britain were associated with the approaching frontal system.



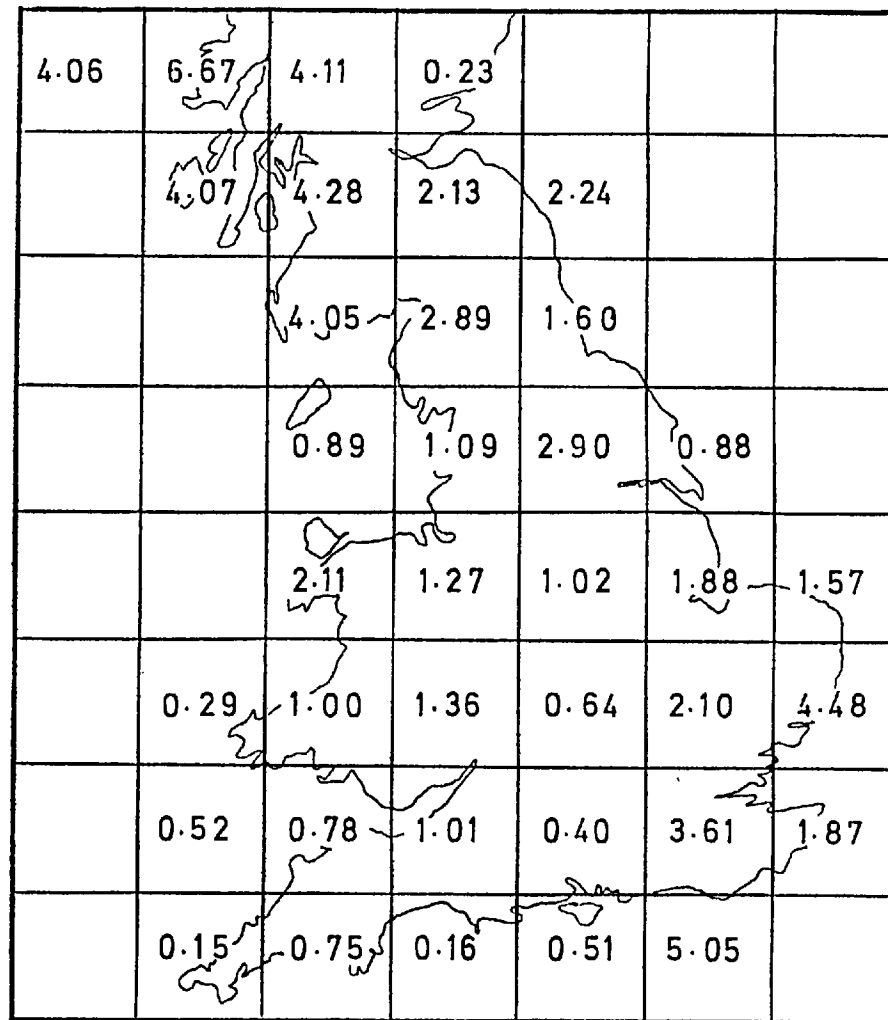
SURFACE ANALYSIS 1200 GMT 17 JUNE 1975

FIG. 2.8

FIG. 2.9



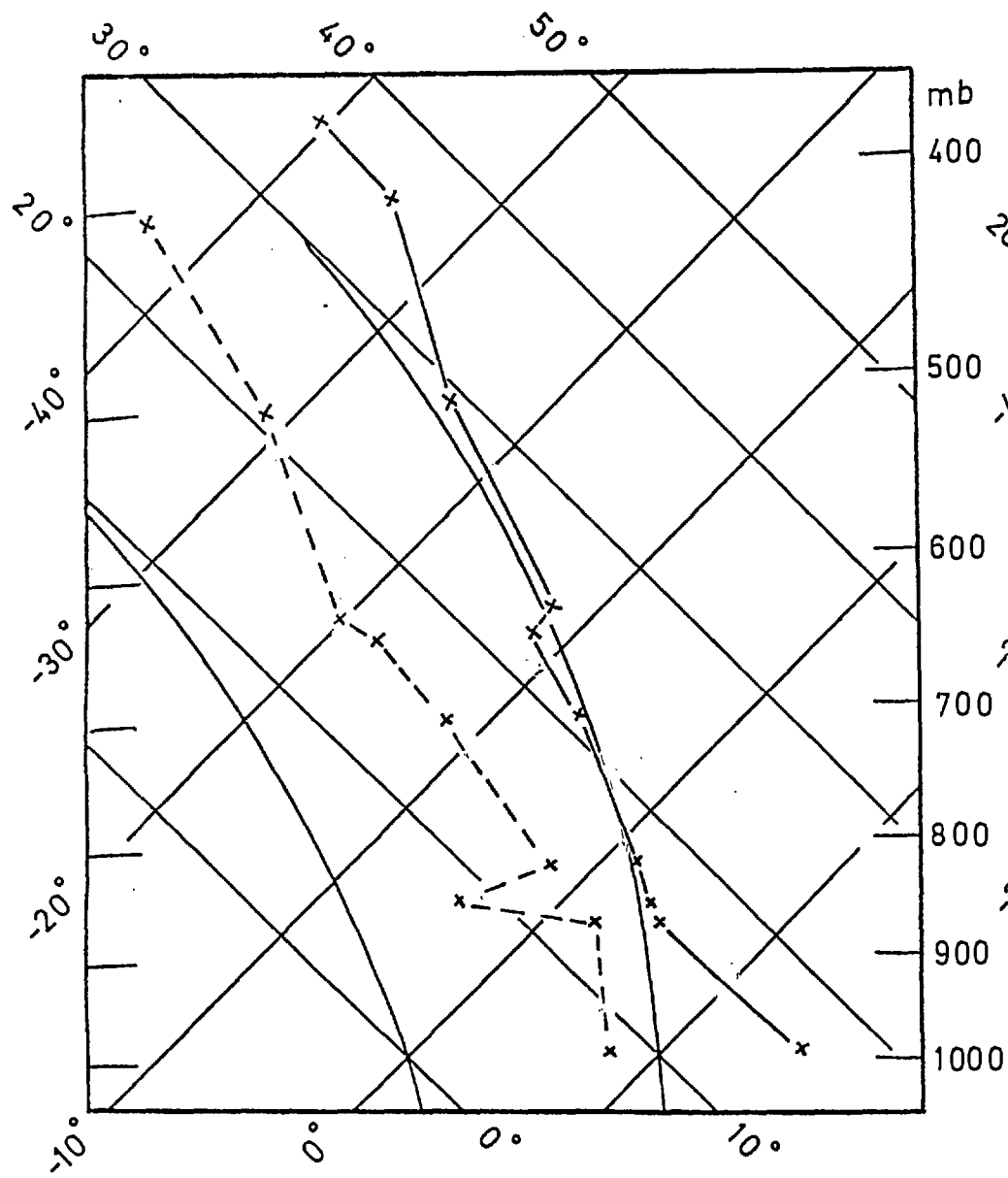
0 and 10 mm isohyets (shaded areas > 10 mm)  
 --- 400 ft contour



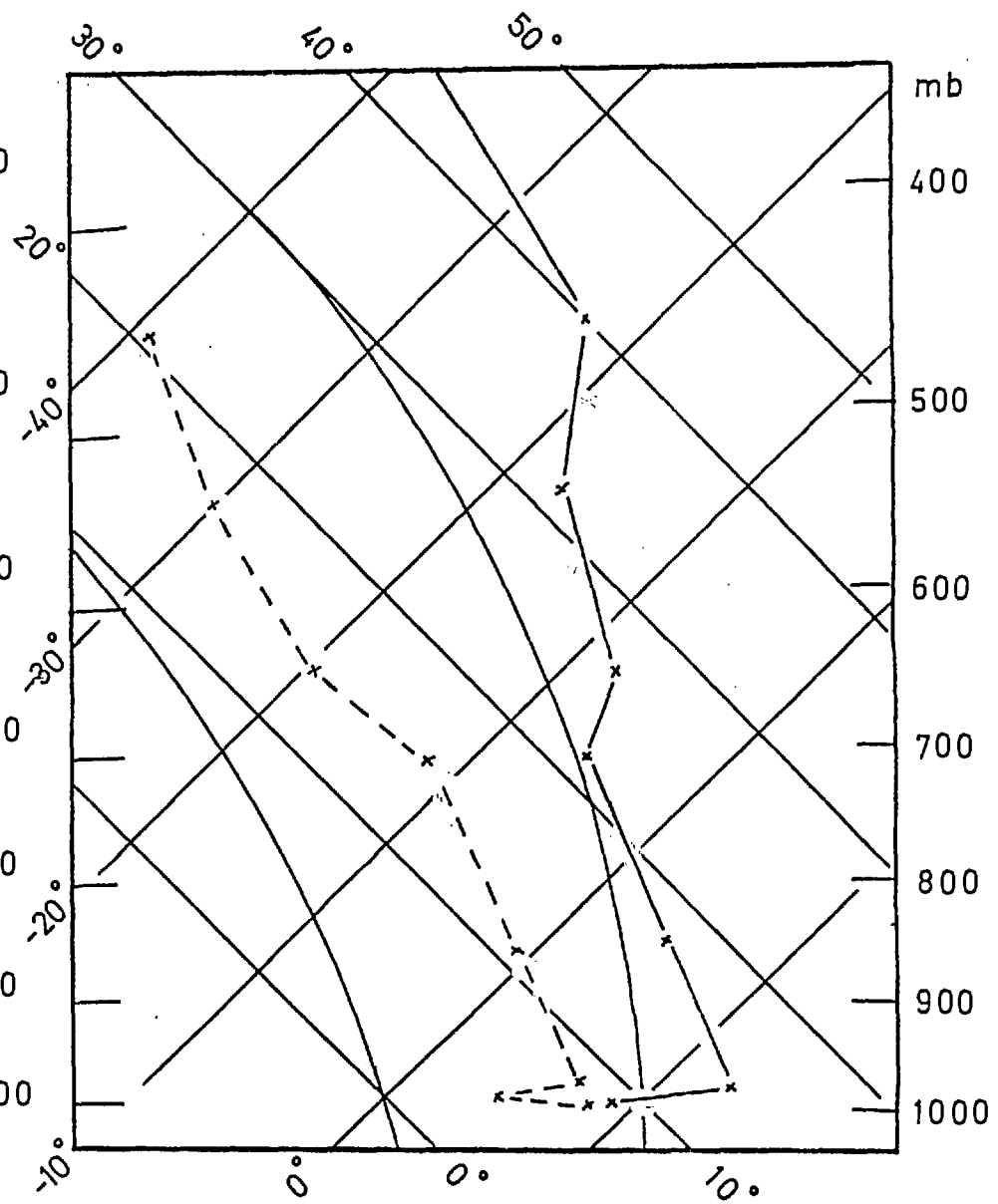
24 hour areal rainfall (mm)

17 JUNE 1975

FIG. 2.10



1100 GMT 17 JUNE 1975



0100 GMT 18 JUNE 1975

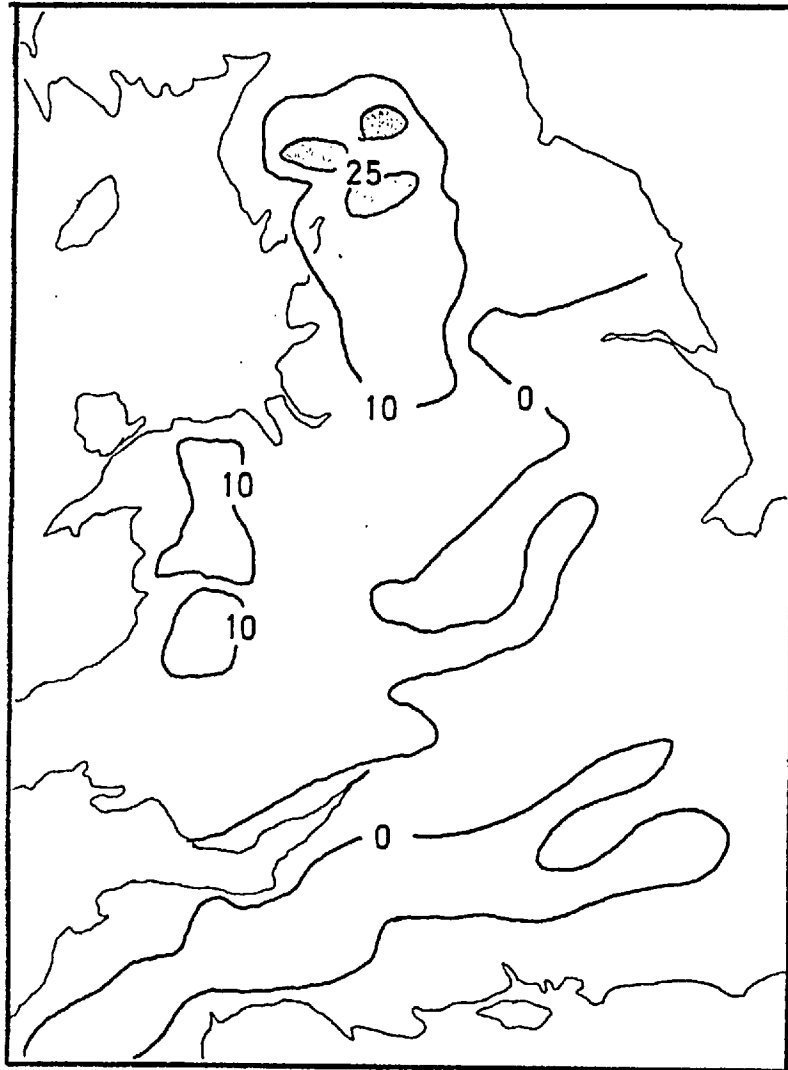
CRAWLEY

30th April, 1975

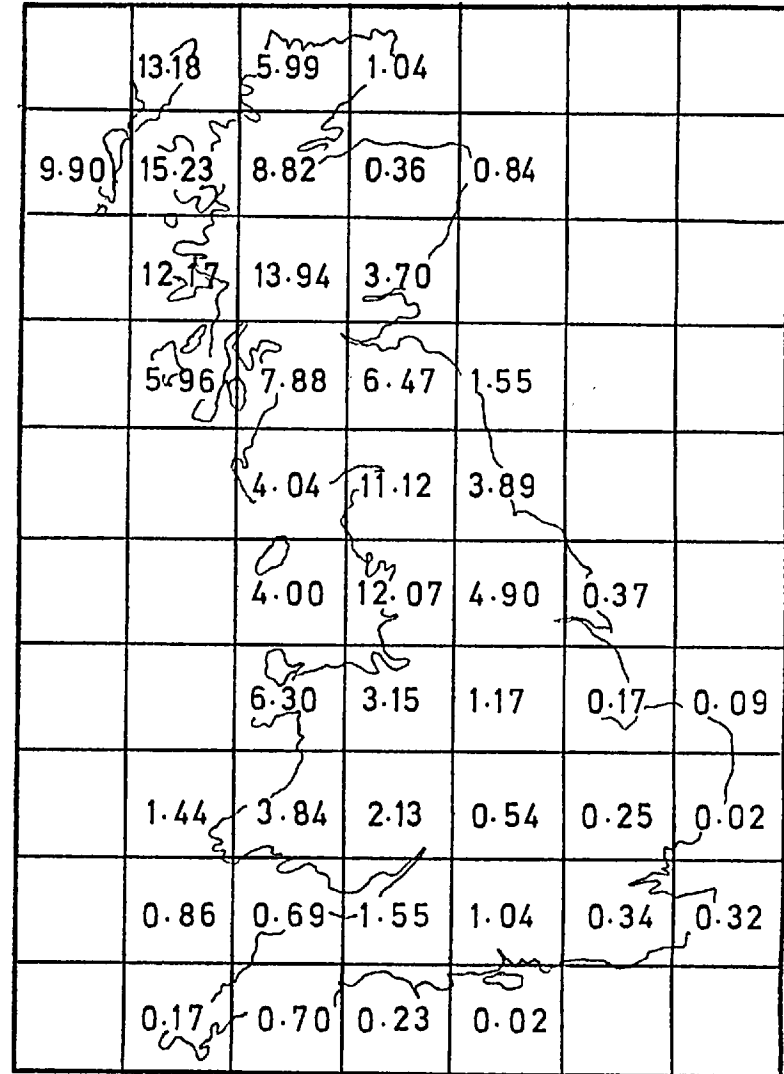
The British Isles lay in a west-south-westerly airstream between a ridge over Biscay and a depression south of Iceland. Most areas experienced some showers, but they were heaviest in the north of Britain, and continued throughout the night in many places. The 24 hour rainfall totals (figure 2.11) show a high degree of correlation between rainfall and elevation, most notably over the western Pennines and the Lake District. Small features are also of interest: the shower-free region around the coast of Devon and Cornwall; the apparent influence of the Chilterns (but not the Cotswolds) on the rainfall distribution and the lower rainfall totals recorded in Scotland compared with northern England. The mean areal values (figure 2.11) give a fairly good impression of the spacial distribution of the showers. The totals of 12 - 15 mm in parts of north-west England and western Scotland are likely to have resulted from several light showers, rather than a few isolated but persistent storms, and the original rainfall data confirm this.

Figure 2.11 suggests an orographic lifting effect with enhanced convection over the windward slopes of the hills, and we may expect this to be reflected in the upper-air soundings from the eastern and western sides of the country. All the British radiosonde stations, however, are situated near the coast; this means that there is no real 'lee' site when winds are westerly. Figure 2.12 shows the midday and midnight soundings for Long Kesh and Shanwell. The differences between the midday soundings are not particularly striking, but they do suggest the possibility of

FIG. 2.11



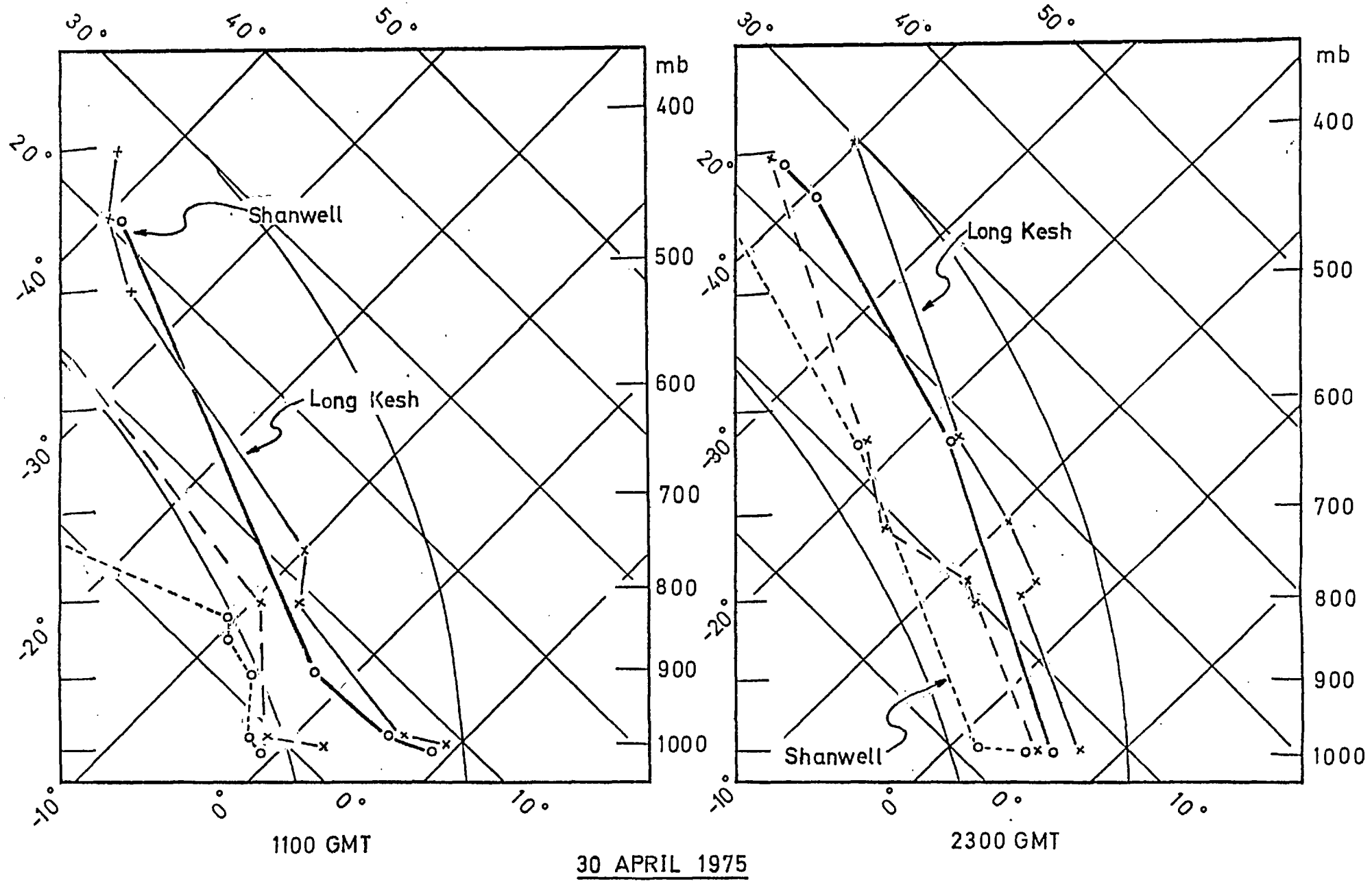
0, 10 and 25 mm isohyets



24 hour areal rainfall (mm)

30 APRIL 1975

FIG. 2.12



cumulonimbus convection up to 500 mb at Long Kesh and only cumulus convection reaching about 800 mb at Shanwell, above which level the air is drier and the lapse rate becomes less than the wet-adiabatic. The midnight Shanwell sounding, however, shows features typical of air in which cumulonimbus convection has taken place, and reference to the surface observations indicates that showers did occur near both stations. The soundings also suggest a higher cloud base in the east, and the surface observations generally show higher values of  $(T - T_p)$  in the lee of the hills.

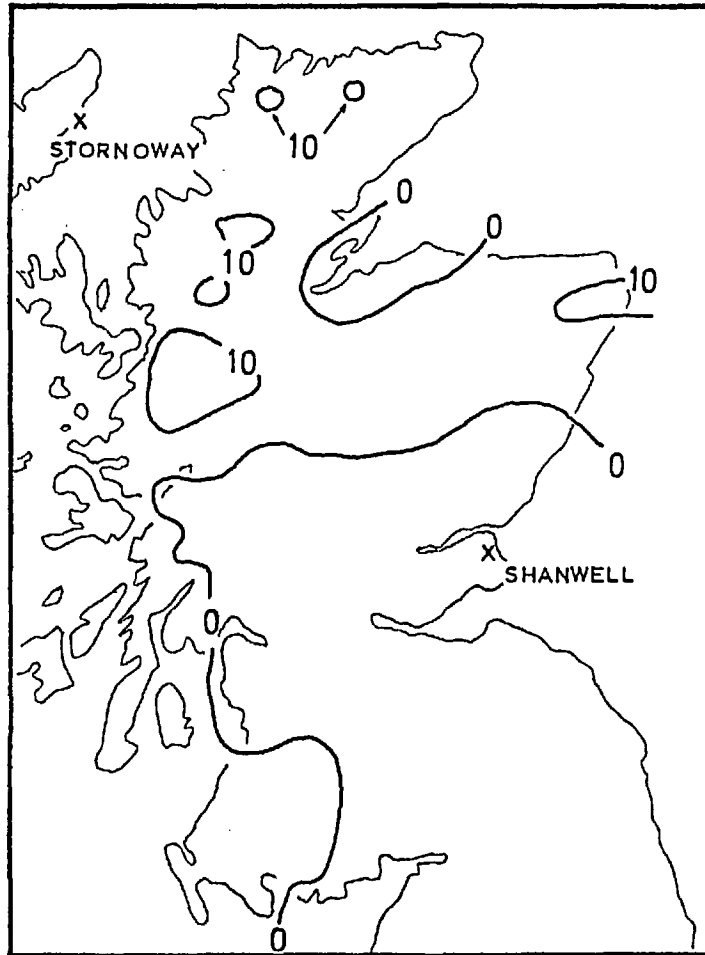
20th October, 1974

On this occasion the British Isles was affected by a showery, north-westerly airstream. The rainfall maps for Scotland (figure 2.13) clearly show the distribution of showers, which were most frequent on the north-west side of the high ground, while areas in the lee (the Moray Firth and south-eastern Scotland) remained dry. The distribution is well represented by the areal rainfall map.

The differences between the midday soundings from Stornoway and Shanwell (see figure 2.14) are remarkably small, considering the contrasting surface observations: Stornoway reported slight showers throughout the day, from cumulonimbus with a base at about 450 to 500 m, while Shanwell remained dry with cumulus and stratocumulus (bases near 750 m and 1500 to 3000 m respectively). The inversion reported from Stornoway suggests that the convection did not penetrate above 820 mb or so, but in fresh maritime air a cloud thickness of 1 km is usually just enough to produce showers. The Shanwell ascent appears rather unstable, and



FIG. 2.13



0 and 10 mm isohyets

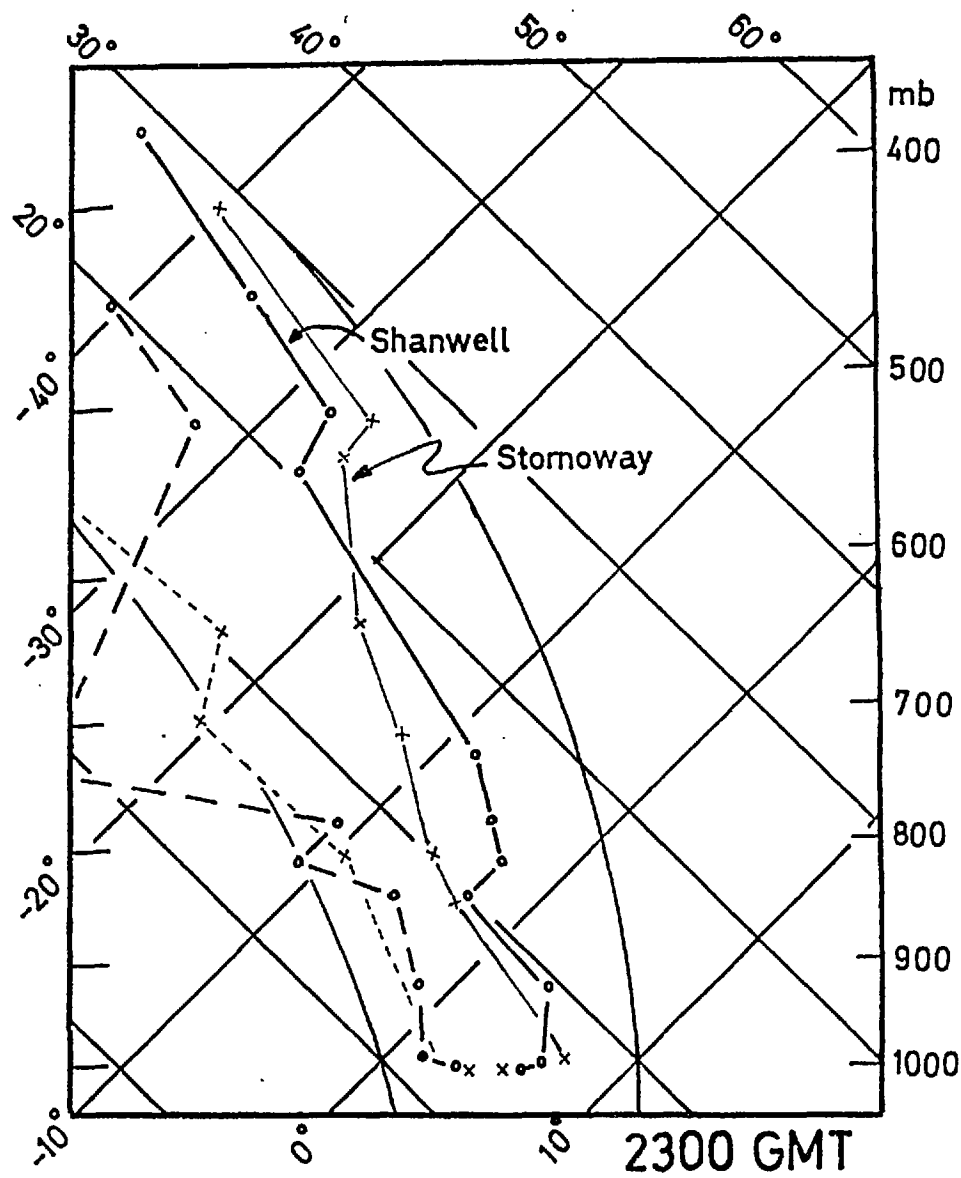
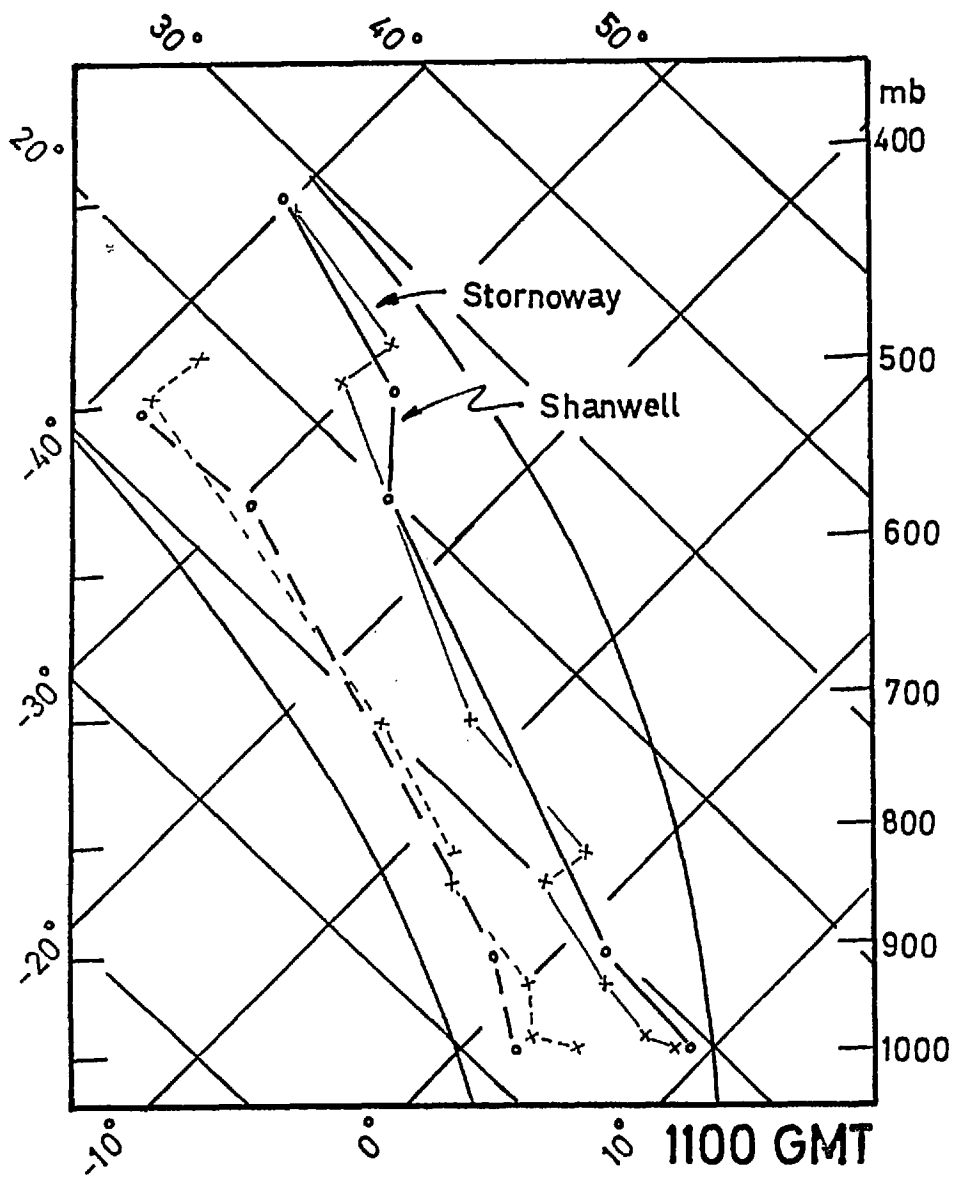
	4.75	5.76	2.81			
3.90	4.60	5.71	3.08	6.88		
	4.29	1.25	0.31			
	4.87	0.89	0.19	0.34		
		2.18	0.42	0.41		
		5.03	2.49	0.39	1.12	
		8.22	10.34	1.34	0.27	1.20
	0.82	9.42	4.11	1.93	0.21	0.39
		2.83	1.46	0.64	1.16	0.38
	4.75	5.43	1.51	0.60		

24 hour areal rainfall (mm)

20 OCTOBER 1974

Temperature soundings for 20 October 1974.

FIG. 2.14



it is perhaps surprising that no showers occurred here. Once again, the soundings for midnight on 20th/21st October are likely to be more representative of the day's convection, and indeed figure 2.14 shows a more stable structure for Shanwell which may be partly attributable to descent in the lee of high ground.

### Summary

In this chapter we have attempted to describe various aspects of shower rainfall under drastic simplifying assumptions, bearing in mind the requirement of qualitative and quantitative forecasting. It has been shown that characteristic stratifications typical of cumulonimbus convection exist, and that they may be of some use in prediction, at least over the oceans, where there is less variation in the microphysical conditions. In maritime airstreams, the quantity of shower rainfall over a large area (a factor which may be of use in hydrological studies) appears to be highly correlated with a simple parameter of the large-scale flow, and again is likely to have some predictive value. Finally we have considered the topographic mechanisms which complicate the distribution and intensity of showers.

CHAPTER III : STATIONARY CUMULONIMBUS

The remainder of this thesis is concerned with a particular class of cumulonimbus convection, the stationary (or slow-moving) local storm. This study was prompted by the Hampstead (north-west London) storm of 14th August 1975, which will be discussed in detail in chapter IV. In this chapter we shall consider several past examples of this phenomenon, together with the meteorological conditions in which they occurred, in an attempt to identify some general characteristics. The chapter includes a short discussion of certain aspects of the influence of a large urban area on cumulonimbus clouds\*.

In chapter I the factors which lead to the intensification and prolongation of cumulonimbus were outlined. Simplified models of severe mid-latitude storms include an appreciable vertical wind shear throughout the troposphere, with the convective system propagating relative to the ground with a speed close to that of the wind in the mid-troposphere. Sometimes persistent, organized storms become stationary or slow-moving, often near a prominent topographical feature (the influence of topography on cumulonimbus convection in general has been discussed in chapter II; its possible influence in the case of stationary storms will be dealt with in chapter IV). Although the intensity of precipitation associated with the severe storm may be no greater than that

\* This and subsequent chapters contain references to a number of locations in and around Greater London. A map is given on p. 83.

of the 'ordinary' cumulonimbus, its continuation for more than an hour or so can have very serious effects over small areas, with particularly disastrous consequences for hill or riverside communities.

According to the 'steering-level' model, an obvious requirement for a mid-latitude storm to remain stationary relative to the ground may be that the wind in the lower troposphere (or at least a component) should be opposed to that in the upper troposphere, so that the wind becomes small at the steering-level. This condition is likely to be satisfied on the poleward side of cyclonic circulations; here the vertical wind shear is typically  $1 \text{ m sec}^{-1} \text{ km}^{-1}$  with the surface wind in the opposite direction to the upper-level westerlies. Some stationary storms in Britain have been associated with depressions of varying intensity over the English Channel or northern France, with the cumulonimbus developing over some prominent ground feature. It seems that these storms are often of only moderate intensity (although persisting for several hours) and produce little or no hail at the ground; they occasionally occur at night (suggesting that perhaps a local heat source is not always an important factor) and may be obscured by middle-level or low-level cloud. For these reasons they have often not been recognized as cumulonimbus, and the rainfall associated with them has been termed 'cyclonic'. The first group of examples given below fall into this category, and instances are quoted from the USA and France as well as southern Britain. In order to distinguish this type of storm from other forms of stationary cumulonimbus, we have given it the title "stationary mid-latitude"; although a rigorous definition has not been

given, it is hoped that its general characteristics will become apparent from the following examples.

### 3.1 STATIONARY 'MID-LATITUDE' CUMULONIMBUS

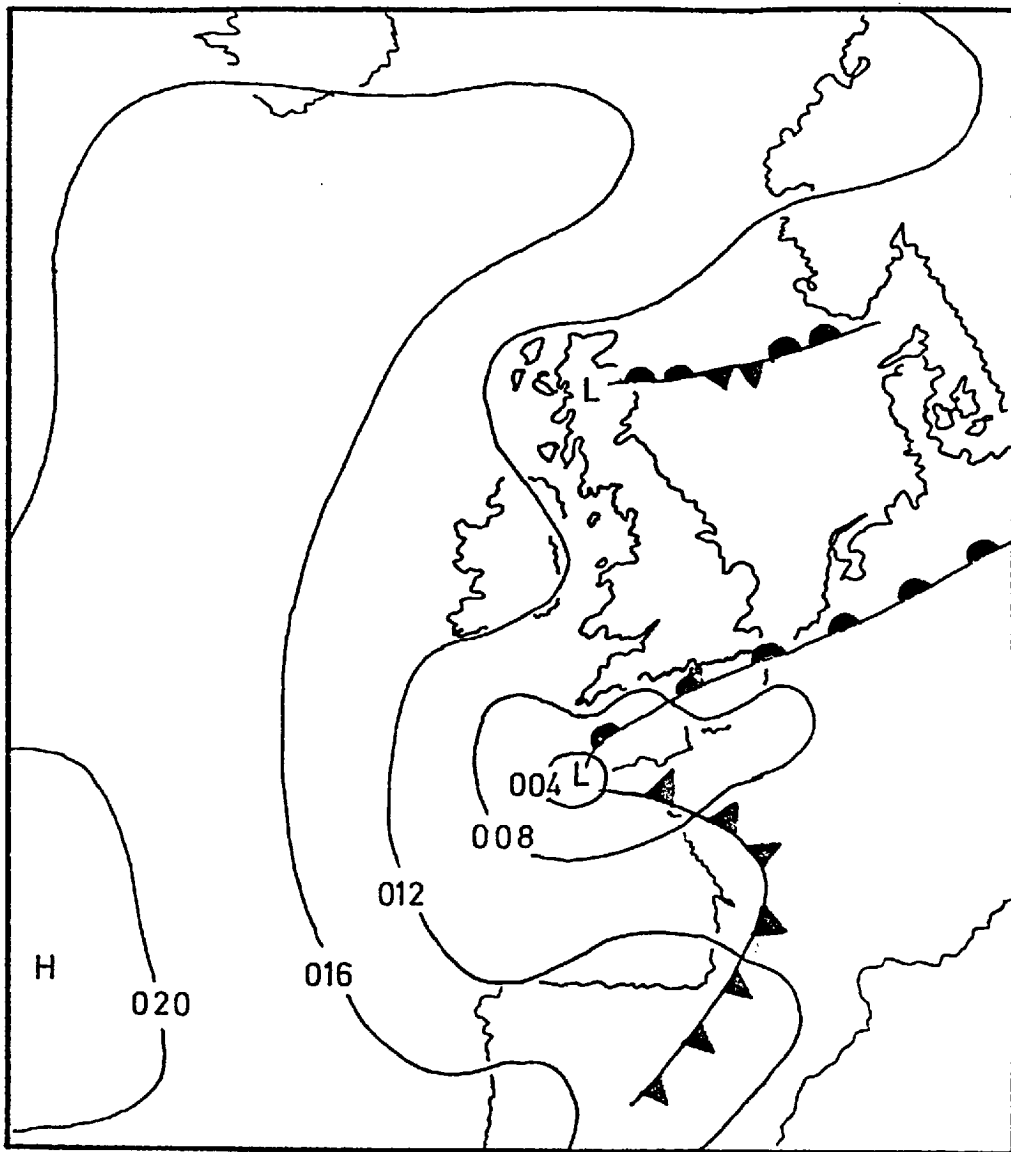
Many examples of prolonged rainstorms have been reported from the USA, most of which were associated with a supply of potentially warm air from the south or south-east below westerly or north-westerly winds in the upper troposphere. These storms will not be discussed in detail here; the reader is referred to accounts by Lautzenheizer and Fay (1966), Richardson et al. (1964), Sayers-Duran and Braham (1965), Carlson (1967), Jetton and Woods (1967) and Dightman (1968). In most cases the heavy rainfalls have occurred near a prominent topographical feature, yet distinctly on the windward side of the obstacle, so that the rain cannot be immediately associated with the ascent of air up a hillslope. One area to the west of a plateau in Texas has experienced several very heavy falls of rain, of which the most remarkable was recorded during a 35 hour period in September 1921, when, according to McAuliffe (1921), rain began at about 0330 local time on the 9th. The period of heaviest rainfall occurred later that day, when from 1845 to 2142 a total of 10.5 inches was recorded.

- (i) Sourbeer and Gentry (1961) describe a persistent storm over Florida in January 1957, which remained stationary near West Palm Beach for about 14 hours and produced 21 inches of rain at three locations in the area. Synoptic charts show low-level south-easterly winds below a strong upper jet from the north-west.

By comparison with those in the USA, storms in Britain

and western Europe are considerably less impressive, but it should be remembered that the southern United States is close to a very large supply of potentially warm air from over the tropical oceans; in Europe, however, the low-level energy arises from the day-to-day solar heating of air over land, and is therefore limited.

- (ii) The most prolonged thunderstorm ever recorded in Europe began near St. Malo, north-west France, on 15th September 1929. The storm continued virtually without a break for almost 2 days, and the total rainfall on 17th September amounted to 25 cm (Lazarus, 1930). The sequence of surface charts for the period show a depression moving slowly across central France, with a cool north-easterly airstream persisting over the north-western part of the country. An associated warm front lay almost stationary in a north-east/south-west orientation, and the horizontal temperature gradient suggests that upper-level winds would have been south-westerly and moderately strong.
- (iii) The Lynmouth storm (Bleasdale and Douglas, 1952) gave rise to some of the most serious flooding ever experienced in Britain, producing as it did a maximum point rainfall of about 10 inches over the high ground of Exmoor; most of the rain fell in a 7 hour period beginning at 1630 GMT. Figure 3.1 shows the surface chart a few hours before the storm started, with a depression moving eastwards over the English Channel, supplying potentially warm air from the south-east at a height of about 2 km above cool north-easterly winds near the surface. Upper air data indicate south-westerly winds at higher levels, and a mean tropospheric wind shear



Met. Office Surface Analysis

06 GMT 15 August 1952

FIG. 3.1



of about  $1 \text{ m sec}^{-1} \text{ km}^{-1}$ .

(iv) On 6th August 1956 a prolonged hailstorm occurred at Tunbridge Wells, Kent (Booth, 1956 and Botley, 1956). Small hailstones fell continuously for about  $1\frac{1}{2}$  hours, and resulted in choked drains, blocked roads and considerable crop damage. At low levels the wind was north-easterly (associated with a weak depression over France) veering to south-south-westerly in the upper troposphere with a mean shear of about  $1 \text{ m sec}^{-1} \text{ km}^{-1}$ .

(v) Rainfalls of over 80 mm were recorded in parts of south-east England on 20th/21st September 1973. The synoptic situation was similar to that during the Lynmouth storm, with an eastward-moving depression over northern France supplying warm air from the north-east or east. The storm started late on the 20th and persisted well into the night as the low-level winds increased in strength. Above 3 or 4 km the wind became southerly, and again the mean shear was about  $1 \text{ m sec}^{-1} \text{ km}^{-1}$ . Only a rather small available potential energy is evident from the Crawley temperature sounding.

### 3.2 OTHER STATIONARY STORMS

Inspection of past weather records reveals that not all prolonged storms are associated with an opposition of lower and upper level winds. Furthermore many seem to occur in locations where there are no significant topographic features, yet their confinement to a very small area is a striking characteristic. Their typical duration is a few hours (perhaps as much as an order of magnitude less than the 'mid-latitude' type of stationary storm) and they are

sometimes noteworthy for the production of large amounts of hail.

- (vi) In the late afternoon of 3rd June 1959 a hailstorm began at Selden in north-western Kansas, USA (Robb, 1959). At first there were strong gusts of wind, and the hail broke many windows. Although the wind soon quieted, the hail continued to fall incessantly for about 85 minutes. An elongated area was affected, 9 miles long (in a north-east/south-west direction) and 6 miles across at the widest point; hail accumulated to a depth of 18 inches and was pea or marble size, many of the stones being soft. In addition to the large quantity of hail, the total rainfall was estimated at between 3 and 5 inches. Synoptic charts indicate a south to south-westerly flow over Kansas and a marked upper trough. Upper winds were fairly light, being southerly,  $3 \text{ m sec}^{-1}$  at 850 mb and westerly  $10 \text{ m sec}^{-1}$  at 250 mb. It is interesting that the surface terrain in this part of north-west Kansas is remarkably uniform.
- (vii) Huff and Changnon (1964) describe an unusual storm which affected southern Illinois, USA, on 16th/17th August 1959. A dense rain gauge network and radar data were used in their analysis and showed that the storm was composed of several groups of cumulonimbus or 'squall lines' which moved across the area from the north-west. During their passage, five of the six individual storms travelled at less than  $5 \text{ m sec}^{-1}$ , and prolonged rainfall resulted; 16-hour totals of up to 270 mm were recorded.
- (viii) Two storms at Camelford, Cornwall on 8th June 1957 gave a total rainfall of about 200 mm; about 140 mm fell

between 1230 and 1500 GMT (mostly in the first hour), with a later storm between 1700 and 1800 GMT (Bleasdale, 1957). A considerable amount of small hail fell with the early precipitation, much of which became congealed and was washed about by flood water. The storms occurred over the windward slopes of Bodmin Moor (affecting an area of about 200 km<sup>2</sup>) in a showery south-westerly airstream, and the role of topography as an obstacle is more plausible in this case, with a fairly small wind shear (less than about 0.5 m sec<sup>-1</sup> km<sup>-1</sup> throughout the troposphere).

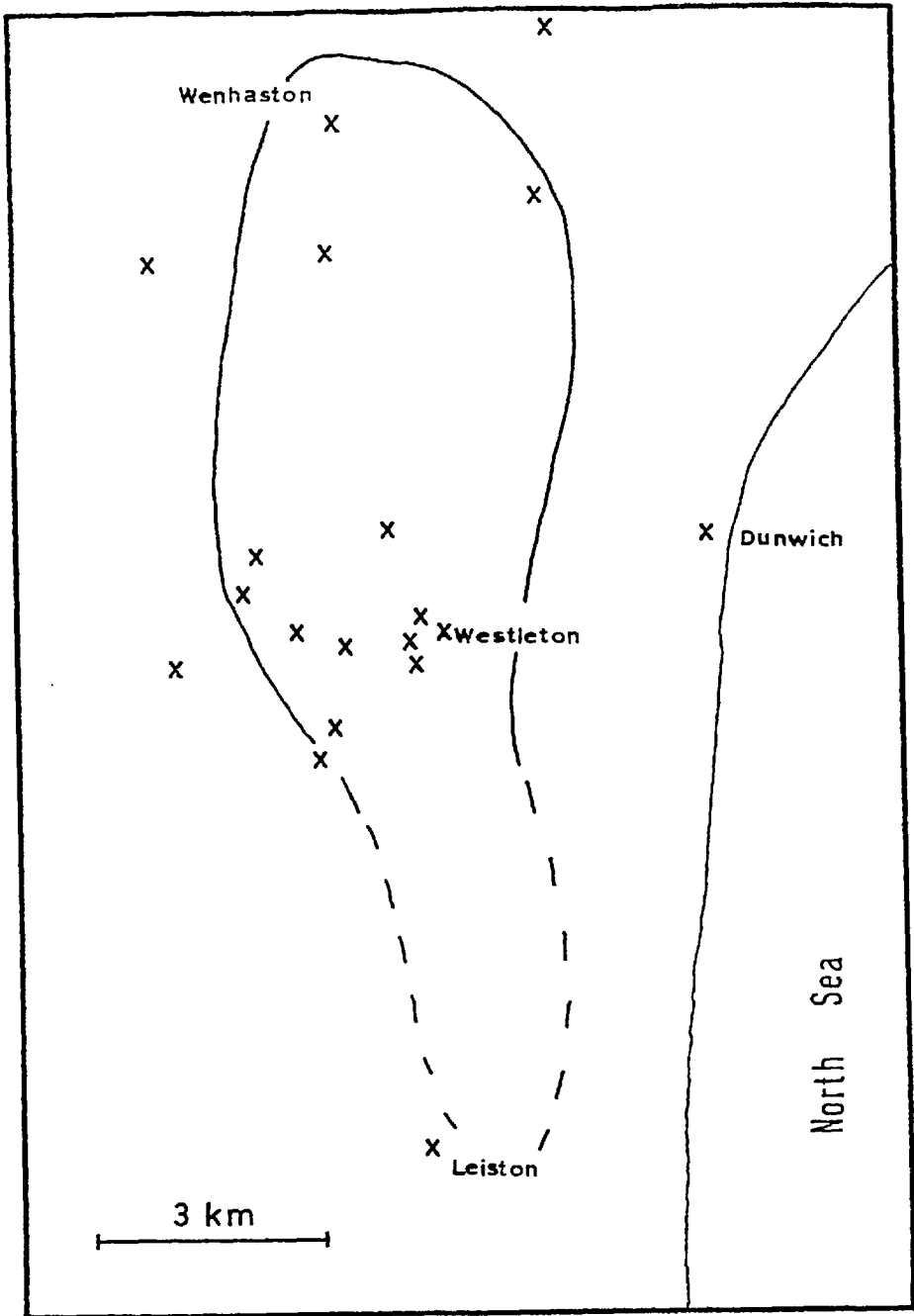
(ix) On 6th August 1952 a severe storm affected parts of north Middlesex and Hertfordshire which gave over 120 mm of rain at Boreham Wood, much of which fell in a 90-minute period (see 'Meteorological Magazine', vol. 81, pp. 302 - 305). There was a line of surface convergence over the area between light southerly and north-easterly winds; above the surface, winds were light (less than 5 m sec<sup>-1</sup>) up to 3 or 4 km, and subsequently south-westerly, with a shear between 3 km and 10 km of about 12 m sec<sup>-1</sup>. No report mentioned hail, and simple parcel theory applied to the available aerological data suggests an updraught of less than 30 m sec<sup>-1</sup>.

(x) The Hampstead storm (14th August 1975) broke out near the convergence between a weak south-westerly airstream and warm continental air from the south-east. Heavy rain fell for nearly 3 hours and caused serious flooding, yet an area of only about 100 km<sup>2</sup> was affected. Chapter IV discusses the storm in detail.

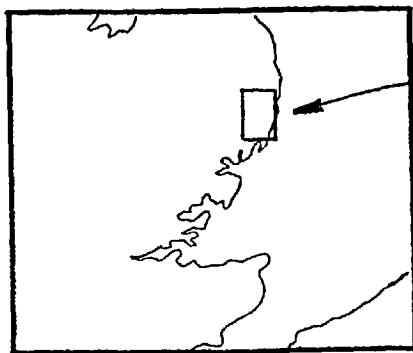
(xi) The Mill Hill storm of 1963 is also considered in

more detail later in the thesis because of its similarity with the Hampstead storm; although the maximum point rainfall was 94 mm (compared with 170 mm at Hampstead), the tropospheric wind shear was also moderately small, and the direction of upper and lower winds differed by about  $90^{\circ}$ . Only one report of hail was found, although the available potential energy was rather large, suggesting updraughts of about  $40 \text{ m sec}^{-1}$ .

- (xii) A severe storm over northern Oklahoma, USA, is described by Merriott et al. (1974). On 10th October 1973 rainfalls of up to 20 inches were produced in a narrow swath between 10 and 40 miles wide. The storm began in the late afternoon, and over 12 inches of rain fell in the first 4 hours of its 12 to 14 hour duration. The cost of flood damage in the area was estimated at \$54 million. The authors describe the most outstanding feature of the storm as the formation of a "stationary and well-defined region of convective activity wherein individual cells formed repeatedly and moved northward, reaching maturity . . . as they passed over the Enid area". The storm occurred near a slow-moving surface front, ahead of a southerly flow of warm, moist air from the Gulf of Mexico. Upper winds were south-westerly, reaching maximum speeds of about  $40 \text{ m sec}^{-1}$ ; individual cell speeds were as high as  $25 \text{ m sec}^{-1}$ .
- (xiii) Around dawn on 23rd September 1976 a severe hailstorm affected a small area of Suffolk between Saxmundham and Southwold (see figure 3.2). According to press reports the village of Westleton was cut off for several hours as a result of both flood water and drifts of hailstones. On



Locations of reports (x) and boundary of hail-affected area (southern limit uncertain)

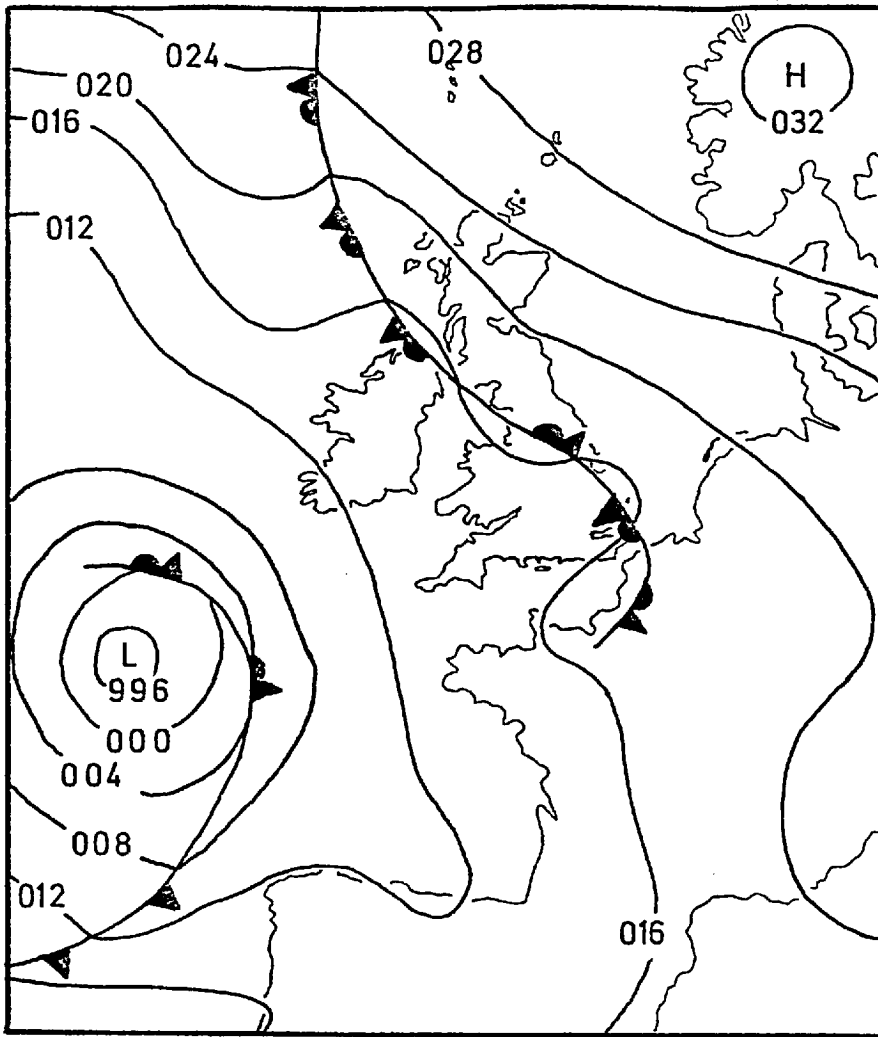


Position of above map

FIG. 3.2

28th September a tour of the area was made, with the intention of establishing more accurately the spatial extent and duration of the storm. It soon became evident that the area affected by hail was remarkably small with quite well-defined edges; Westleton itself was very close to the eastern limit. Many residents were interviewed (at locations indicated in figure 3.2), and it was possible to determine the approximate extent of the hail area, which was only 15 km long and about 5 km across at the broadest point. Many people in the district were awakened by thunder at about 0500 (all times are BST), but no hail fell until about 0600. Hailstones were over 2 cm in diameter and continued falling for nearly 1 hour; the storm itself, with heavy rain, did not cease until about 0730. Crops suffered considerable damage; fruit was badly bruised and leaves were shredded. Hail had lain up to 1 ft deep in places, with drifts of 3 or 4 ft where it had been washed up against walls or fences by the floodwater. The storm evidently moved over the area from the south, but no-one interviewed was aware of any strong winds at the time, and rain and hail apparently fell vertically.

At 00 GMT on 23rd September a depression off south-west Ireland was moving slowly eastward (see figure 3.3). The surface analyses marked an occluded front lying almost stationary across Britain, which evidently marked a confluence between south-easterly continental air and cooler air to the south-west. This front may have moved slowly across the area during the early hours of the 23rd; there was certainly a marked change in the upper-level winds at Hemsby (40 km to the north-north-east), which became light south-westerly



SURFACE 00 GMT 23 SEPTEMBER 1976

FIG. 3.3

by 06 GMT having been strong (up to  $28 \text{ m sec}^{-1}$ ) southeasterly at 00 GMT.

In an attempt to summarize the characteristics of stationary or slow-moving storms, table 3.1 has been compiled which lists the principal features of examples of both types of cumulonimbus. Those entries which are not self-explanatory are referred to below. It is hoped that upper-air data included in the table are as representative as possible, but it should be remembered that the nearest radiosonde station to some of the storms in the USA were up to 300 miles distant.

The fallspeed of hailstones uses the formula given by Browning et al. (1963). The vertical velocity near the equilibrium level of the simple parcel theory is given by  $w = \sqrt{2 \times \text{available potential energy}}$ .

The 'vertical wind shear' gives the difference in direction between lower and upper winds, and so is a relative, not an absolute vector. The 'resolved wind shear' gives the magnitude of the vertical shear when the environmental winds are resolved in the direction of the wind at the equilibrium level. The shear between the ground and the equilibrium level is denoted as  $\Delta U$ .

The mean Richardson number is defined as

$$(-\overline{Ri}) = \frac{\text{available potential energy}}{\frac{1}{2} (\Delta U)^2}$$

It was mentioned in chapter I that the Richardson number has been found to be a useful parameter of the large-scale flow in which cumulonimbus may develop. Efficient conversion of available potential energy in a well-organized, persistent



TABLE 3.1

	(i) Florida 21 Jan 1957	(iii) Lynnouth 15 Aug 1952	(iv) Turnbridge Wells 6 Aug 1956	(v) S.E. England 20 Sept 1973	(vi) Selden 3 June 1959	(vii) Illinois 16 Aug 1959	(viii) Camelford 8 June 1957	(ix) Boreham Wood 6 Aug 1952	(x) Hampstead 14 Aug 1975	(xi) Mill Hill 7 June 1963
Maximum point rainfall (mm)	546	230	34*	86	~100*	270	200	120	171	94
Duration of storm (hours)	~18	~7	1.5	few hours	1.5	~16	2.5 (1st storm)	2	2.5	2
Maximum measured rainfall rate (mm hr <sup>-1</sup> )	60 (in 2 hrs)	50 (in 6 min)	-	-	-	70 (in 1 hr)	100 (in 1 hr)	100 (in 30 min)	125 (in 10 min)	100 (in 35 min)
Maximum hailstone diameter (cm)	no report	none reported	1.6	none reported	2	+	1	no report	3	no report <sup>†</sup>
fallspeed in upper troposphere (m sec <sup>-1</sup> )	-	-	28	-	30	-	22	-	38	-
Simple Parcel Theory: θ <sub>s</sub> in updraught (°C)	20	15	12	15	19	24	13	18	18	15.5
maximum temperature excess (deg C)	6	3	2	3	5	4	4	3	4	3
H - height of equilibrium level (km)	10.6	7.2	7.9	7.2	10.6	11.1	8.7	10.6	10.4	10.3
positive area (available potential energy, m <sup>2</sup> sec <sup>-2</sup> )	1415	280	300	370	860	1255	900	675	680	870
vertical velocity near equilibrium level (m sec <sup>-1</sup> )	53	24	24	27	40	50	42	37	37	40
Vol. of inflow (degrees, m sec <sup>-1</sup> )	110,10	015, 7	020, 3	030,10	205, 3	180, 4	190, 7	080, 4	130, 3	090, 5
Vol. of wind at equilibrium level (degrees, m sec <sup>-1</sup> )	320,43	175, 8	195,15	145,11	260, 9	235,22	200,17	205,15	215,17	180,16
Vertical wind shear (degrees, m sec <sup>-1</sup> )	200,52	160,15	175,18	115,23	060, 8	055,25	010,10	125,19	085,18	090,17
Resolved wind shear (m sec <sup>-1</sup> ) ground → 5 km	13	9	9	15	5.5	5	1	10	10	6
ground → equilibrium level (ΔU)	50	15	18	18	7.5	20	10	19	18	16
Mean Richardson number (-Ri)	1.1	2.5	1.8	2.3	~30	6.2	18.0	3.8	4.2	6.8
Predicted motion: H/H <sub>0</sub>	1.5	1.0	1.1	1.0	1.5	1.5	1.2	1.5	1.4	1.4
steering level (z*, km)	4.2	3.7	3.9	3.7	6.7	5.9	5.6	5.2	5.2	5.7
propagation speed (m sec <sup>-1</sup> ) in direction of resolved winds	+5.0	+0.6	+5.0	+2.0	+9.0	+7.0	+8.0	+5.0	+8.0	+6.0

Notes: \* Rainfall total does not include hail

† Hail reported, but no size given

‡ One press report of "giant" hail

cumulonimbus takes place when  $-\overline{Ri}$  approaches 1: then the buoyancy is appropriately matched to the windshear. For larger values of  $-\overline{Ri}$  the convection is generally more intermittent and impulsive.

The entries under 'predicted motion' refer to the theory of cumulonimbus propagation developed by Moncrieff and Green (1972). They considered an idealized dynamical model of steady two-dimensional convective overturning, in which integration of the vorticity equation led to the determination of a steering-level for the system in terms of a Richardson number and a density scaling parameter. The steering-level in turn defined a propagation speed, which compared very favourably with the movement of actual storms in a number of case studies. Since they applied the results of a two-dimensional model to a three-dimensional atmosphere, the available kinetic energy ( $\frac{1}{2}\{\Delta U\}^2$  in the expression for the Richardson number) was obtained from the wind component parallel to the direction of motion of the storm. In our application this is, of course, not possible; instead we have taken components in the direction of the wind at the equilibrium level of the parcel theory.  $H_0$  is the density scale height of the atmosphere, and is equal to 7.3 km.

Table 3.1 serves to emphasize the distinctions between the two types of stationary storm. The mid-latitude type is characterized by a Richardson number close to 1, with rather smaller values of available potential energy. Their motion (or lack of it) is accounted for fairly well by the steady, two-dimensional theory; storms (iii) and (v) have very light

winds at their steering-levels, and the value of  $5 \text{ m sec}^{-1}$  for the Tunbridge Wells storm (iv) is acceptable, since it implies a movement of only about 25 km during the lifetime of the storm. The Florida storm (i), however, is exceptional in many respects, and the predicted propagation velocity of  $5 \text{ m sec}^{-1}$  towards the east is unsatisfactory if the storm is to be regarded as a single system. It may be that more careful examination of the upper wind data is required, since in a situation where the vertical shear is as great as  $5 \text{ m sec}^{-1} \text{ km}^{-1}$ , the steering-level must be determined with considerable accuracy.

The behaviour of the other type of storm (numbers (vi) to (xi) ) cannot be accounted for by the steering-level model. They are characterized by rather higher values of  $(-\overline{Ri})$ , having generally larger available potential energies than those of the mid-latitude type. The most fundamental difference appears to be in the environmental wind field which is clearly of a three-dimensional nature, and, since upper and lower winds are not in opposite directions, the resolution of the wind field in this direction is not of immediate significance.

It is evident that a fundamental difficulty arises in applying the theoretical results of Moncrieff and Green to stationary storms, because there is no obvious direction in which to take a two-dimensional projection. Clearly we can select any level in the atmosphere, resolve the wind field in a direction perpendicular to the wind at that level, and immediately obtain there zero wind relative to the ground; this level could easily be chosen close to the steering-

level of the convective system. With any given orientation of upper and lower winds we can select a direction along which the value of  $\Delta U$  becomes zero, and hence the Richardson number becomes infinite. It would seem reasonable, therefore, to select the direction perpendicular to this for the evaluation of  $(-\overline{Ri})$ ; in the case when upper and lower winds are in opposite directions this is, of course, equivalent to resolving along the upper wind direction. In later chapters we shall suggest that the circulation of these storms is indeed three-dimensional, and that the vector wind shear plays a crucial role in maintaining the convective system.

### 3.3 URBAN INFLUENCES ON CUMULONIMBUS

Chandler (1965) referred to the overall "comparative lack of literature on the climatic implications of the urban sprawl". Since then there has been a considerable increase in research into the effects on the environment of urbanization, but the influence on convective precipitation is not easy to isolate. Differences in rainfall between cities and surrounding rural areas are much less obvious than other urban effects, such as increased temperatures or reduced visibility, so that a meaningful study would require a dense raingauge network, not only in the city but also in the environs, operating over a long period without changes in site or exposure. Added to this is the overall complexity of the processes involved in precipitation; in general the uniqueness of each urban site makes it very difficult to transpose results from one location to another.

Most writers list four possible mechanisms whereby

precipitation could be influenced by an urban area: (i) higher temperatures near the surface; (ii) higher humidities (as a result of industrial processes); (iii) higher pollution levels which may be associated with a greater number of available condensation nuclei; and (iv) a greater degree of turbulence near the surface due to city buildings. While all these symptoms of urbanization have been identified and measured, it is by no means clear in what way each may influence the amount of precipitation; for example, as Gunn and Phillips (1957) pointed out, for a given amount of water vapour, the greater the number of condensation nuclei, the less chance each drop has of growing, and consequently cloudiness rather than rainfall is characteristic of highly polluted air masses.

In the USA most studies have been climatological, in that precipitation statistics of various forms were analyzed in attempts to show spatial variations of rainfall in and around a given city over a number of years. Considerable interest in this field was aroused by data from La Porte near Chicago (Changnon, 1968). During the period 1951 - 1965, La Porte (situated 30 miles east of the large industrial complex on the southern shores of Lake Michigan) experienced 31% more precipitation, 38% more thunderstorms and 246% more 'hail days' than surrounding weather stations. The author discusses the opposing arguments that the increase may be either fictional (resulting from changes in instrument exposure or observer error) or genuinely resulting from urban effects. He ultimately decides in favour of the latter, but makes only passing reference to the topographic factors involved, which, in view of the proximity of Lake Michigan,

may be of considerable importance.

Research in other American cities (Changnon, 1969 a and b) revealed apparent urban-produced increases (over the surrounding rural areas) of 5 to 16% in annual precipitation and 'rain days', and 7 to 20% in summer thunderstorm days. It was claimed that the four mid-west cities in the study were without orographic features which might have influenced the rainfall distribution. A later paper (Huff and Changnon, 1973) examined historical weather records of eight American urban areas. The six largest cities experienced increases of between 9 and 17% in seasonal rainfall during the period 1955 - 1970, and significantly higher frequencies of summer 'thunder days' (up to 41% higher) and 'hail days' (90 to 450% higher), these differences being predominant in the morning hours. The increases in precipitation were found to be due to enhancement, rather than initiation, of moderate or heavy rains, and the typical locations of maxima were, for thunder, over and near the city and, for rain and hail, between 25 and 55 km downwind. The results also suggest that the degree of precipitation enhancement was related to city size.

Research in the USA culminated in project METROMEX, an intensive observational programme on the interaction between urban areas and climate; several articles reviewing the results appear in 'Bull. Amer. Met. Soc.', vol 55, number 2 (February 1974).

A case study approach was used in the USA by Harnack and Landsberg (1975). They examined historical precipitation data for the years 1968 - 1972, and extracted days on which the rainfall distribution was highly localized in or downwind

of the city of Washington. All available observations were then employed in order to explain the rainfall patterns. A "prediction area" of precipitation was computed for each occasion by first applying the parcel theory to air rising over the city to give a mean updraught speed. Assuming initial droplet radii of  $40\mu\text{m}$ , the minimum cloud depth necessary for precipitation by coalescence was calculated, and finally upper wind observations were used to determine the horizontal advection of cloud during precipitation. There was encouraging agreement between observed and 'predicted' rainfall distributions, and the authors conclude that the urban thermal effect on precipitation is real (the selected case studies were days of isolated storms in or near the city).

Studies in Britain and Europe were confined at first to urban influences on single thunderstorms, although precipitation anomalies were first postulated by Schmauss (1927), who found an 11% increase in mean annual precipitation for the eastern (downwind) part of Munich. Case studies in Britain were carried out by Parry (1956) and Barnes (1960), who dealt with storms over Reading and the east Midlands respectively. Barnes suggested a correlation between rainfall and urban area during a thundery outbreak in 1952, relating not to initiation, "but to some influence on the course of development of mature cells initiated 10 to 12 miles from the rainfall maxima". Parry, on the other hand, believed the urban influence in his study to be one of initiation, the local heat island (with a magnitude of about 4 deg F) being responsible for "touching off the convective mechanism of the rainstorm".

A more climatological approach was made by Atkinson (1968), who examined the distribution of thunder rainfall over south-east England during the period 1951 to 1960. Despite the difficulties inherent in the definition and identification of 'thunder' precipitation, the author suggests a real urban effect on the rainfall distribution, with a frequency of thunder of 10 to 12 days per year over much of the London conurbation, compared with typical values of 6 to 8 days for the surrounding countryside. It seems possible that this higher frequency may have resulted from a higher density of observers in the built-up area, but Atkinson claims that the audible range of thunder together with the remarkably high number of observers in the environs of London, mean that all the storms occurring in the region during the period would have been noted by at least one station.

Further analysis of these data (Atkinson, 1969) led to the conclusion that the urban maximum was due to about ten summer storms out of a total of over 600 which occurred over south-east England during the period in question. Case studies (e.g. Atkinson, 1971) examined the urban effect in more detail, and revealed both initiation and intensification over the London area. The author concludes that the urban effect is real, but only manifests itself in precipitation patterns when conditions are "just right".

The clearest manifestation of an urban effect on cumulo-nimbus convection appears to be the 'heat island' of high surface temperatures, and its presence will be apparent when the atmosphere is marginally unstable. In this role, cumulo-



nimbus may be initiated preferentially over the city; furthermore it is possible that such storms will have a longer duration than those away from the built-up area, having access to a larger supply of low-level warm air. It is not clear, however, that an urban area may influence the propagation of cumulonimbus, unless we postulate some interaction between the downdraught outflow and the increased surface roughness over the city. These ideas are considered later in the particular case of the Hampstead storm, where the behaviour of the downdraught is of crucial importance to the longevity of the system.

We conclude this chapter with some further examples of heavy, localized falls of rain in the vicinity of Greater London. They are treated separately because, at the time of their occurrence, synoptic weather data was either unavailable or unreliable; it is felt, however, that the graphic descriptions do yield useful information. Unless otherwise stated the source of all material was "British Rainfall" (published originally by the British Rainfall Organization, and latterly by the Meteorological Office).

1. 23rd June 1878

Over 3 inches of rain fell during two storms in the afternoon. The first, from 1332 to 1412 hours, gave rise to a five minute total of as much as 0.54 inches, and resulted in 2.32 inches in 40 minutes. No rain fell for 34 minutes, then a second storm from 1446 to 1502 gave 0.86 inches (all figures are for Camden Square, central London). The heavy rainfall was confined to north London; other totals recorded were 3.1 inches at Leyton and 2.86 inches at Camden Road.

2. 14th June 1914

More than 3 inches of rain fell in a narrow band, 18 square miles in area, extending from Richmond to Staines (a distance of about 10 miles). Fairgrieve (1914) produced 'rain-fields' which show the distribution of rainfall for every  $\frac{1}{4}$  hour during the storm. These suggest that isolated falls of rain occurred over London between 1015 and 1215; these subsequently increased in size and number, and, by mid-afternoon, rain affected south Wiltshire and Dorset. These maps are not quantitative, however, and no indication of intensity is given. A number of interesting eye-witness accounts appear in 'Meteorological Magazine' (1914), pp 110 - 112, and several storms are mentioned, each with heavy rain and sometimes hail. One description suggests rather impulsive convection: "Billowy masses were constantly rising out of it (the cloud tower) with rapid changes".

3. 6th May 1915

A very localized storm produced over 3 inches of rain between the city and Kings Cross. Bonacina (1915) described it as "the first heat thunderstorm of the season", and remarked on its long duration (about  $2\frac{1}{2}$  hours) and the absence of "the violent gust which so often springs up during a storm".

4. 16th June 1917

This storm began at about 1600 over north London and produced a very similar rainfall pattern to the previous example, with over 4 inches of rain near Kensington. Eye-witnesses ('Meteorological Magazine', vol 52, pp 61 - 63) describe how the storm "came up against the wind - that is

the vanes showed throughout N to NW - while the clouds moved or gathered from the south". The storm lasted for about 2¼ hours. (The rainfall of June 1917 was overshadowed by widespread heavy falls on the 28th. Much of the south of England was affected, and in the south-west the greatest 24 hour fall ever recorded (9.56 inches) was measured. Similarities with the Exmoor storm of 1952 are evident, with a small depression moving eastwards up the English Channel, and the heaviest rainfall occurring over high ground.)

5. 11th July 1927

For this occasion meteorological information is included in the descriptions of the storm, namely the existence of a shallow low pressure area over southern Britain with light south-easterly winds near the surface. The aircraft ascent from Duxford (about 40 miles north of London) suggests cloud condensation level at 550 m, and a temperature excess of about 5½ deg C up to 5 km. The storm over London was apparently slow-moving in a southerly upper current. Rain started at about 1345 (in South Kensington and Balham) and at 1430 (in Kings Cross and north-east London) and ceased between 1600 and 1630.

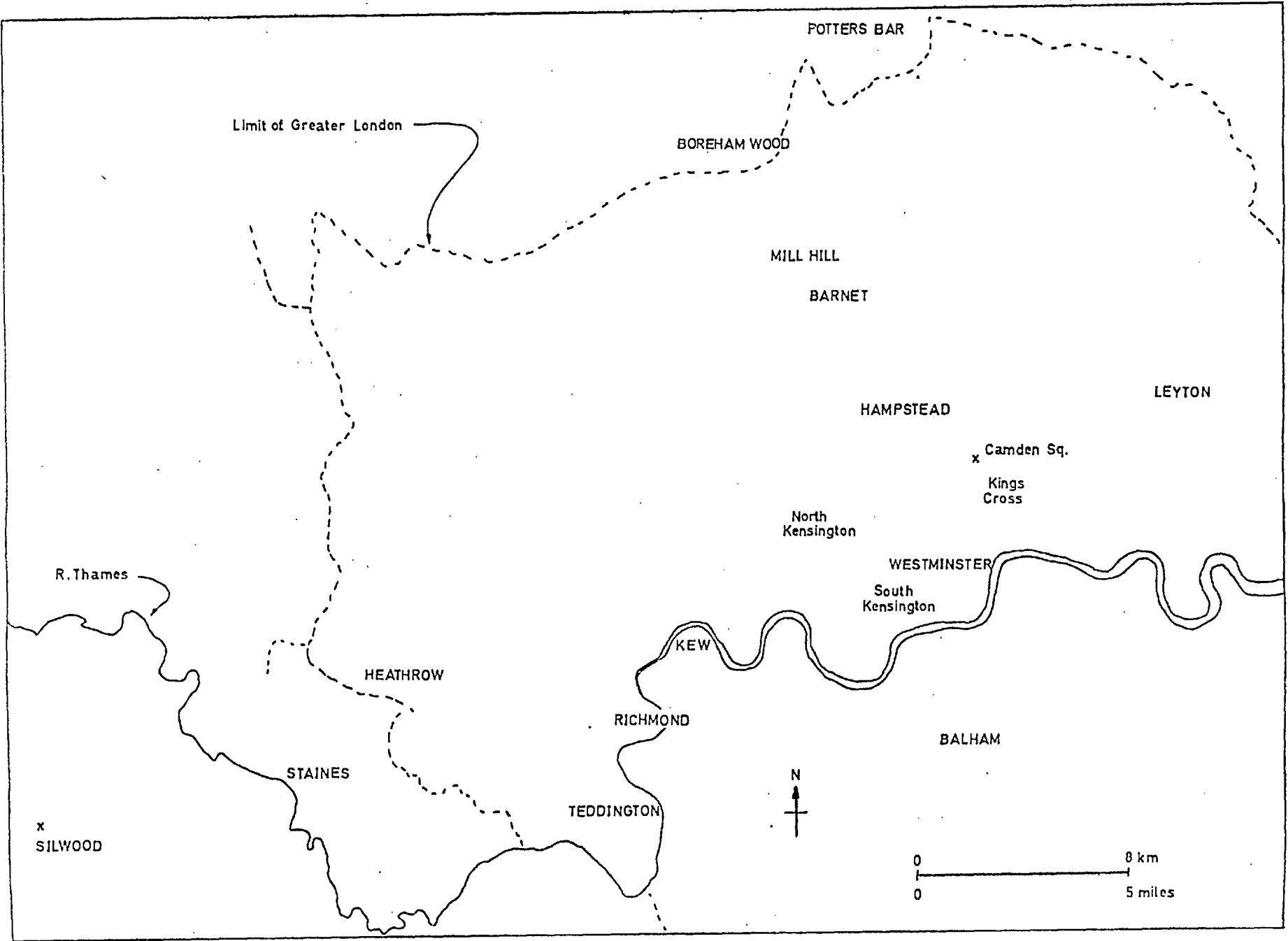
Summary

Consideration of past weather data has shown that winds in the upper and lower troposphere need not be in opposite directions to sustain a persistent cumulonimbus which is stationary or slow-moving relative to the ground. Published reports suggest that these severe storms occur somewhere in the northern hemisphere as often as once per year.

Despite the difficulties involved in identifying an

urban influence on cumulonimbus convection, it appears likely that higher surface temperatures in cities may be responsible for the initiation of thunderstorms in certain conditions, and that a large supply of warm air could encourage their persistence.

Map showing locations of places in and around London which are mentioned in the text.



CHAPTER IV : THE HAMPSTEAD STORM - OBSERVATIONAL STUDY

On 14th August 1975 a severe thunderstorm developed over north London (a preliminary description has been given by Keers and Westcott, 1976, and a number of other more graphic accounts were published, such as the one by Hillaby, 1975). Heavy rain fell for nearly three hours and serious flooding resulted in the region immediately around Hampstead Heath, with damage assessed at more than £1 million. Many homes were made uninhabitable by floodwater and overflowing sewers, which in addition presented a serious health hazard. Public transport was badly disrupted for several days. Despite its longevity the storm affected a very small area of approximately 100 km<sup>2</sup>.

This chapter presents an observational description of the storm itself, and a discussion of the meteorological situation (including both synoptic and meso-scale features) in which it occurred. The area of the ground affected by severe cumulonimbus, particularly when they are slow-moving or stationary, is often small enough for them to escape satisfactory observation by the network of routine meteorological stations. Our description of the Hampstead storm was facilitated by the fact that it occurred over a densely populated urban area; voluntary observers were invited (through the medium of local newspapers) to contribute any relevant information, with special regard to hail size, duration and intensity; lightning frequency; and the strength, direction and gustiness of the wind. About 50 voluntary reports have been incorporated in the following description, together with routine surface observations and aerological

data from Crawley (about 30 miles south of London). All times referred to are GMT.

#### 4.1 OBSERVATIONAL DESCRIPTION OF THE STORM

Figure 4.1 shows the rainfall map for 14th August, and illustrates the remarkably small area affected by the storm. The total of over 17 cm recorded at Hampstead Heath was the highest 24 hour total ever measured in the London area; the rate of rainfall, averaged over the 2 to 3 hour duration of the storm was between 60 and 70 mm hr<sup>-1</sup> at Hampstead, and about 40 mm hr<sup>-1</sup> at Parliament Hill. (Both stations operate autographic raingauges, and the latter recorded a maximum rainfall rate of 125 mm hr<sup>-1</sup> over a ten minute period before it failed. These figures are unreliable, however, because of funnel blockage by hailstones and other debris.)

Cumulus cloud began to develop around midday on 14th August over central London, and by about 1530 the sky was almost completely overcast. Two observers reported that the first rain fell at Hampstead as early as 1500 to 1530; certainly the storm had matured by about 1630, and the rain was most intense between 1700 and 1800. By about 1900 the rainfall had ceased.

Certain features of the storm updraught may be inferred from reports of hail at the ground; it is also important to obtain some indication of the significance of the ice phase in the dynamics of the storm, particularly since the computer simulation (discussed in chapter V) does not explicitly incorporate the formation of hail. Table 4.1 classifies the hail sizes and assigns code numbers (after Browning and Ludlam, 1960) which are plotted in figure 4.2. Although

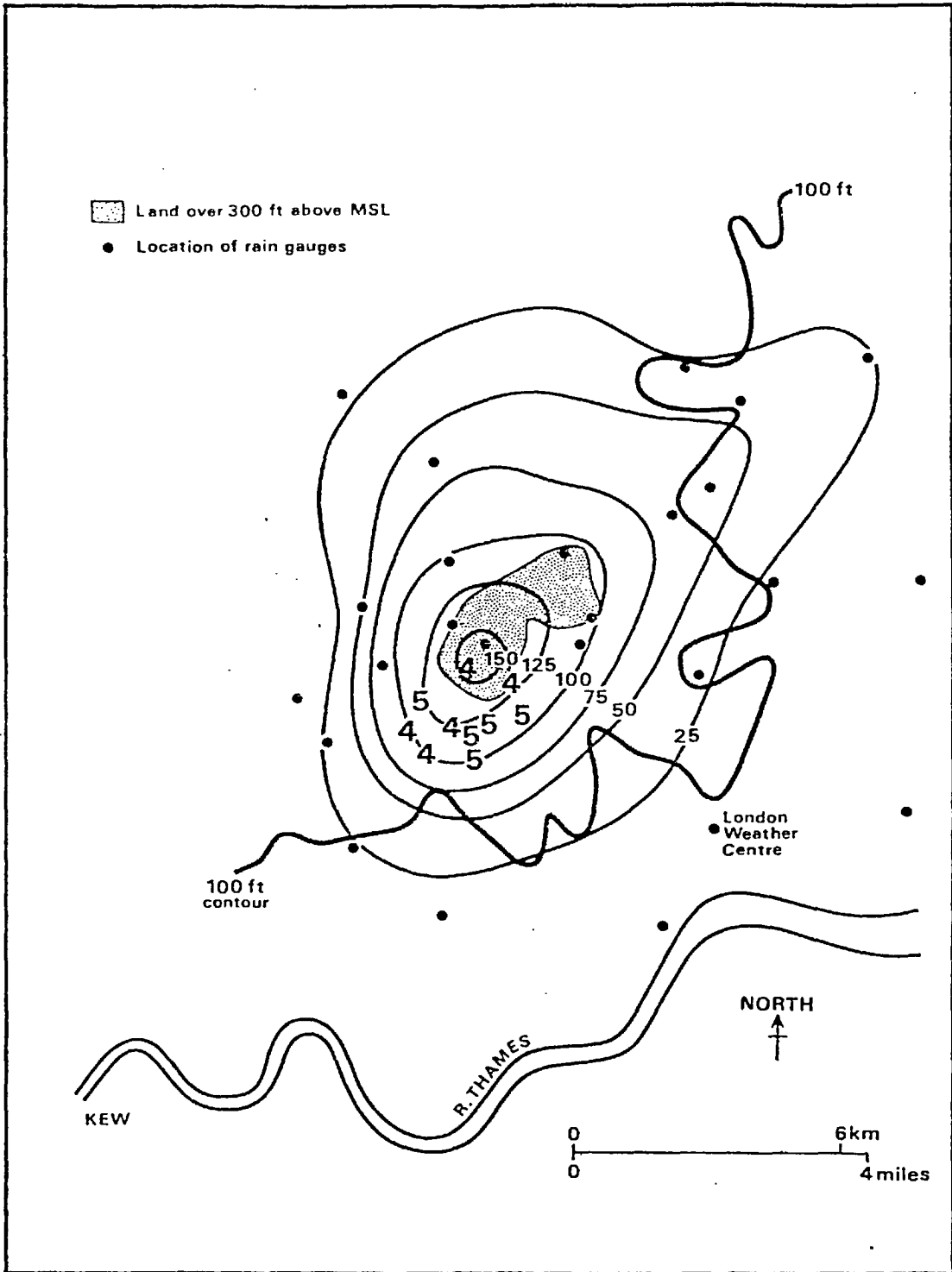


FIG. 4.1

Isopleths of total rainfall (at intervals of 25 mm) for the period 09 GMT 14th to 09 GMT 15th August 1975 over north London, together with the 100 and 300 ft height contours. Numbers '4' and '5' refer to hailstone size (see text and following fig.).



TABLE 4.1

Classification of hailstone sizes  
(after Browning and Ludlam, 1960)

<u>Hailstone size</u>	<u>Diameter</u>		<u>Code</u>
	<u>inches</u>	<u>cm</u>	
Grain	$< \frac{1}{4}$	$< 0.6$	1
Pea	$\frac{1}{4} - \frac{1}{2}$	$0.6 - 1.3$	2
Grape/cherry	$\frac{1}{2} - \frac{3}{4}$	$1.3 - 1.9$	3
New Penny	$\frac{3}{4} - 1$	$1.9 - 2.5$	4
Walnut/10 p. piece	$1 - 1\frac{1}{4}$	$2.5 - 3.2$	5

In figure 4.2 a report of no hail is signified by '0'.



there were few observations to the north of Hampstead, it appears that the largest hail fell to the south of the area of greatest rainfall; this fact is of use when inferring the location of the storm updraught. Some observers reported that hail fell for an hour or more, apparently in up to four 'bursts', each of 10 to 15 minutes' duration.

Two interesting observations were made from locations well away from the storm itself. The first, from a point 16 km to the west of Hampstead, records that a cumulus was beginning to tower over central London (in the vicinity of Westminster) from about 1600. As it grew and moved slowly northwards to reach a maximum height of about 8 km, it was succeeded by two more clouds at intervals of about  $\frac{1}{2}$  hour. The observer remarks on the apparent smallness of the anvil cloud, and rather few 'sferics'. The second observer was travelling west and when about 60 km west of the storm, described "towers growing on the south side of the cloud and moving northwards where they merged with a massive anvil". Both these observations suggest a type of regenerating, multicell storm (this 'unsteadiness' is an important feature, and will be discussed in chapter VI).

Data collected and described by Atkinson (1977) support this view of the storm. He presents isochrones of the start of the heaviest precipitation during the storm (perhaps resulting from the second of the three cells referred to above). They are consistent with a progressively deepening cloud moving in the direction of the ambient wind field, reaching its most intense phase over Hampstead, and moving to the north-east as it decays.

#### 4.2 THE STORM ENVIRONMENT

The surface and upper air charts (figures 4.3 and 4.4) show a depression centred west of Ireland with a surface front and upper trough moving slowly eastwards across Britain. A small low pressure area over north-west France can also be identified, and this was probably associated with the incursion of continental air into south-east England. The low-level convergence associated with the confluence of westerly and easterly air masses is demonstrated by the surface streamlines (figure 4.5) which indicate a well-marked confluence zone extending northwards through London; this feature persisted throughout the afternoon. During 14th August other thunderstorms were reported along this zone, some giving rainfalls of up to 40 mm. Figure 4.6 shows the 24 hour rainfall map for the whole of eastern England; it is interesting to note the elongation of the isohyets in a north-easterly direction, and the rather small areas of most intense falls (of which the most striking is that near London).

The appearance of the surface convergence zone suggests that it may have been associated with sea-breezes from the south and east coasts opposing the weak westerly flow. It is, however, unlikely that a sea-breeze could penetrate so far inland by midday (Simpson et al. (1977) describe the inland penetration of sea-breeze fronts from the south coast of Britain, which occasionally reaches 100 km by about 2200); furthermore some convergence of the surface winds is clearly indicated by the observations for 0600 and 0900. In fact a similar feature can be identified on the previous day, 13th August, but is located further north and west. As on 14th

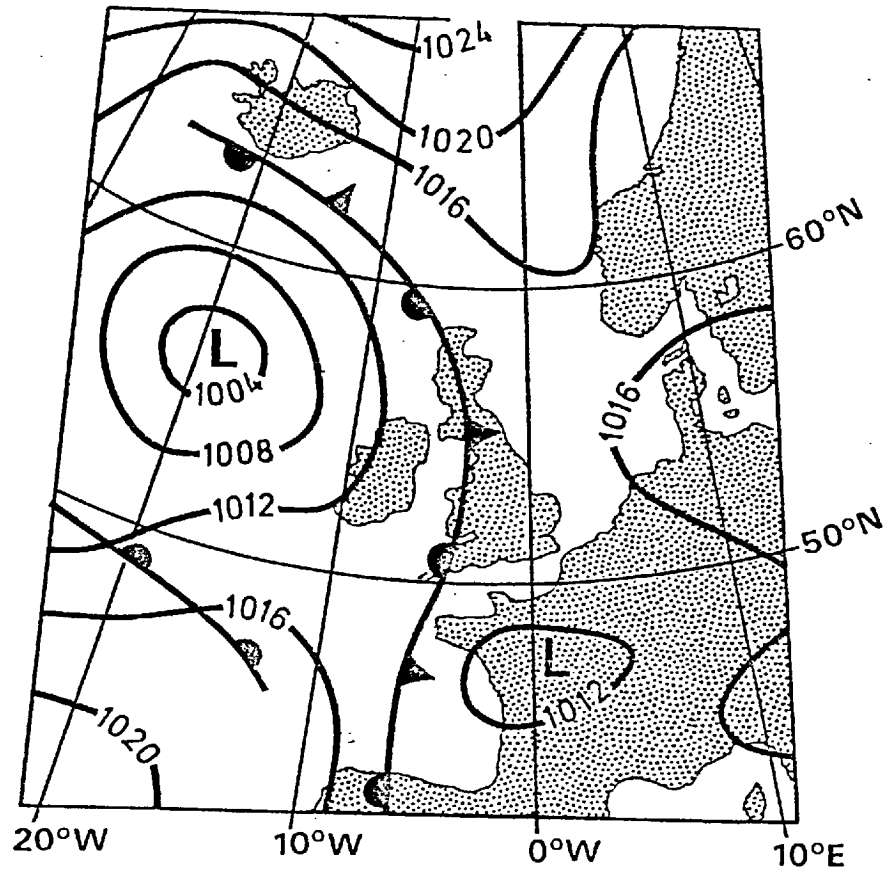


FIG. 4.3

Surface chart for 12 GMT, 14th August 1975  
(based on Meteorological Office analysis).

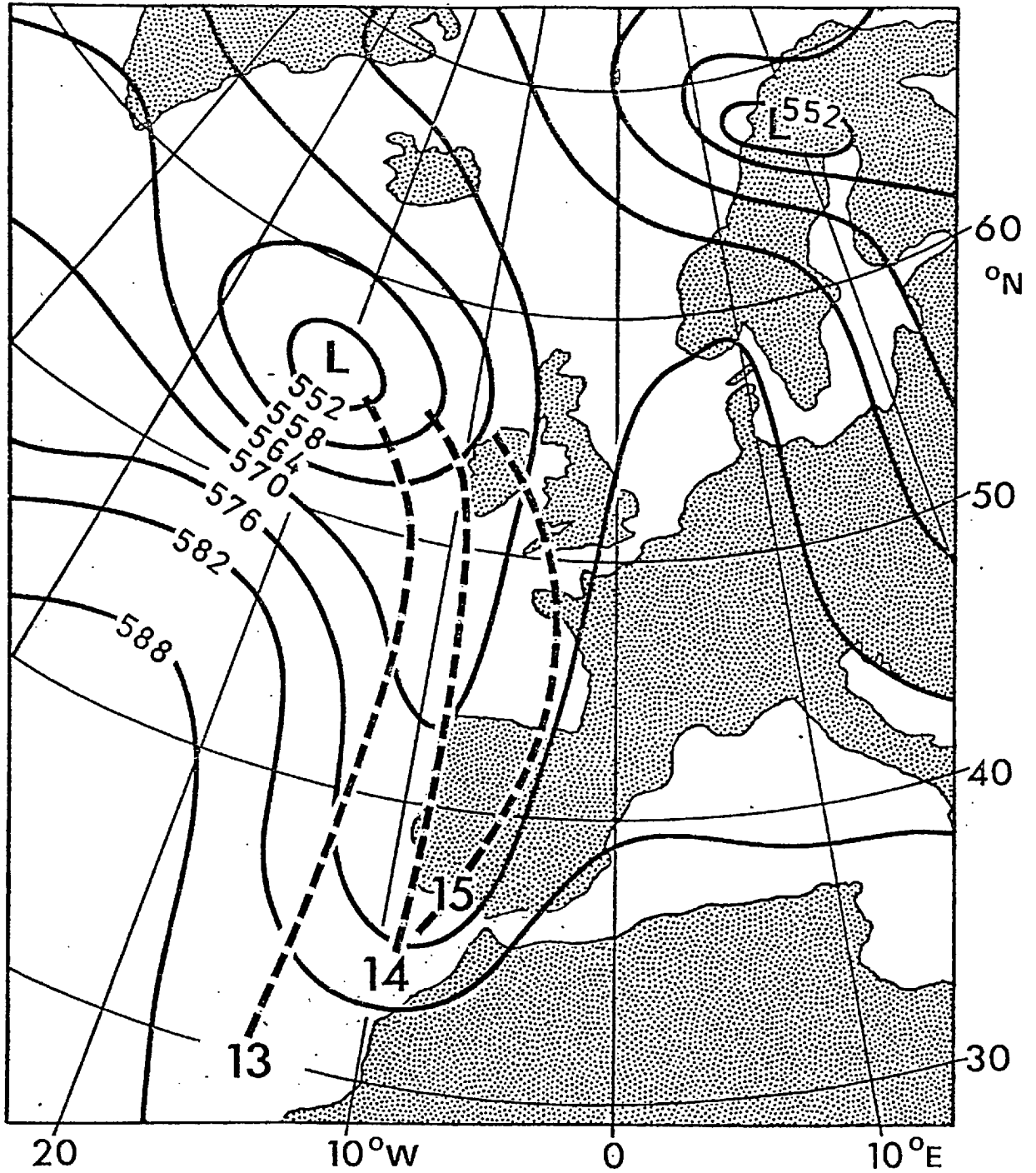


FIG. 4.4

Successive positions of the upper trough (pecked lines) at 00 GMT on 13th, 14th and 15th August 1975, superimposed on the 500 mb chart for 00 GMT 14th August. Height contours labelled in units of 10 gpm.

# Surface streamlines for 12 GMT, 14 August 1975

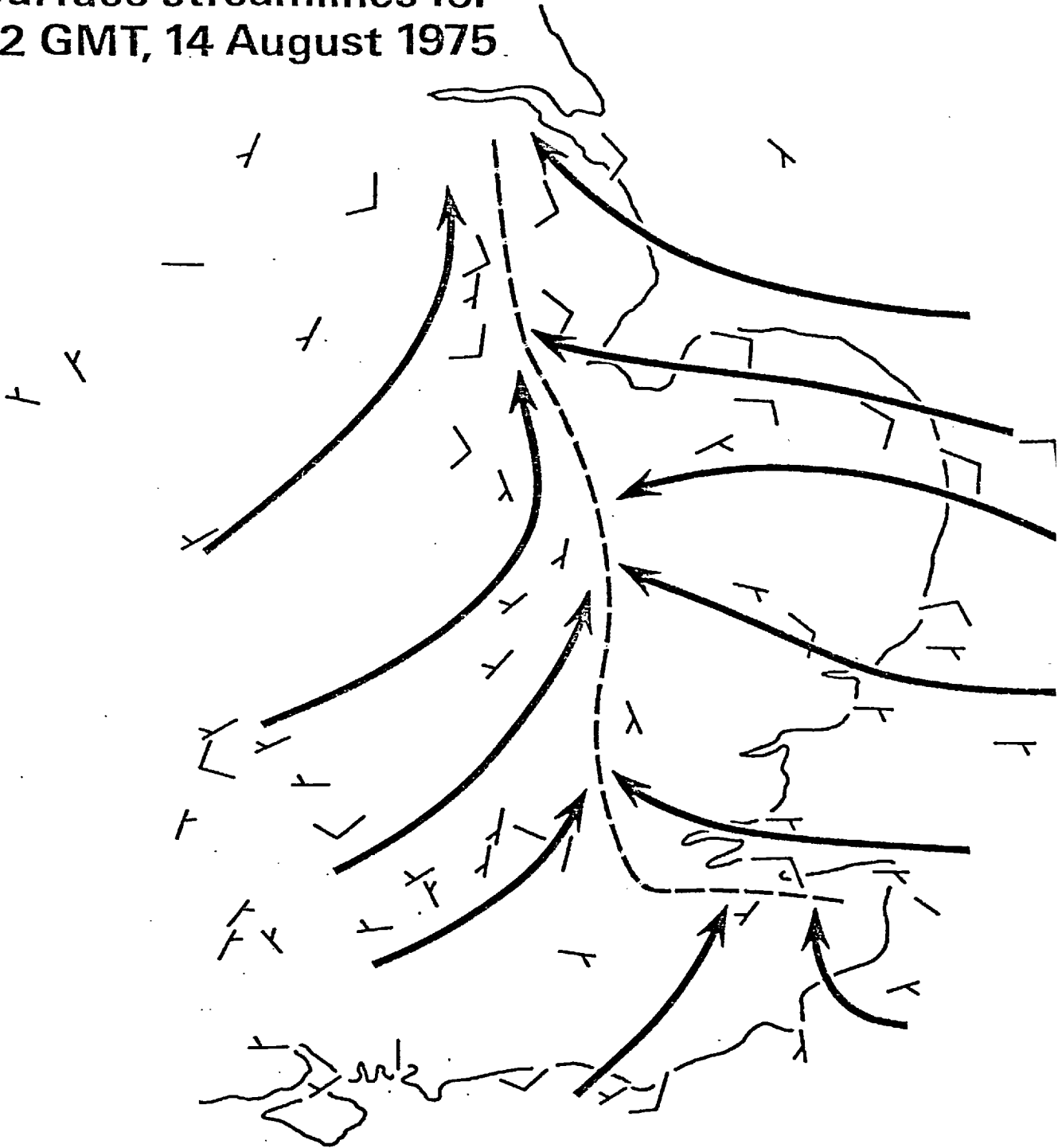


FIG. 4.5

Approximate position of the confluence zone (see text) is indicated by the pecked line. Surface wind data are presented in the standard form, each half 'feather' corresponding to a wind speed of 5 knots.

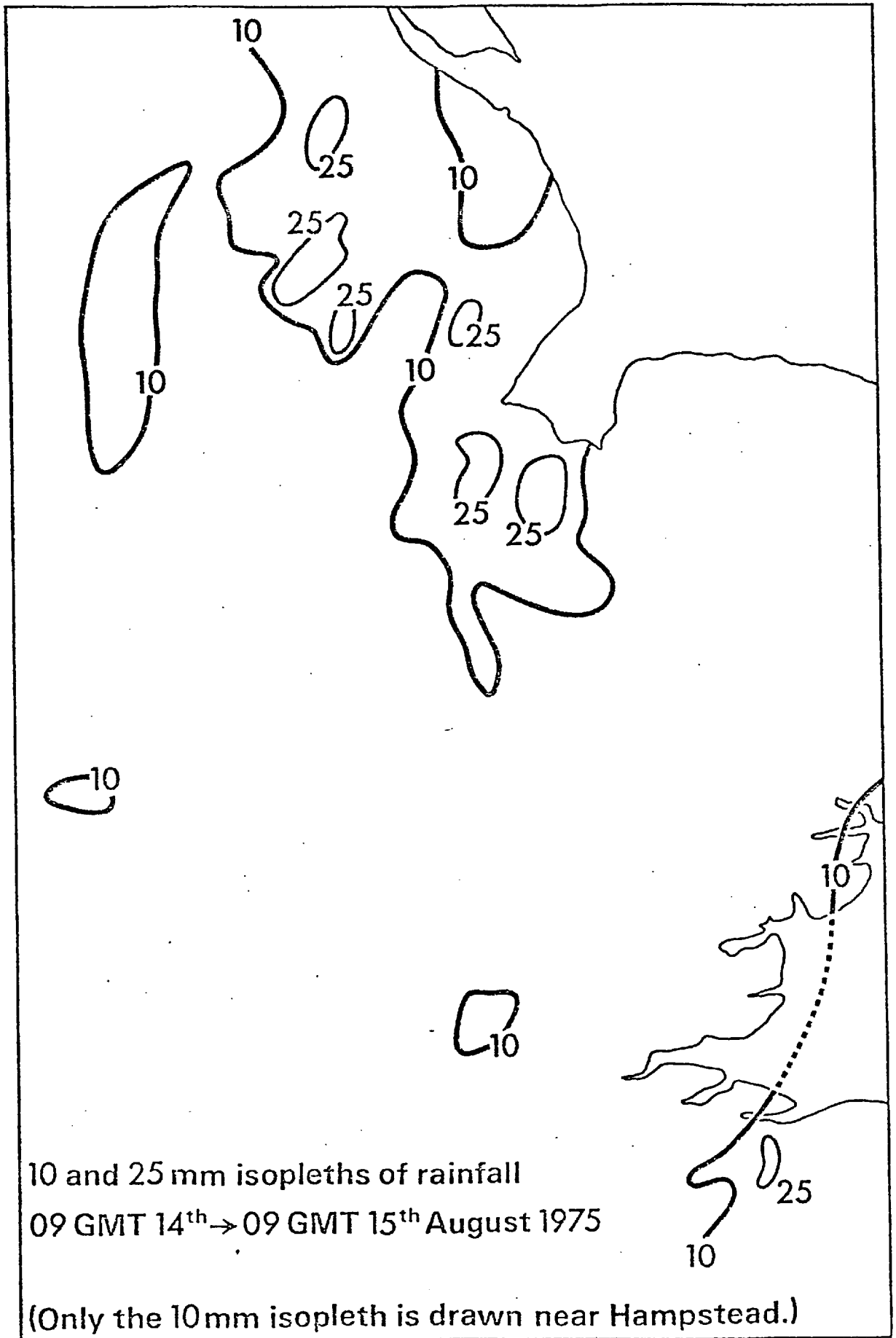


FIG. 4.6

Rainfall map for eastern England. Compare the locations of the highest totals with the position of the confluence zone in fig. 4.5



August, thunderstorms were reported along this line, and over the Pennines rainfalls of over 60 mm were recorded. It is interesting that the German surface analyses consistently interpret the confluence as a cold front, although satellite photographs indicate a fairly thick band of cloud further west, thus supporting the British Meteorological Office's analyses. There were, however, marked changes of temperature and dewpoint across the convergence zone, and in view of the associated convective activity, the German analysis is not unreasonable.

Figure 4.4 shows the eastward progress of the upper trough at the 500 mb level, and a time-height section based on aerological data from Crawley (figure 4.7) illustrates the associated cooling (decreasing  $\theta_s$ ) in the middle and upper troposphere. Although quite small ( $\theta_s$  decreases by about 1 deg C in 24 hours) there is a noticeable change in the stability from 0000 on 14th August. Evidently deep convection was prevented on 13th August by a stable layer between  $1\frac{1}{2}$  and 2 km; we recall from chapter I that such low-level inversions often presage deep convection. Rather more apparent from the time-height section is the increase in  $\theta_w$  in the lowest kilometre of the atmosphere, which at midday on 14th August was between 1 and 2 deg C higher than 24 hours previously. This may indicate a storage of energy in the boundary layer beneath the inversion, or possibly potentially warm air advected from the south-east, as suggested by the trajectories plotted in figure 4.8. The time section also shows the development of stronger winds at upper levels, which are likely to be an important requirement for a severe, persistent convective storm. Winds throughout

# CRAWLEY Time-height section, 12-15 August 1975

---  $\theta_s$  °C  
 —  $\theta_w$  °C  
 / wind direction and speed (knots)

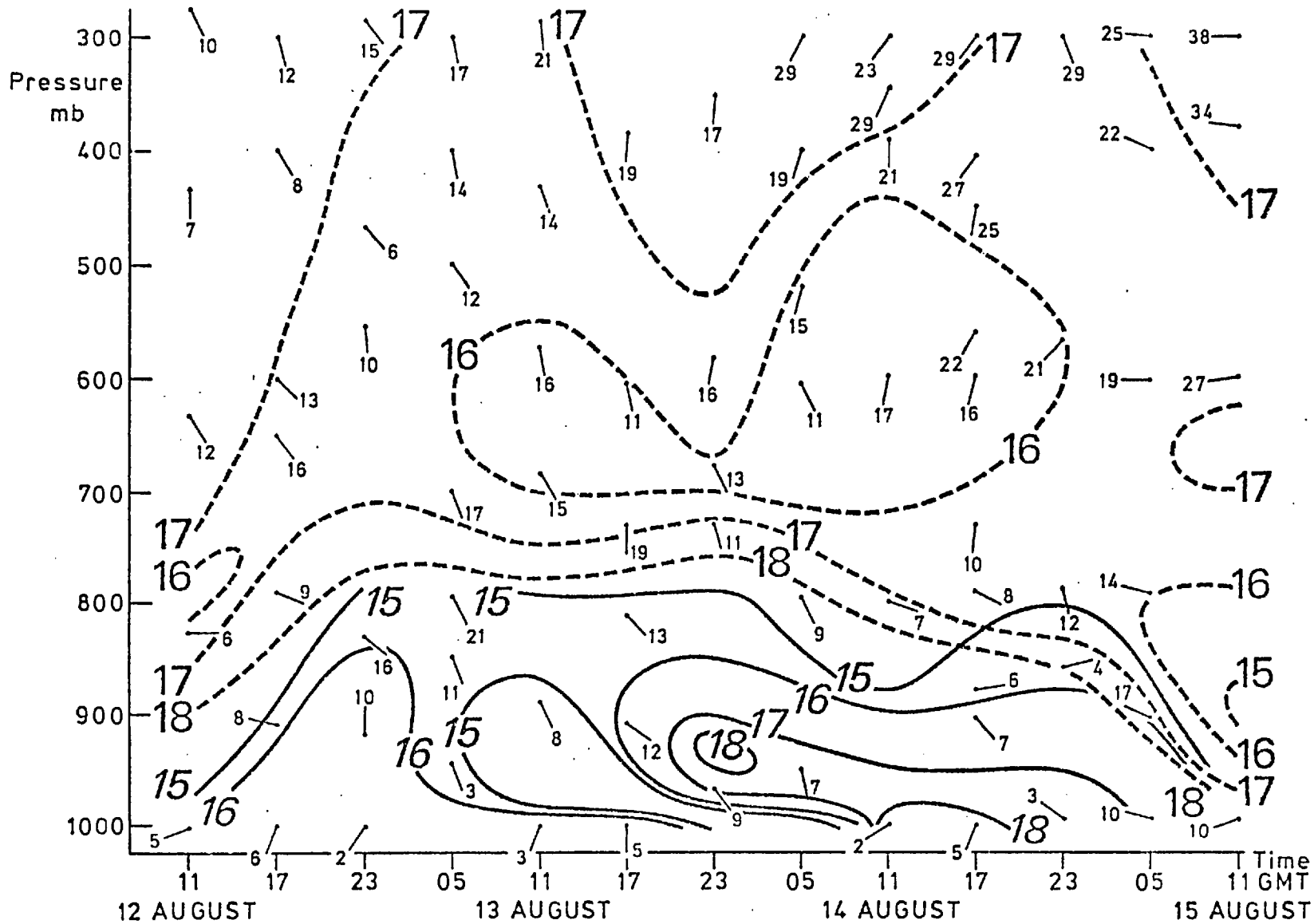
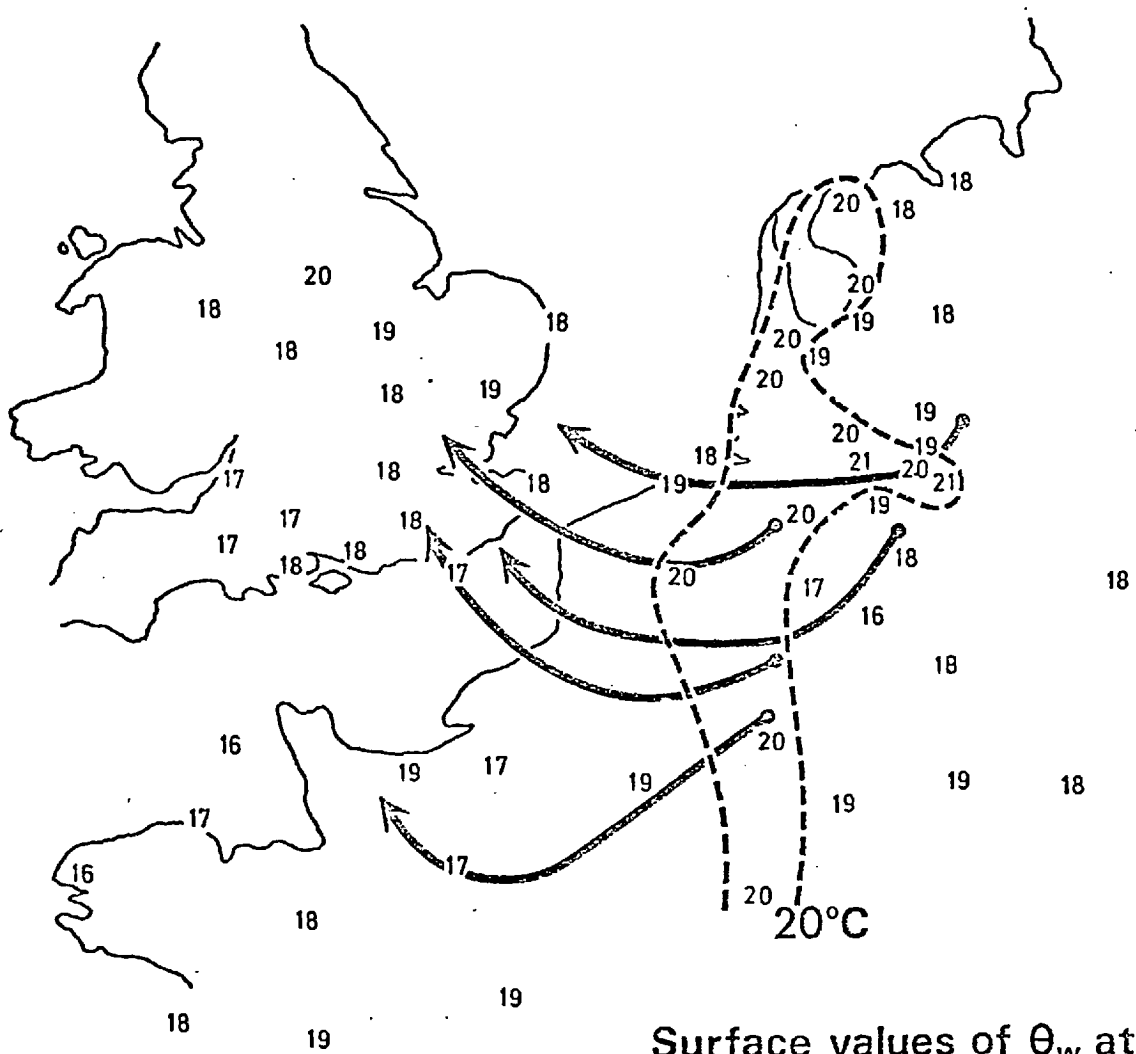


FIG. 4.7  
 Time-height section using aerological data from Crawley.  
 For clarity  $\theta_w$  above 800 mb and  $\theta_s$  near the surface are not shown.



Surface values of  $\theta_w$  at  
12 GMT, 13 August 1975

➤ Trajectories of air near 900 mb for 24 hours, from 12 GMT 13<sup>th</sup> → 12 GMT 14<sup>th</sup> August

FIG. 4.8

A possible origin of boundary-layer air with high  $\theta_w$  is suggested by low-level trajectories.

the troposphere were very light until late on 13th August, when speeds greater than  $10 \text{ m sec}^{-1}$  first became evident.

#### The local environment

It is important that the upper air sounding (used as input for the numerical model) is representative of the storm's immediate environment. While the midday ascent from Crawley on 14th August (shown in figure 4.9) is adequate in some respects, the reported boundary layer is unlikely to be an appropriate description of air over London some 4 hours later. Strong cumulus convection was observed over the city at midday, with cloud base near 1500 m. In such conditions the mixing ratio ( $r$ ) usually decreases very slightly upwards, often by less than  $1 \text{ g kg}^{-1}$  over the whole adiabatic layer (see chapter II); the Crawley sounding, however, shows  $r$  decreasing from  $10 \text{ g kg}^{-1}$  near the surface to about  $5 \text{ g kg}^{-1}$  near the level of observed cloud base, so that an adjustment to the sounding is necessary. Some alteration is also made to the dry bulb temperature by taking account of the mid-afternoon surface temperatures attained in London of  $30^\circ\text{C}$ , and allowing for a superadiabatic layer in which the potential temperature decreases by about 3 deg C. The modified sounding, which was used as input for the numerical simulation, is shown in figure 4.10.

The greater degree of mixing in the boundary layer over London is accounted for by vertical motions induced by low-level convergence not effective near Crawley. Our modification to the dewpoint temperature stratification requires the top of the moist layer to have risen by about 1 km in 4 hours. If we consider an approximate two-dimensional continuity equation of

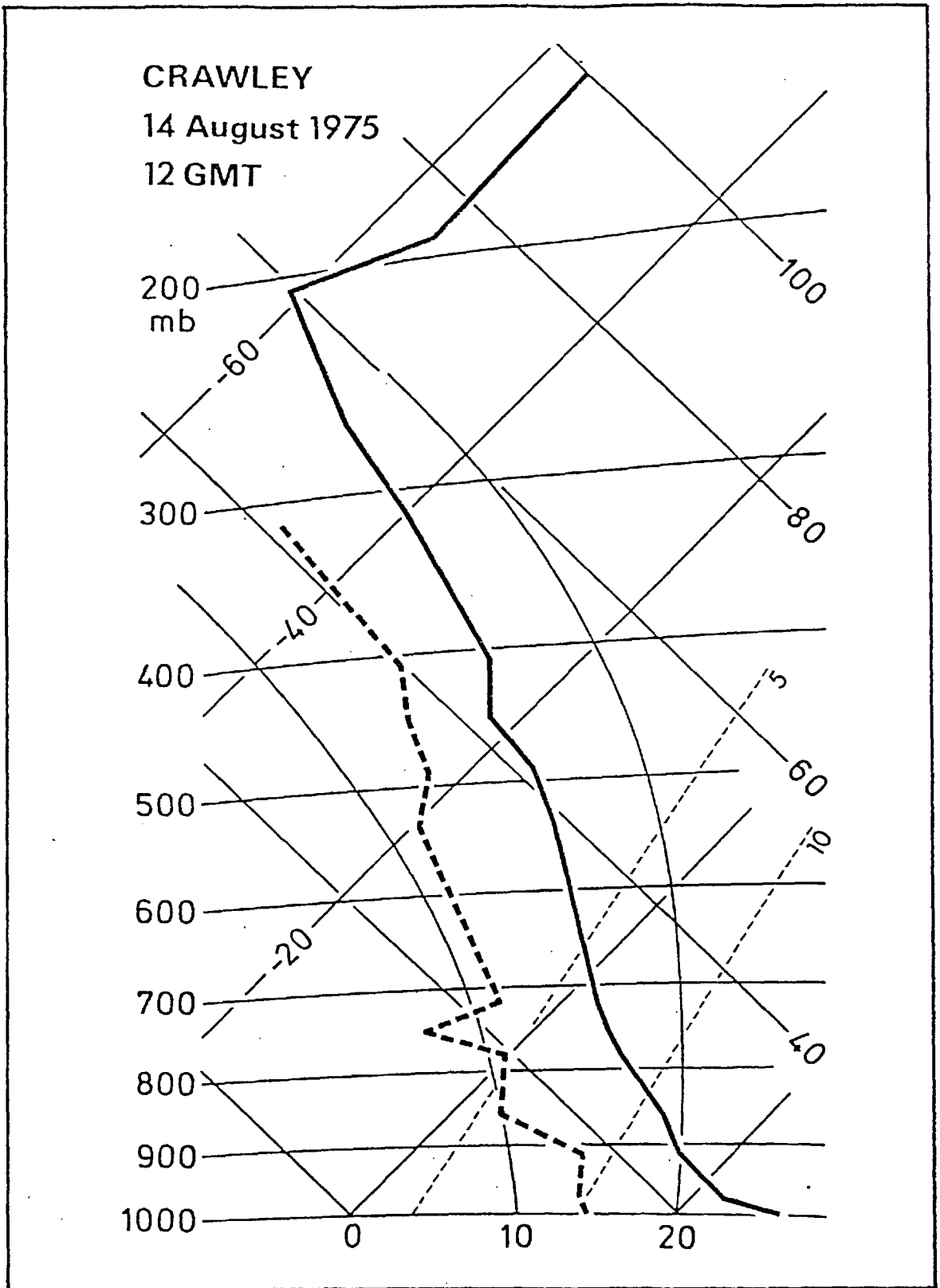


FIG. 4.9

Original Crawley sounding, plotted on a tephigram.

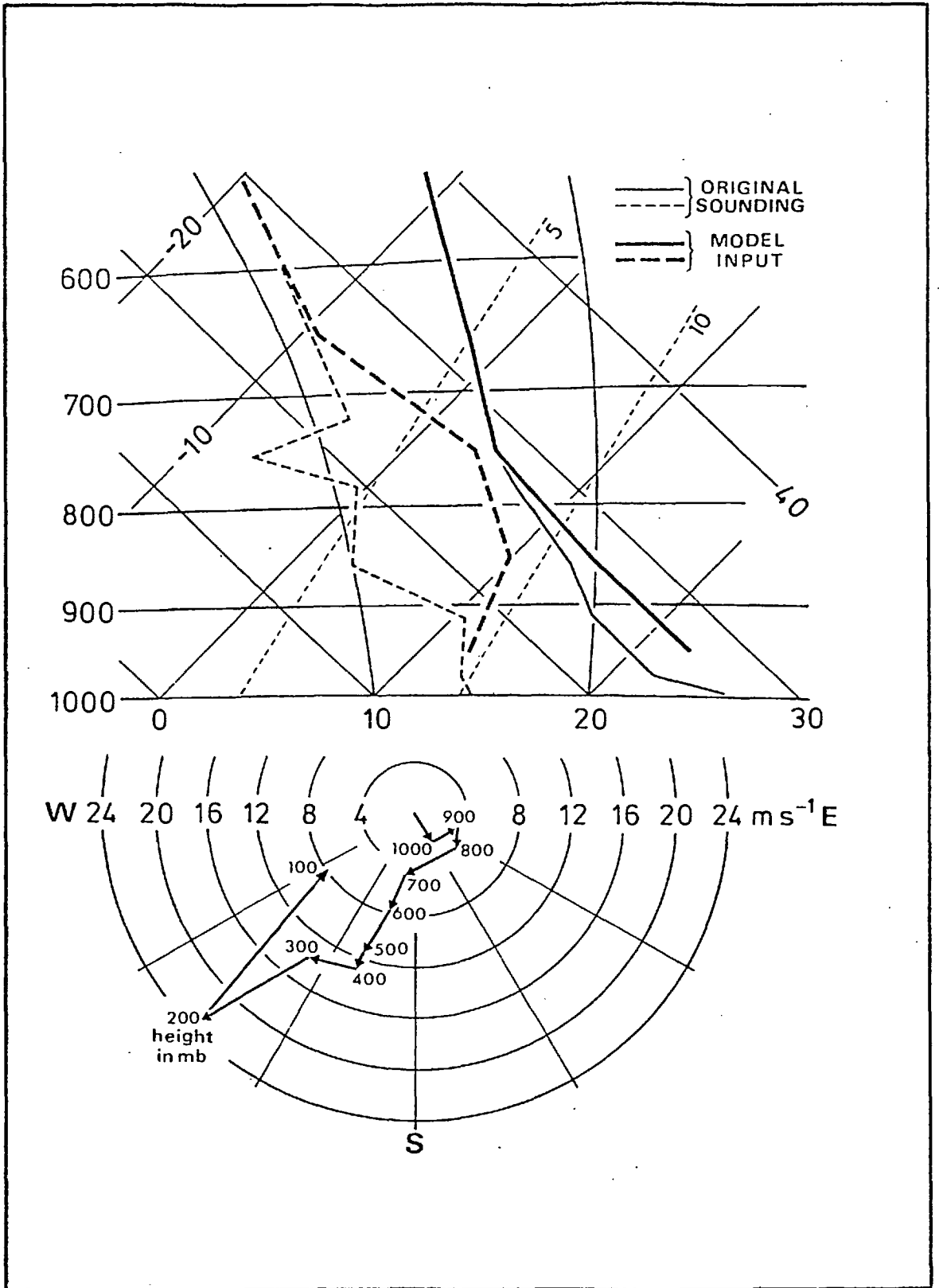


FIG. 4.10  
Representative temperature and wind data  
for the Hampstead storm environment  
(used as input for the numerical simulation).

the form  $|\delta w/\delta z| \sim |\delta u/\delta x|$ , the necessary vertical motion can be achieved by a change in horizontal velocity (averaged over the lowest kilometre) of  $\delta u \sim 5 \text{ m sec}^{-1}$  across a convergence zone of width  $\delta x \sim 100 \text{ km}$ . These values are seen to be consistent with the reported surface winds (figure 4.5), the configuration of which was maintained throughout the day.

Figure 4.11 shows the divergence field computed on a grid of spacing 50 km from the reported surface winds at midday on 14th August. Large errors are, of course, inherent in this calculation, partly because the divergence is often the difference between two terms of similar magnitude, and partly as a result of the unreliability and unrepresentativeness of the surface wind observations. Nevertheless, the computed field is consistent with the observed winds, and the magnitude of the convergence is in accord with the modification made to the boundary-layer thermodynamic structure. However, the dewpoint modification does represent a large input of moisture into the boundary layer; this is readily estimated from figure 4.10 as about  $5 \text{ kg m}^{-2}$ . A simple calculation shows that this quantity could be accounted for by a surface latent heat flux of  $200 \text{ W m}^{-2}$  (a typical value for a summer day) continuing for as long as 15 to 20 hours. Clearly the moist boundary layer cannot be explained by evaporation alone, and the effects of advection must be of importance.

Figure 4.10 also shows the wind field used in the numerical model. This was interpolated from the 1200 and 1800 Crawley data, with the addition of south-easterly surface winds (as observed in London).

The convergence of air over London was evidently of great

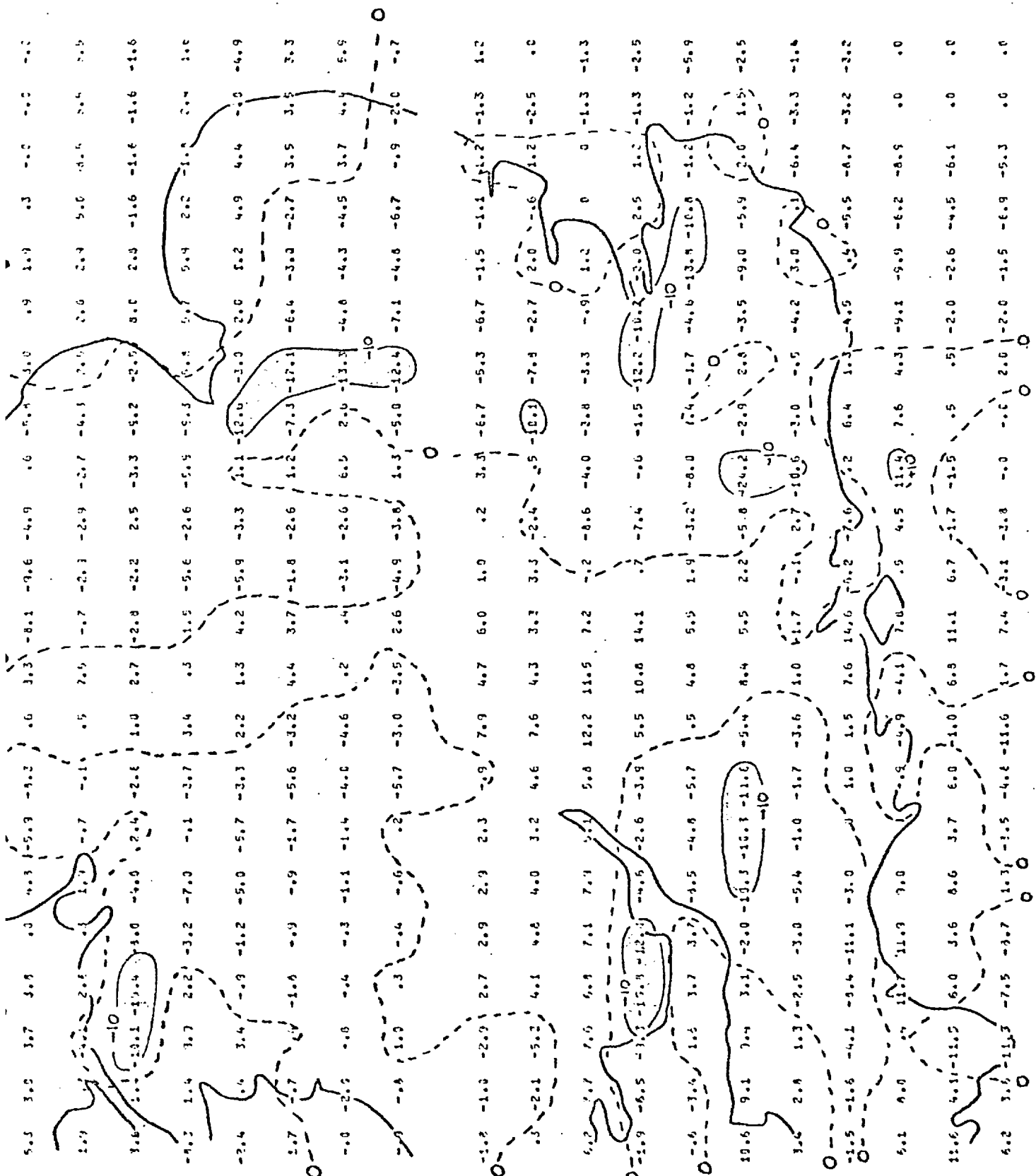


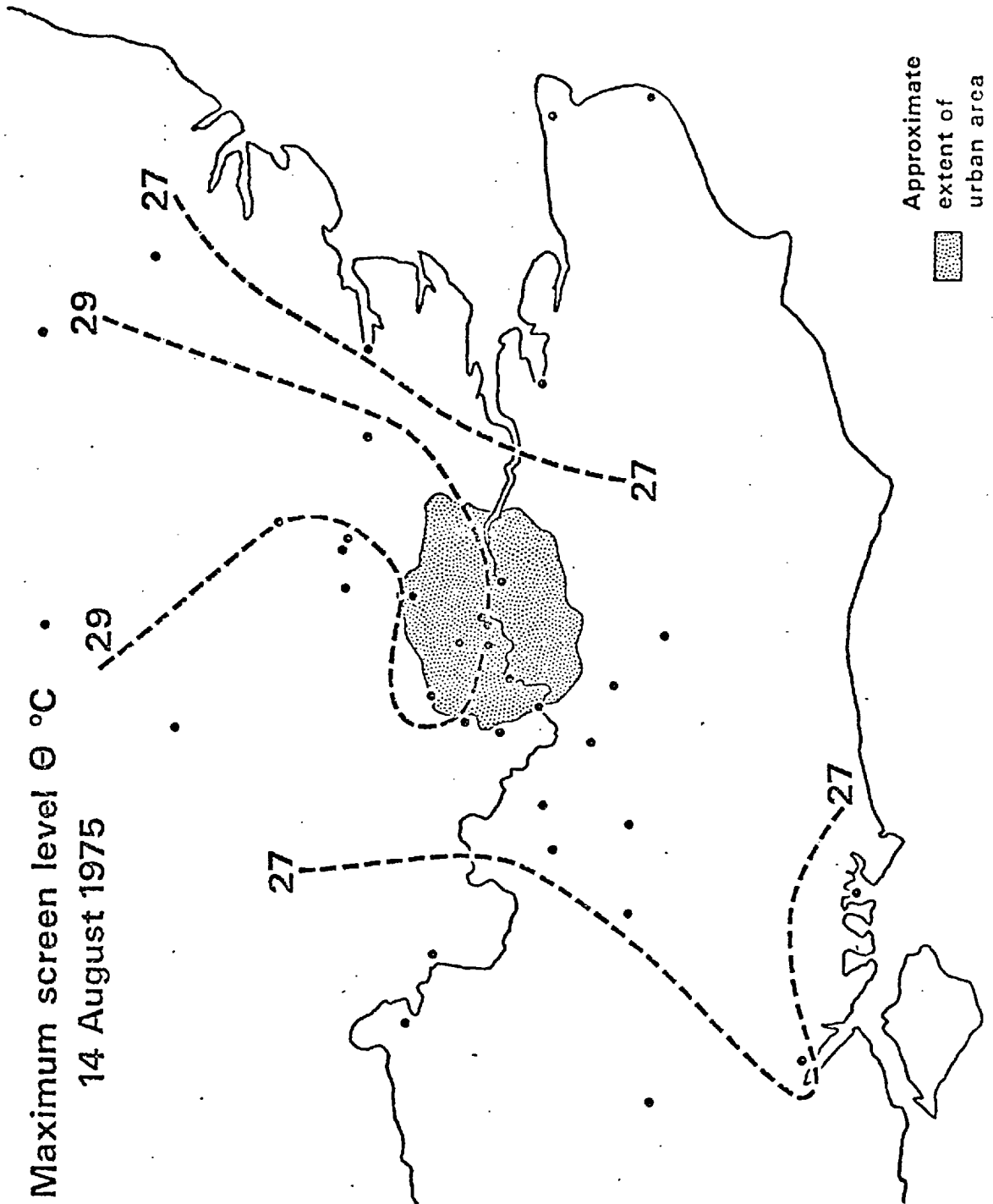
FIG. 4.11

Divergence computed from surface winds at 12 GMT, 14th August 1975. Units are  $10^{-5} \text{sec}^{-1}$ .



importance in the provision of an environment suitable for cumulonimbus convection. Although no precise calculation can be made, it seems likely that the large-scale conditions described in this section were enhanced by the presence of an urban 'heat island' (see figure 4.12). While the effect was not particularly well-marked on this occasion (compare Atkinson, 1970 for example), it is clear that with a boundary-layer value of  $18^{\circ}\text{C}$  for  $\theta_w$ , surface potential temperatures of about  $29^{\circ}\text{C}$  would have been necessary for deep convection, and that the Greater London area was evidently a favourable source. Away from the built-up area, surface temperatures were probably too low to allow the development of any cloud other than small cumulus. Application of the simple parcel theory gives an available potential energy of about  $680 \text{ J kg}^{-1}$ , using a value of  $18^{\circ}\text{C}$  for  $\theta_s$ . This suggests a maximum updraught speed of  $37 \text{ m sec}^{-1}$  at a height of 10.2 km, and a maximum cloud top height of 12.8 km. These values are rather greater than those suggested by the observer in section 4.1, but the magnitude of the updraught is consistent with the maximum reported hailstone diameter of 3 cm, as given in table 3.1.

Atkinson (1977) identified another urban effect, which gave rise to remarkably high values of surface vapour pressure over north and north-east London. He states: "This extreme localization of high vapour pressures defies explanation at present but . . . must provide an important key to the similar localization of the storm later in the day." One of his figures shows the surface vapour pressure for 0900 on 14th August; at an atmospheric pressure of 1000 mb, a vapour pressure of 22 mb as reported from part of north-west London is equivalent to a dewpoint temperature of approximately  $19^{\circ}\text{C}$ .



Maximum screen level  $\theta$  °C  
14 August 1975

FIG. 4.12

Approximate isotherms showing the distribution of maximum screen-level potential temperature on 14th August 1975. Data points are indicated by a dot.

Chandler and Gregory (1976) refer to the problem of high vapour pressures on the 'down-breeze' side of cities overnight, which arise from the differences in the water balance of urban and rural areas when conditions are relatively calm. The high vapour pressure over London on the morning of 14th August may be accounted for as follows.

On the previous afternoon, vapour pressures at the surface would have been fairly uniform over the whole area (at about the same value as the maximum value the following morning). During the night, when conditions would have been calm under the nocturnal inversion, the surface temperature in rural areas would have fallen well below dewpoint, and water vapour could have been extracted by the ground (without necessarily forming dew). In urban areas, however, the temperature would have remained above dewpoint, so that the vapour pressure would have remained near the previous afternoon's high value. When small-scale convection resumed the next morning, the nocturnal inversion would soon be removed, and vapour pressures should eventually return to values close to those of the previous day.

It appears then that while the locally high vapour pressures are due to the presence of a large urban area, the contrast between the city and the surrounding countryside would only have been apparent in the early morning, and is unlikely to have any influence on the localization of the storm later in the day.

#### 4.3 DOWNDRAUGHT OBSERVATIONS

The identification of the cool outflow from the storm is greatly facilitated by the rather sudden associated change in

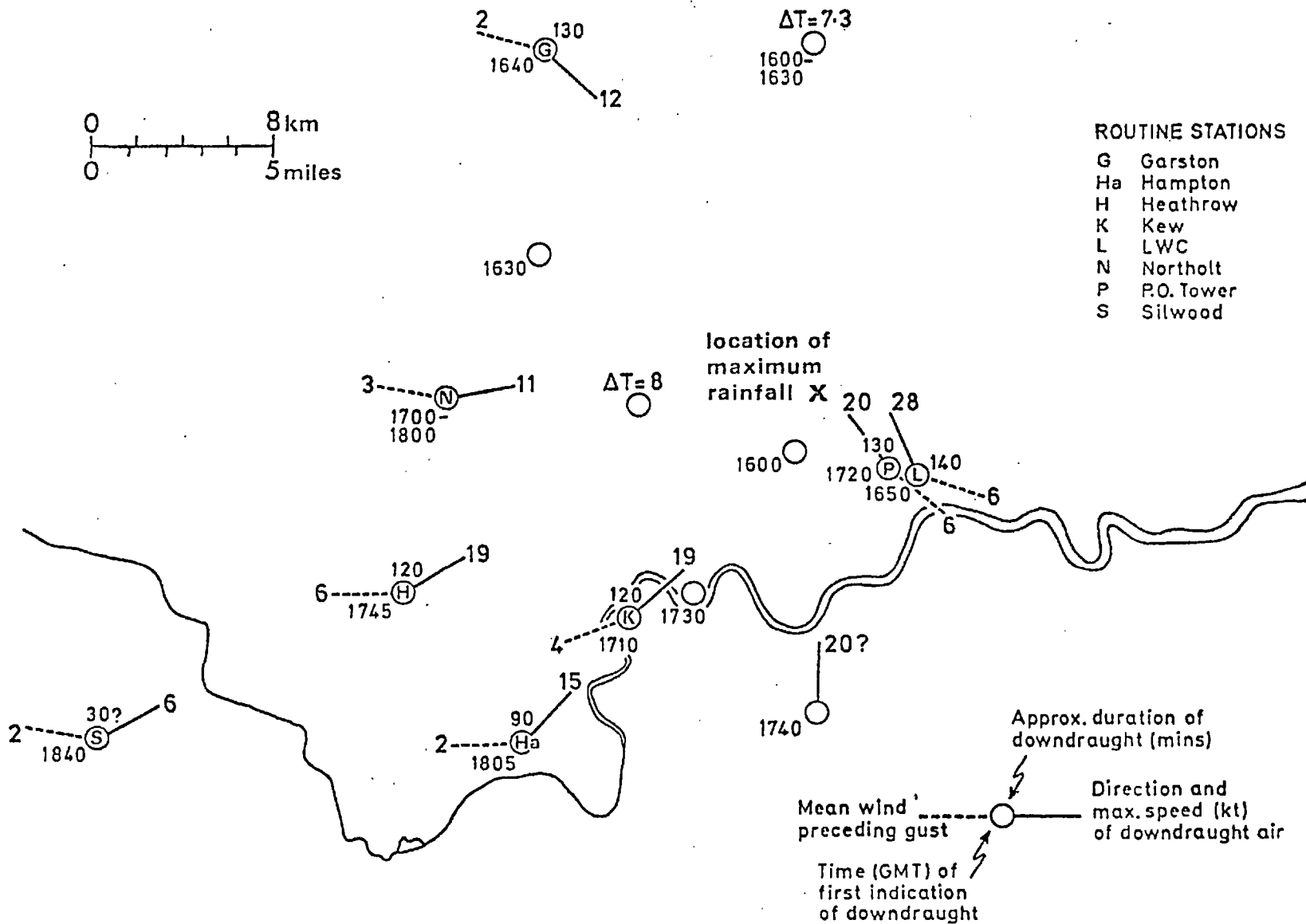
the weather at the ground, and the resulting impression made on voluntary observers, many of whom noticed a change in wind speed or a rapid fall in temperature. Some of these observations (including reports from the routine meteorological stations) are presented in figure 4.13. Figure 4.14 illustrates the way in which the arrival of downdraught air was registered by recording instruments at Garston (near Watford) and Heathrow. The main features of the downdraught outflow are as follows:

- (i)            Soon after the onset of heavy rain at 1600 to 1630, the cool air was noticed close to the centre of the rain area. It apparently spread out most rapidly towards the north-west, reaching Watford at about 1640. Two observers provide indications of rapid falls in temperature (8 deg C at a point 5 miles west of Hampstead, and 7 deg C from a thermograph at Potters Bar, about 10 miles to the north), although some of the decrease may be accounted for by increased cloudiness and diurnal cooling. The times given suggest a mean outflow speed in this direction (north-west) of 10 to 15 m sec<sup>-1</sup>.
  
- (ii)           Downdraught air spread out more slowly to the south and south-west into the prevailing surface winds, at a fairly steady rate (between 3 and 4 m sec<sup>-1</sup>) reaching Silwood, near Ascot, at 1840. The passage of a 'squall-front' was marked at Kew by a sudden fall in temperature of about 2 deg C and an increase in humidity from 37 to 50%; at Silwood the value of dry bulb minus wet bulb temperature (the wet bulb depression) fell by 1.5 deg C (corresponding to an increase in humidity of about 10%).

(It is difficult to make any reliable estimation of  $\theta_w$  in

Observations of the Hampstead storm downdraught, including data from routine stations (see code letter) and voluntary observers. Sudden temperature falls indicated by  $\Delta T = (\text{deg C})$  at top of station model. Centre of storm indicated by the position of the maximum point rainfall.

FIG. 4.13



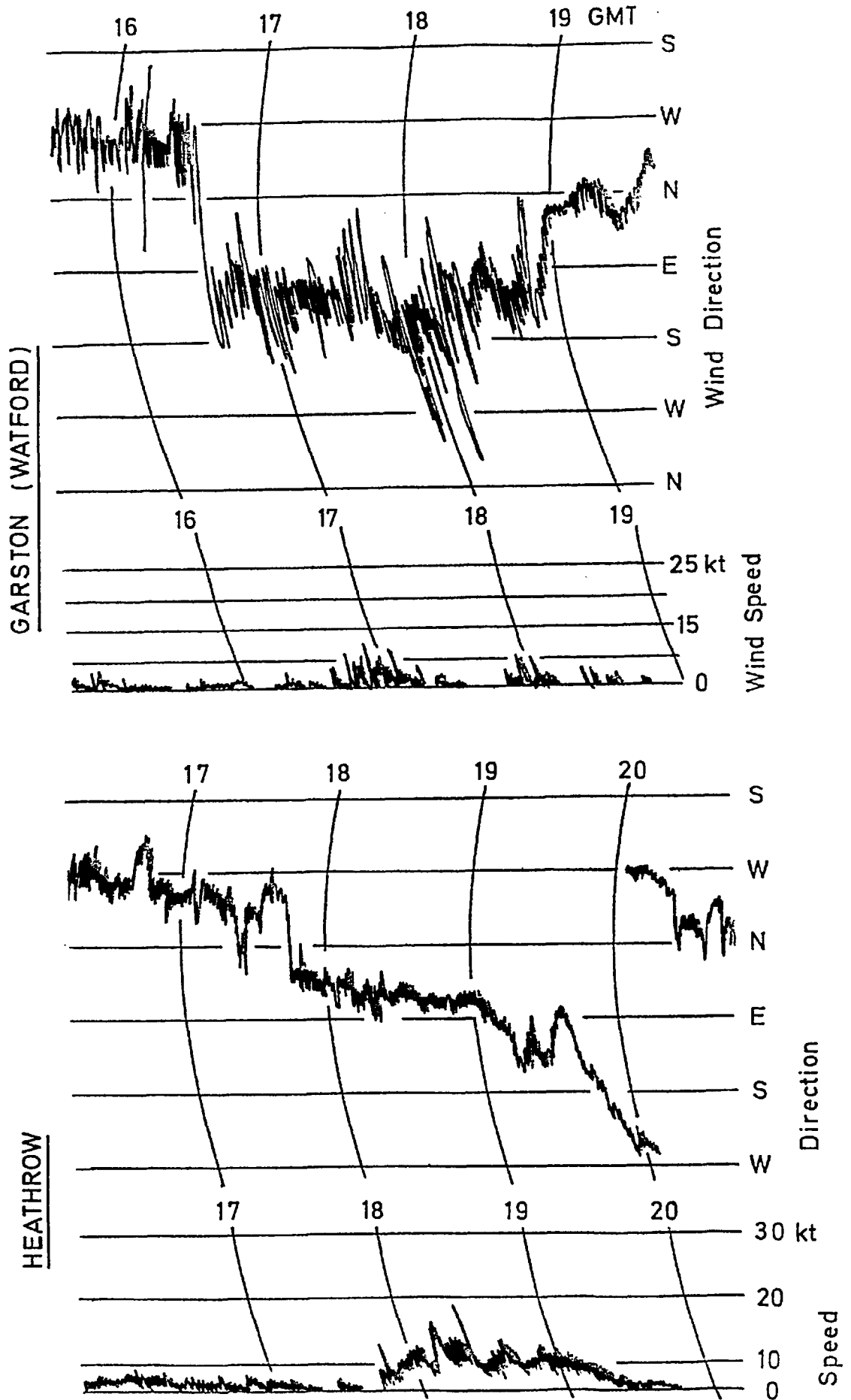


FIG. 4.14

Wind records from Garston and Heathrow showing arrival of downdraught air from the Hampstead storm (see also fig. 4.13).

the downdraught air, but if we accept the above report of a sudden temperature fall of 8 deg C, then  $\theta_w$  is about 15°C, so that the outflow may have originated from levels up to about 550 mb.)

The above observations suggest that downdraught air was detected up to 40 km away from its origin. Such distances are unusual, but not unprecedented; Scorer (1953b) describes cumulonimbus convection in Spain, from which the cool outflow was measured 65 km distant. The storms were located over mountains, which may have provided some initial assistance to the downdraught current, but the intervening terrain was generally flat.

(iii) As Atkinson (1977) points out, "the irregularities of the wind speed and temperature changes" following the initial gust front "suggest a succession of downdraughts . . . in bursts of very heavy precipitation", and lends weight to the view of an impulsive, cellular storm.

(iv) Virtually no observations, routine or voluntary, could be obtained from east and south-east London, and this is a considerable disadvantage in the analysis of the storm. It is believed, however, that this lack of observations can be attributed at least partly to the absence of any significant weather in this area, and it seems that the cold outflow was confined to the west side of Hampstead. Clearly the storm could not have produced a symmetrical outflow without its supply of warm air being cut off.

We can show that an asymmetric outflow consistent with these observations is likely by considering the formula for

the rate of advance (c) of a model gravity current given by Simpson et al. (1976). They showed that

$$c = 0.4\bar{u} + 0.8 \sqrt{g \frac{\Delta\theta}{\theta} H} ,$$

when the current of depth H and average temperature deficit  $\Delta\theta$  penetrates a medium in which there is some mean fluid flow (velocity  $\bar{u}$ ). Although  $\Delta\theta$  and H can only be estimated, it is easy to show that, given the ambient wind field, an 'ideal' density current would flow out fastest to the north of Hampstead, rather slower into the weak south-westerly winds, and become almost stationary to the south-east, where the surface flow was somewhat stronger. A stationary (or slow-moving) downdraught front in such a position could have induced ascent of air over it, and ensured a regeneration of the convection. This feature is emphasized in the results of the computer simulation, and appears to provide a crucial mechanism for the persistence of the storm.

#### 4.4 THE ROLE OF TOPOGRAPHY

In view of the striking localization of the rainfall over the relatively high ground of north London, as shown in figure 4.1, it is pertinent to consider the possible influences of the topography on the initiation or persistence of the storm. The general question of topographic features and their influence on convection has been considered in chapter II; here we shall attempt to identify an influence in a particular case.

The highest point of Hampstead Heath is a little over 400 ft above sea level, so that the maximum gradient of the south-facing slope is about 1 in 20 over a horizontal distance of 1 to 2 km. This gradient is too small for the slope to be a



better source of thermals than the environs (the ratio of solar flux per unit area falling on a sloping surface to that on a horizontal surface is simply  $\sin(\alpha + \beta)/\sin \beta$ , where  $\alpha$  is the gradient of the sloping surface and  $\beta$  is the angle of elevation of the sun. With  $\beta \sim 50^\circ$  and  $\alpha = \tan^{-1}(1/20) \approx 3^\circ$ , the ratio is less than 1.05). Orographic lifting could in theory account for a vertical velocity of (gradient x horizontal velocity), but this effect is unlikely to be important on such a small horizontal scale.

By virtue of its height, the surface potential temperature on Hampstead Heath is likely to be about 1 deg C above that of the surrounding area, and this might be expected to ensure that the high ground was a preferred location for the initiation of convection. It is clear, however, that in a south-easterly low-level wind, no cloud can have developed and released precipitation over the same area; furthermore the source of the convection was observed to be some distance upwind from Hampstead.

The effect of sloping terrain on a cumulonimbus outflow has been mentioned in chapter III (section 3), but if as before we regard the downdraught as a gravity current, the influence of a slope on the propagation speed is readily shown to be small for a gradient of only 1 in 20.

It appears then that the coincidence of the maxima of height and rainfall, which is one of the most striking features of figure 4.1, results from both occurring just the same distance downwind of the area where convection was initiated, which at first was the 'heat island' of central London, and subsequently the quasi-stationary squall front lying to the south-east of

Hampstead. As we shall see, the results of the computer simulations strengthen the view that the high ground of north London had no influence on the storm, since the model contains no representation of surface topography.

#### 4.5 SUMMARY

The Hampstead storm formed ahead of a slow-moving upper trough, and its initiation was determined by low-level convergence, increased values of  $\theta_w$  in the boundary layer (compared with preceding days), and a local maximum of surface potential temperature over Greater London.

The storm relied on an important heat source over central and south-east London which the downdraught did not flow over and remove; rather the environmental wind at low levels probably constrained the edge of the outflow to remain almost stationary to the south-east of Hampstead. This 'squall front' provided extra lift for the inflow and ensured the regeneration of convection.

Although rain fell continuously for nearly 3 hours, the convection is not described as 'steady'; the storm was composed of at least three cells, each of which grew over central London and reached cumulonimbus proportions when in the vicinity of Hampstead. It is suggested that the relatively high ground of north London had no influence on the location or duration of the storm.

It is now possible to suggest a model of the three-dimensional airflow through the storm. It has warm air in a low-level inflow from the south-east, rising over a squall front, and eventually flowing out to the north-east as the

anvil cloud at a height of about 10 km (as suggested by the parcel theory). Downdraught air is drawn in from the south or south-west at low to middle levels, and spreads quickly out to the north and north-west. Some of the outflow leaves more slowly to the south-west, but surface winds give rise to a quasi-stationary squall front lying approximately north-east/south-west on the south-eastern side of the storm.

Our observational description of the storm is based on data of variable reliability, and there are clearly some aspects of the simple, qualitative model which may be open to doubt. It was decided, therefore, to attempt a three-dimensional numerical simulation of the Hampstead storm, using a computer model already well-established in the representation of tropical cumulonimbus convection. The objects of the experiment were firstly to obtain further insight into the important dynamical features of the storm and relate these to observational details, and secondly to extend the applicability of the model to situations of 'mid-latitude' convection. As we shall see in chapter V the experiments were fruitful, regarding both the understanding of the Hampstead storm and also the model's parameterization of microphysical processes.

CHAPTER V : THE HAMPSTEAD STORM - NUMERICAL STUDY

Examination of the observational data has suggested a qualitative model of the Hampstead storm. However, its most important feature, the quasi-stationary squall front which initiates fresh convective cells on the south-eastern side of the storm, has been proposed partly on the basis of a lack of observations, and clearly requires further dynamical justification. The results of the numerical simulations described in this chapter allow us to relate the dynamical character of the storm to observed details; the ultimate intention was not to derive and compare two independent models of a stationary storm, but rather to use the two techniques of observational and numerical analysis in a complementary fashion to suggest a 'unified' cumulonimbus model (in the same way that Moncrieff and Miller, 1976, combined analytical and numerical techniques).

5.1 THE NUMERICAL MODEL

The numerical model employed in the simulation is a three-dimensional primitive equation model, using pressure as a vertical coordinate and a grid of 30 x 30 x 10 points (giving a domain 29 km x 29 km x 900 mb). We shall not describe the model in detail here; its development and some initial simulations are discussed by Miller (1972) and Miller and Pearce (1974), and some recent modifications to the lower boundary condition, the grid configuration and other aspects are given by Moncrieff and Miller (1976). Simulation of the Hampstead storm required some adjustment to the microphysical parameterization to take account of the ice phase, and this will be discussed more fully later.

## Methodology

Previous simulations with the numerical model utilized the thermodynamic and wind sounding from a radiosonde ascent made just before the passage of a travelling storm. The sounding was used as an initial horizontally stratified model atmosphere, and was perturbed by a low-level heat or moisture source to trigger convection. In the case of the Hampstead storm, however, several factors precluded the adoption of a similar approach.

The nearest radiosonde station to London is at Crawley, which provides a temperature and wind sounding at 1200 and pilot balloon winds at 0600 and 1800. Section 4.2 of the previous chapter has already discussed the midday sounding and its representativeness, and how it was considered appropriate to modify the sounding as shown in figure 4.10 before using it as initial data for the simulation.

The first simulation (using the modified sounding) was initiated by a heat source of  $0.3 \text{ deg C min}^{-1}$  at four grid points and  $0.2 \text{ deg C min}^{-1}$  at the surrounding twelve points at the 850 mb model level. The heat source was applied for the first three minutes of simulation time, and resulted in a maximum perturbation of about  $0.6 \text{ deg C}$ . (It is important that the energy input of the applied temperature perturbation is small compared to the convective available potential energy, otherwise the resultant motion is dependent on the nature of the initial heat source rather than the stratification of the model atmosphere.)

The initial perturbation developed rapidly, and after 25 minutes of simulation time had deepened sufficiently to produce

the first rain at the ground. However, despite large quantities of liquid water aloft, only a few millimetres of rain reached the surface, and after 50 minutes the cumulonimbus cell had almost dissipated with only some medium and high cloud remaining. A downdraught outflow appeared at the surface, but it was short-lived, rapidly spreading out and losing its identity.

The failure of the model to produce significant rainfall at the surface is likely to be due to one of two factors. Either the convection was insufficiently deep and vigorous to generate adequate concentrations of liquid water aloft, or the microphysical parameterizations (which determine the phase changes and fall-out of the water substance) were at fault. As mentioned above, the convection in the first simulation was of considerable depth and intensity; updraughts within the model cloud attained speeds of up to  $25 \text{ m sec}^{-1}$ , and liquid water concentrations reached  $10 \text{ g kg}^{-1}$ . These values should be sufficient for substantial amounts of rainfall at the ground, and so it was decided to consider possible inadequacies of the microphysical parameterizations used in the model.

#### The model microphysics

Four main processes relating to the evolution of water substance are modelled. They are:

- (i) the auto-conversion of cloud droplets to raindrops,
- (ii) the coalescence process of raindrop growth,
- (iii) the evaporation of raindrops, and
- (iv) the fallspeeds of raindrops.

The basic equations are

$$\frac{D}{Dt} (q + l_c) = - \text{PROD} \quad (5.1)$$

and 
$$\frac{D}{Dt} l_r = \text{PROD} - g \frac{\partial}{\partial p} (\rho l_r V_t) \quad (5.2)$$

where  $l_c$  and  $l_r$  are the cloud water and rainwater concentrations (in  $g \text{ kg}^{-1}$ ),  $q$  is the specific humidity and  $V_t$  is the mean terminal velocity of raindrops relative to the air.

The rainwater production term, PROD, is given by

$$\text{PROD} = P_1 + P_2 + P_3$$

where  $P_1$  (the evaporation of raindrops) is parameterized as

$$P_1 = \beta (q - q_s)$$

Here  $\beta$  is a variable parameter and  $(q - q_s)$  is the saturation deficit. The accretion of cloud water by rainwater (parameter  $P_2$ ) is taken as

$$P_2 = \gamma l_c l_r^{0.95}$$

and the conversion of cloudwater to rainwater as

$$P_3 = \alpha (l_c - l_{crit})$$

where  $\gamma$  and  $\alpha$  are variable parameters.  $l_{crit}$  is a cloud water value below which there is no auto-conversion; once  $l_c$  exceeds  $l_{crit}$  the rate of production of cloudwater is largely determined by the value of  $\alpha$ . (Note that the only distinction between cloudwater and rainwater is that the former moves only under the influence of the local air motion, while the latter possesses an additional terminal fallspeed.) The factors  $\alpha, \beta$

and  $\gamma$  and the fallspeed  $V_t$  were all unchanged from the tropical simulations described in Moncrieff and Miller (1976).

The lack of rainwater reaching the surface suggested either that too great a proportion of the water substance aloft was in the form of cloudwater which never fell from the cloud and eventually evaporated at upper levels, or that although ample rainwater was present in the cloud, it was unable to escape from the updraught and fall to the ground. In order to identify the problem a second simulation experiment was carried out, in which the conversion and coalescence rates (factors  $\alpha$  and  $\gamma$ ) were both increased by a factor of five. This resulted in large concentrations of rainwater in the cloud (particularly at middle levels) but only a doubling of the rainfall reaching the surface.

One of the most important features of the numerical model's parameterization scheme is that it takes no explicit account of the formation of ice. In the case of tropical convection, to which the model had previously been applied, the ice phase is generally unimportant; in mid-latitude cumulonimbus, on the other hand, the freezing of water at upper levels is a significant feature. (One reason for the scarcity of hail in the tropics was suggested by Ludlam (1963); because the environmental wind shear associated with severe cumulonimbus causes the anvil to trail behind the storm rather than in front, the small hailstone embryos which fall from the upper level outflow mostly enter the downdraught and so are denied the opportunity of being recycled and growing into large hailstones in the updraught.) Because rainwater was unable to escape from the model cumulonimbus updraught rapidly



enough to produce significant quantities of rain at the ground, it was decided to attempt a simple modification to the parameterizations which would take account of the presence of hail.

The mean terminal velocity of raindrops relative to the air (equation 5.2) is given by

$$V_t = \delta l_r^{0.2}$$

where  $\delta$  in the original simulations took the value  $5.32 \text{ m sec}^{-1}$  (after Liu and Orville, 1969). It was envisaged that the presence of hail could be crudely modelled by incorporating a weighted average of raindrop and hailstone fallspeeds, so the factor  $\delta$  was increased to  $10.0 \text{ m sec}^{-1}$ . This action almost doubled the parameterized rainwater fallspeed, and had fundamental consequences on the rainfall from the storm and its ultimate structure and behaviour, in striking contrast to the lack of sensitivity shown in the modification of other microphysical parameters.

The initial cumulonimbus cell in the first simulation with the increased raindrop fallspeeds now produced up to 20 mm of rain at the ground - almost ten times the amount which resulted from earlier simulations.

An important feature of the numerical experiments described in Moncrieff and Miller (1976) was the way in which the downdraught from the primary cumulonimbus cell propagated outwards near the surface as a density current, thereby giving rise to convergence in the boundary layer and subsequently initiating fresh convective activity. However, although the increased rainfall from the primary cell of the

Hampstead simulation produced a strong downdraught and convergence near the surface, it failed to initiate further convection. Inspection of the moisture and temperature fields generated by the model revealed that low-level convergence had, nevertheless, brought large regions of air very close to saturation; in view of the modifications already made to the original thermodynamic sounding, it was decided to make a further small increase in the mixing ratio at the 750 mb level, so that at least parts of these regions would attain saturation when the simulation was repeated.

## 5.2 THE SIMULATION

Following the initial experiments described above, an extended simulation was carried out, in which the model continued to run for over 90 minutes (simulation time). The initial perturbation (situated south-south-east of the centre of the horizontal grid) moved slowly towards the north-west at a speed of about  $4 \text{ m sec}^{-1}$ , but rapidly grew into a mature, precipitating cumulonimbus cell while moving towards the north-north-east. Figure 5.1 shows a vertical section through the primary cell, 30 minutes after the initiation of convection. The precipitation-generated downdraught can be clearly seen, and is already beginning to spread out at the surface; figure 5.2(a) shows the cool air outflow in plan view. At this stage an important feature is apparent, namely the elongation of the rainwater and height and potential temperature deviation fields in the north-east/south-west direction (see figures 5.2(b) and (c)). As we shall see, this elongation of the fields across the low-level winds is of considerable significance in the regeneration of convection, and it was maintained throughout the simulation.

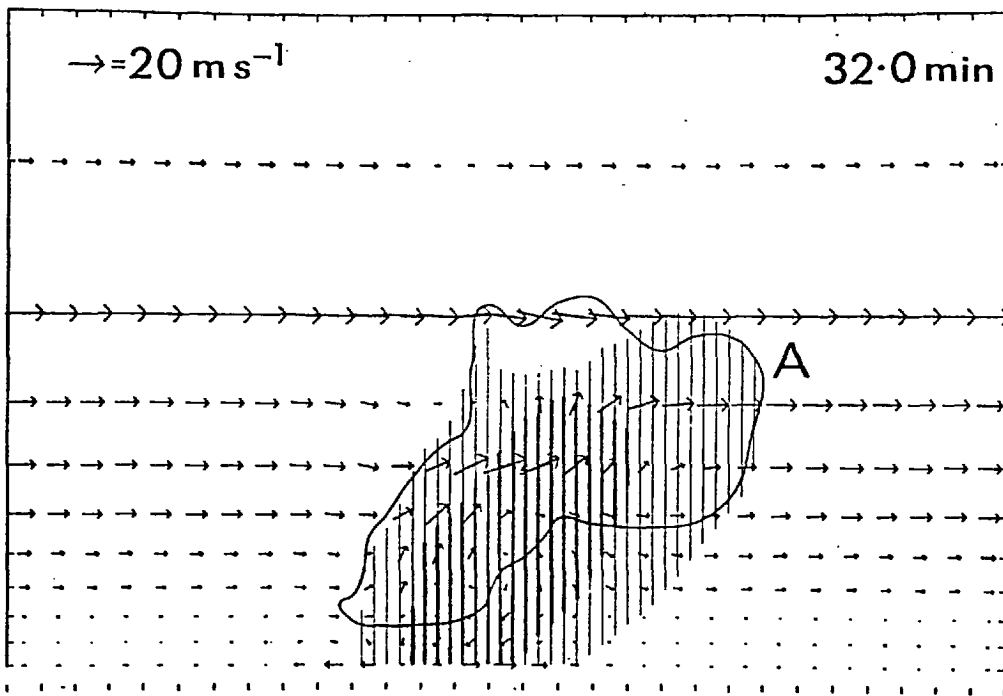


FIG. 5.1

Vertical section through numerical model showing flow (relative to the ground) in the plane aligned along  $210^\circ/030^\circ$  (left to right); vector arrows are formed from the wind components in this plane only. Diagram includes  $0.1 \text{ g kg}^{-1}$  cloudwater contour and hatching for rainwater (light  $>0.1 \text{ g kg}^{-1}$ , dark  $>2.0 \text{ g kg}^{-1}$ ).

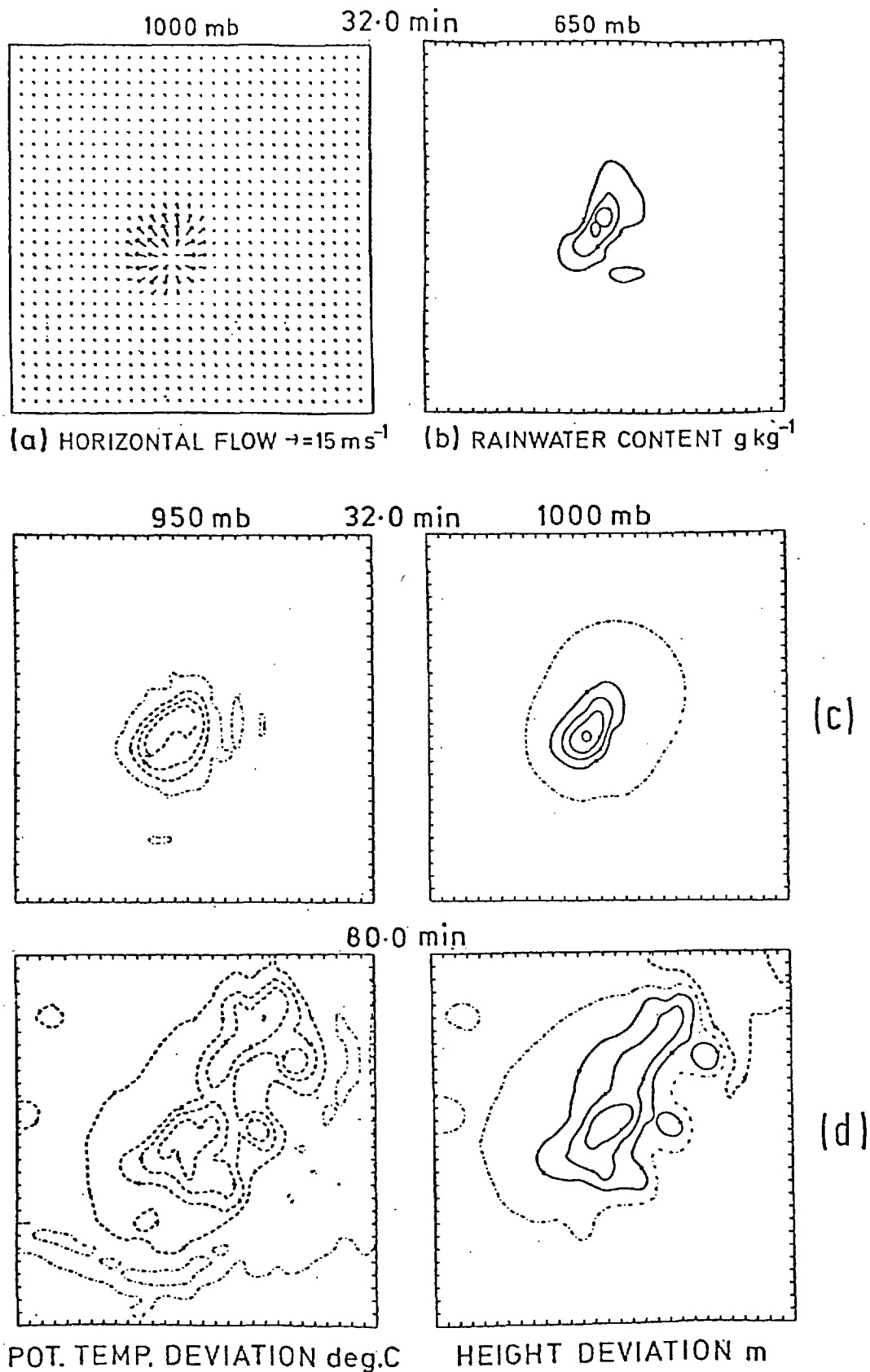


FIG. 5.2

- (a) Horizontal winds on a pressure surface in vector form.
- (b) Rainwater concentrations; 0.1, 2.0 and 4.0  $\text{g kg}^{-1}$  contours.
- (c) } Potential temperature deviation; contours every 1 deg C.
- (d) } Height deviation; contours every 3 m.

Positive contours are continuous, negative contours are pecked.  
The zero contour is 'dot-dash'.

Development of secondary cell and downdraught

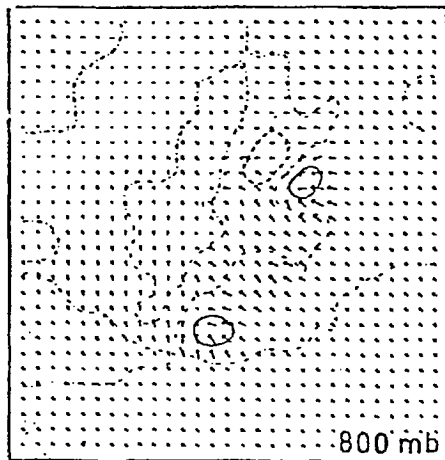
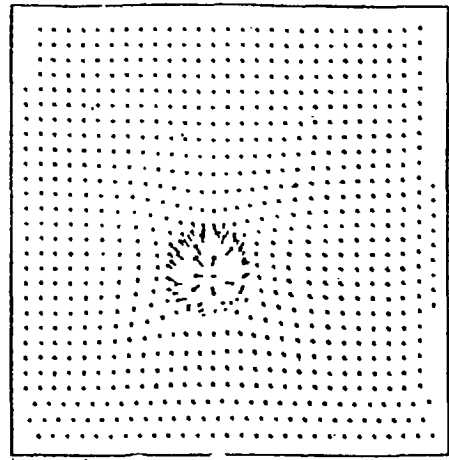
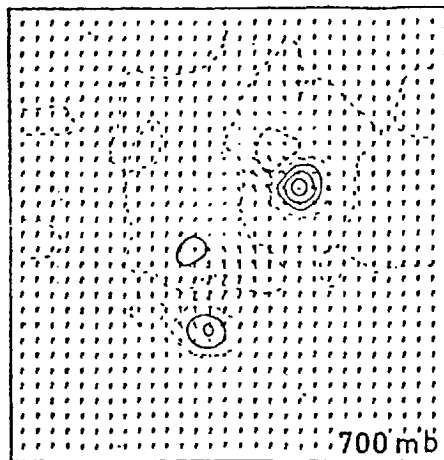
Figure 5.3(b) shows that the spreading downdraught from the primary cell gave rise to a shallow ring of cloud near the surface which was generally short-lived and soon dissipated in most regions. The strongest boundary-layer convergence was on the south-east flank of the downdraught outflow where it opposed the low-level winds; here new convective cells were generated which evolved through a life-cycle similar to that of the primary cell, moving from the south while growing until they merged with a larger region of raining and decaying cells. Once mature and producing precipitation, the cells moved in a north-easterly direction, thus contributing to the elongated anvil and rain area. The multi-cellular development of the storm is clearly evident in figure 5.3(a) which shows two distinct areas of horizontal convergence and updraught, and in figure 5.5, which is a vertical section through the cumulonimbus system.

After about 80 minutes of simulation time further cells began to develop along the downdraught squall front. One of these was, after 96 minutes, so close to the northern boundary of the grid that the simulation was terminated due to the model's inability to handle strong updraughts at grid points near the edge of the domain.

The development of the cool outflow at the surface is shown in figure 5.3(c), (d) and (e). The downdraught from the primary cell spread out rather rapidly to the north and north-west, less so towards the north-east and south-west, and only very slowly to the south-east; this shape evolves as a consequence of the interaction between the outflow and

FLOW FIELD ON A PRESSURE SURFACE (except (b))

$\rightarrow = 15 \text{ m s}^{-1}$



(a) 60.0 min

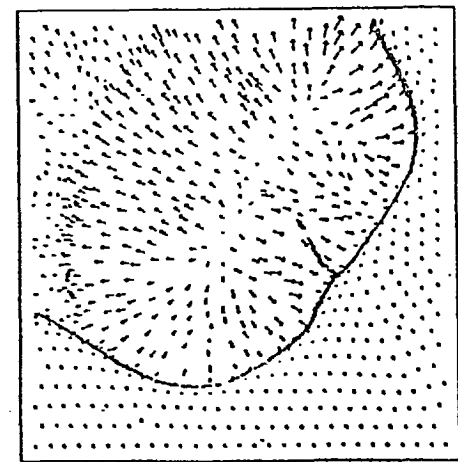
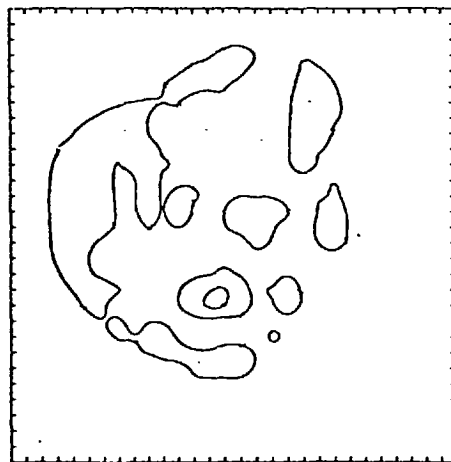
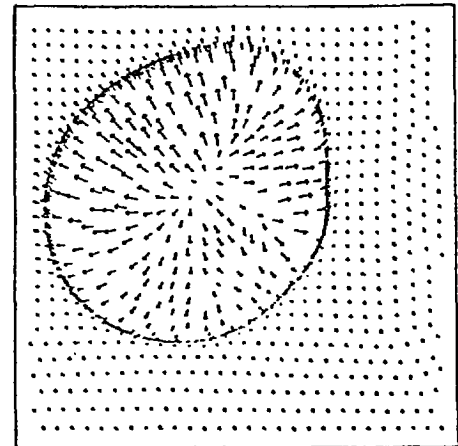


FIG. 5.3

- (a) Horizontal winds on a pressure surface in vector form, with vertical velocity contours every  $3 \text{ m sec}^{-1}$ .
- (b) As fig. 5.2(b) for cloudwater.
- (c) to (e) Horizontal winds on a pressure surface, allowing vectors to move with their local velocity

the ambient flow near the surface (the model is unable to resolve the depth of the outflow since the vertical grid spacing is equivalent to a 100 mb layer of atmosphere). The quasi-stationary south-eastern edge of the outflow is located about 6 km to the south-east of the rainfall maximum, and moves only about a kilometre or so during an hour of simulation (equivalent to a speed of less than  $0.5 \text{ m sec}^{-1}$ ). Towards the north-west the downdraught 'squall-front' moved at about  $10 \text{ m sec}^{-1}$  and at about  $3 \text{ m sec}^{-1}$  towards the south-west. These figures compare remarkably well with observed values (see chapter IV, section 3).

#### Rainfall

Figure 5.4 shows the simulated rainfall rates and totals after 40 and 80 minutes. The rainfall pattern produced by the primary cell is maintained by subsequent cells with a pronounced local maximum of 45 mm; inspection of the computer output indicated that this maximum was formed mainly during two periods of more intense rain between 24 and 44 minutes and again between 60 and 84 minutes. Typical rainfall rates were between 25 and  $50 \text{ mm hr}^{-1}$ , but during the intense rain values of up to  $200 \text{ mm hr}^{-1}$  for one minute occurred. The agreement between simulated and observed rainfall rates, totals and distribution (compare figures 5.4 and 4.1) are encouraging, and suggest that the crude modification made to the micro-physical parameterization scheme is adequate in many respects.

#### Multicellular structure

Figure 5.5 is a vertical section through the cumulonimbus system, along a line orientated  $210^{\circ} - 030^{\circ}$  from north. It is, of course, difficult to show meaningful cross-sections, since

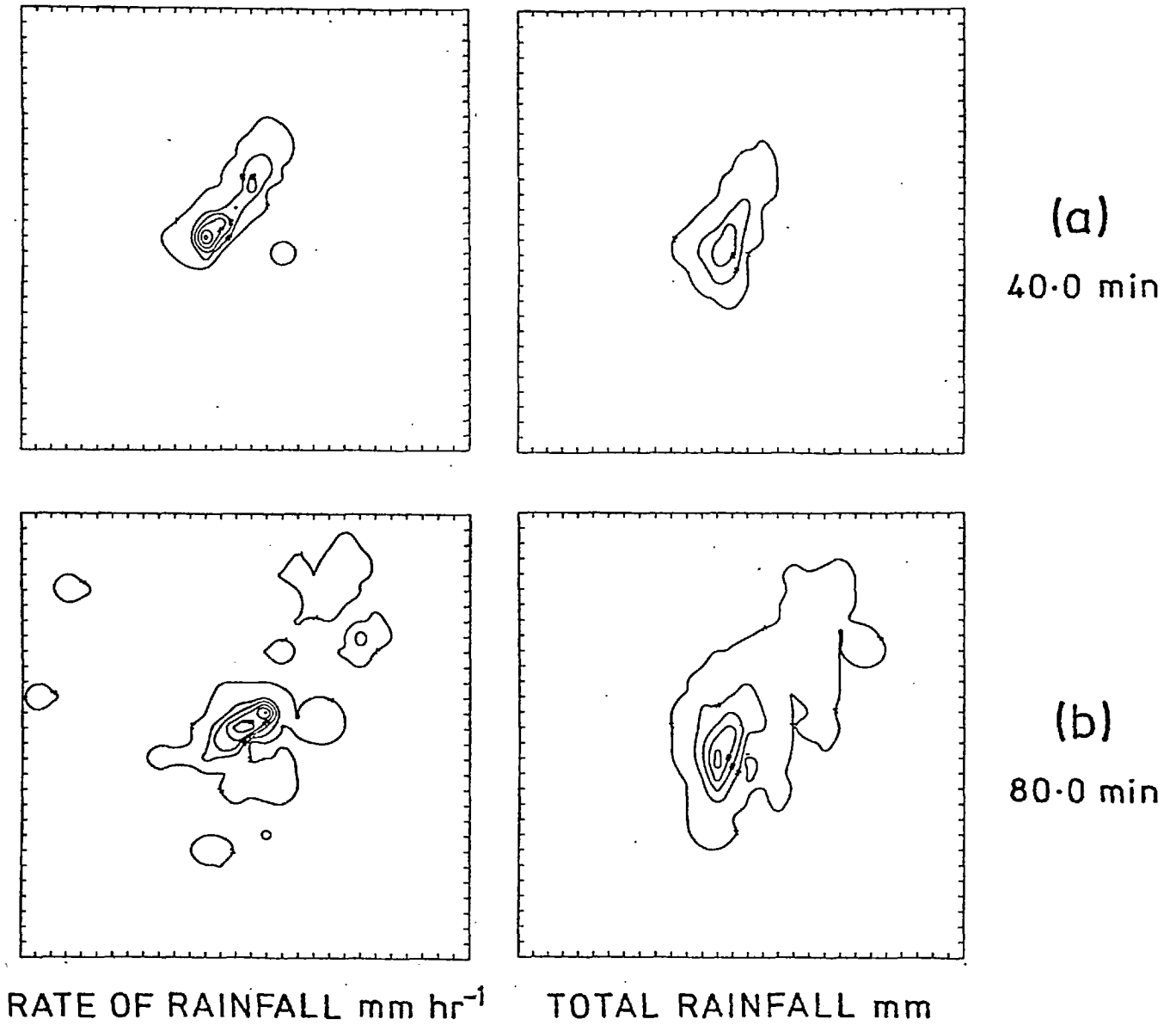
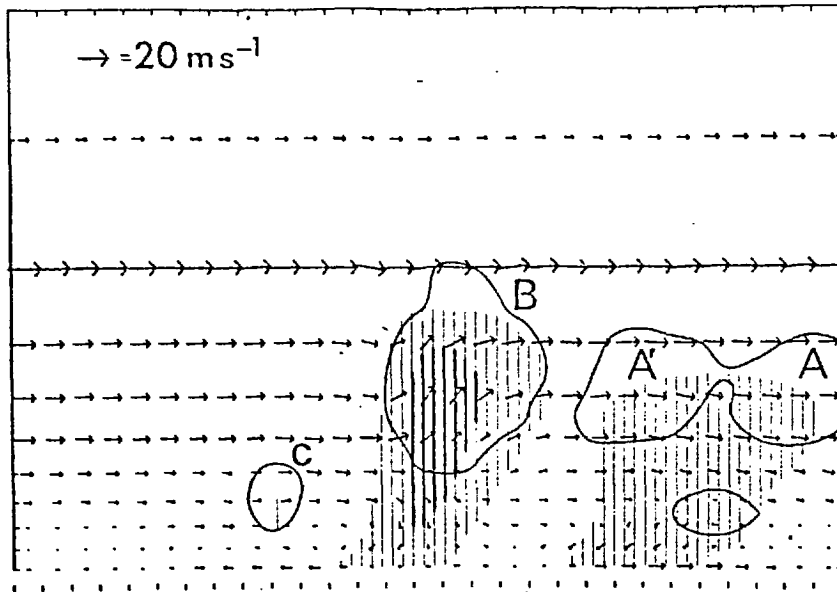


FIG. 5.4

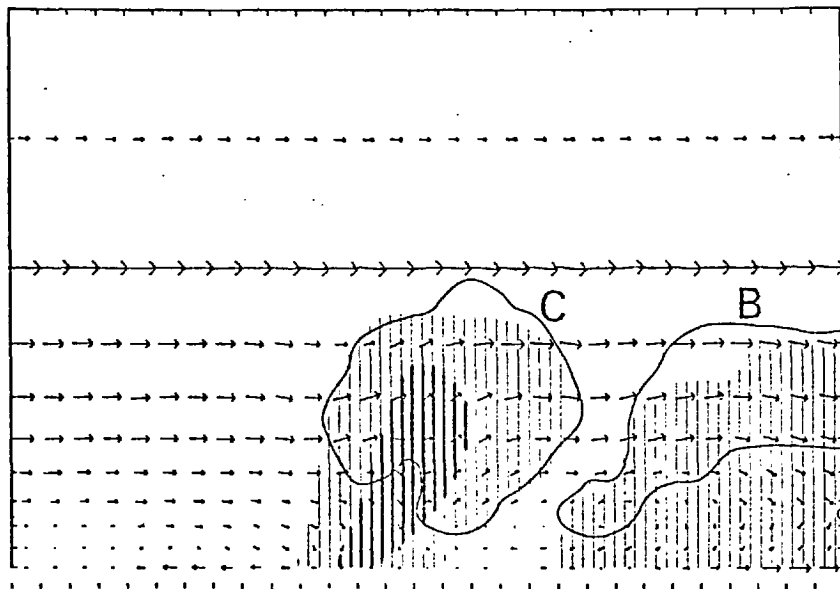
Rainfall rates (contours every 25 mm hr<sup>-1</sup>) and totals (contours every 10 mm).





(a)

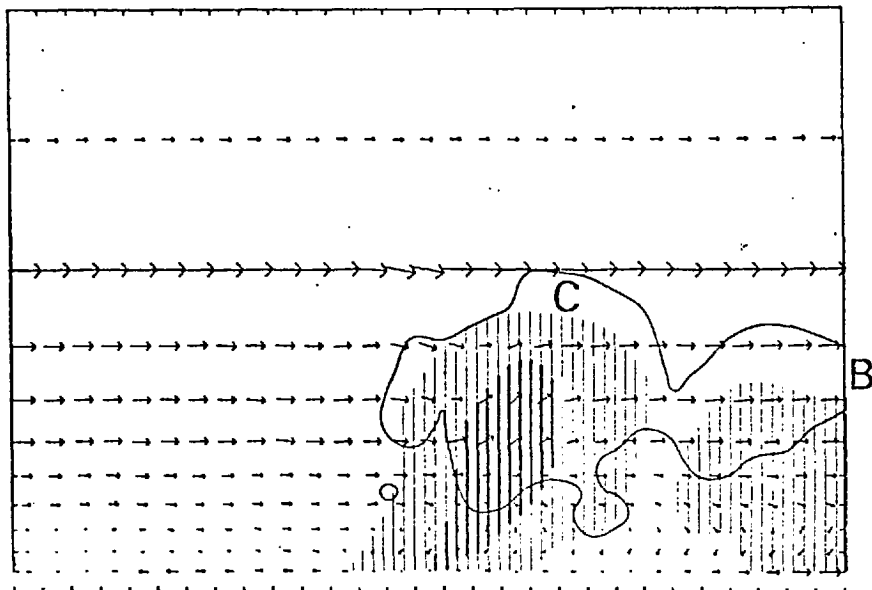
64.0 min



(b)

76.0 min

(A')



(c)

80.0 min

FIG. 5.5

Vertical sections through model, as fig. 5.1.

the individual cells of the storm move in rather curved paths. However, when the cells are in the mature and decaying stages they do move approximately in the direction  $210^{\circ} - 030^{\circ}$ , and the cross-sections are a reasonable two-dimensional representation of the three-dimensional structure. (Rotation of the simulated fields is necessary since the line  $210^{\circ} - 030^{\circ}$  is not parallel to a line of grid points. Such a rotation required some simple interpolation, and results in the loss of data close to the boundaries of the grid domain, although this is not serious.)

The section clearly shows the consecutive evolution of three cumulonimbus cells (labelled A, B and C). After 64 minutes (figure 5.5(a)) the primary cell A is decaying, producing only moderate rain and containing no upward vertical motion. Cell B is approaching the peak of its maturity, and contains strong updraughts with heavy rain (indicated by the darker hatching) about to reach the ground. Further to the south-west, cell C, still at the 'cumulus' stage, has recently moved into the plane of the section.

After 76 minutes (figure 5.5(b)) cell B is dominated by downdraughts as it decays, merging as it does so into the anvil extending in a north-easterly direction. Cell C is now fully mature, producing heavy rain at the ground. Its evolution continues as the rainfall becomes less intense and it eventually begins to merge with the remains of cell B (figure 5.5(c)).

### 5.3 THE HAMPSTEAD STORM MODEL

Comparison of the numerical simulation results and the observational details described in chapter IV reveals considerable agreement in many aspects of the storm, most notably with

regard to the rainfall rates and distribution, the shape of the downdraught outflow and the multicellular structure. The model results support the earlier suggestion of a stationary squall front on the south-eastern flank of the storm, which, through convergence near the surface, initiated fresh convective cells. Because the edge of the outflow was stationary (or at least very slow-moving) in this position, each cumulonimbus cell reached maturity and produced rain over the same area of ground, that is in the vicinity of Hampstead. The movement of individual cells was consistent with the ambient wind field; while still in the initial cumulus stage cells were subject to the low-level wind and so moved in a north or north-westerly direction. When they reached the mature and dissipation stages the cells were of greater vertical extent and so were affected by the wind at higher levels, moving in a north-easterly direction.

While the impulsive nature of the storm was clearly an important feature, it appears that the basic configuration of low-level inflow, updraught region and anvil outflow, as well as the low-level downdraught outflow, were relatively steady throughout the simulation. In chapter IV we suggested a model three-dimensional airflow for the cumulonimbus system based on various observational data; the flow configuration in the model simulation was studied by computing trajectories from the four-dimensional fields provided by the computer (see Miller and Betts, 1977, for a description of this technique). Consideration of a large number of these computed trajectories (together with the figures already discussed) lead to a simple description of the storm's macrostructure in terms of major updraught and downdraught branches. Figure 5.6 is a schematic

view of the airflow; note that these trajectories approximate to streamlines relative to the ground since, on the time scale of the storm, they are sufficiently steady (in the sense that trajectories generated at different starting times have similar configurations). It seems reasonable to consider the storm as being impulsive on the scale of individual cells, but steady on the scale of the entire cumulonimbus system. We shall consider the question of 'steadiness' more fully in chapter VI.

The computed trajectories suggest a relatively deep updraught inflow (occupying the lowest 200 mb of the atmosphere) which approaches the storm from between  $135^{\circ}$  and  $115^{\circ}$ . Almost all of the upper-level outflow is contained within the 400 mb and 250 mb layers, and extends towards the north-north-east ( $030^{\circ}$ ). Downdraught air is largely drawn from the layer between the 600 mb and 800 mb levels, and flows into the storm from between  $210^{\circ}$  and  $160^{\circ}$ , and out at the surface (below the 900 mb level) towards the north-west (between  $300^{\circ}$  and  $340^{\circ}$ ).

The way in which the updraught and downdraught flows are 'interlocked' is reminiscent of a model proposed by Browning (1964) of a severe right-moving storm (that is one which travels appreciably to the right of the wind in the middle troposphere). There are, of course, considerable differences between Browning's large single supercell with its continuous propagation relative to the ground, and the stationary yet impulsive multicellular characteristics of the Hampstead storm; nevertheless the configurations of winds relative to the storms are similar, as is the way in which downdraught air enters the storm and curves

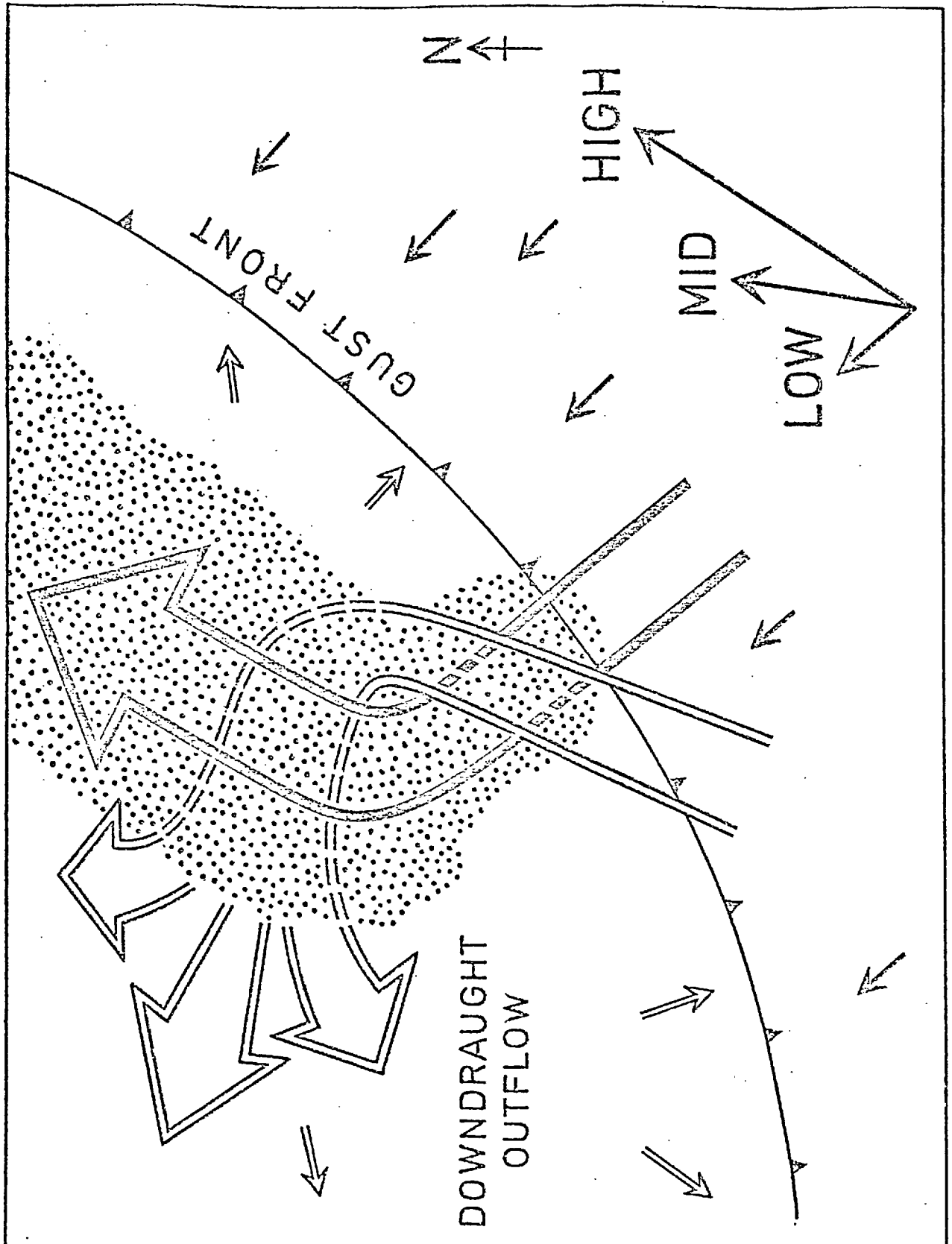


FIG. 5.6

A schematic representation of the main features of the Hampstead storm model.

cyclonically around the updraught.

#### 5.4 MODELLING IMPLICATIONS

As we have suggested in earlier chapters, showers in a generally unstable atmosphere are likely to be widespread and not very intense. In the case of the Hampstead storm, conditions were not notably unstable, so that the convection was localized by processes operative over London. The modifications made to the upper air sounding (see sections 4.2 and 5.1) are therefore fundamental to the occurrence of cumulonimbus convection over the London area, and were effected by typical daytime boundary layer evolution enhanced by a meso-scale convergence field and the urban 'heat island' (the relative importance of these two mechanisms is unresolved). Preliminary simulations indicated that the generation of new convective cells near the edge of the downdraught outflow was rather sensitive to the boundary layer properties of the sounding used as input data; the sounding which was used in the final simulation probably represented marginally too great an ability to support the growth of new cells, and it was this feature which led to the premature termination of the simulation. A numerical model of much better resolution would be required to examine this sensitivity further.

Even though the simulation experiments are based on highly simplified parameterizations, some of the microphysical implications seem rather complex. As we have suggested, the transition from the simulation of tropical to colder, mid-latitude clouds requires an increase in the mean fallspeed of water substance within the cloud. This increase is a simple representation of the presence of hail, which is not specifically

parameterized in the model. That the average size (and hence fallspeed) of raindrops is larger in mid-latitude clouds is supported by the recent results of List and Gillespie (1976); they discuss and quantify in some detail the distinction between 'warm' (tropical) rain and 'cold' rain (which arises from the melting of ice particles).

As far as the cloud dynamics is concerned the most important role of the ice phase (or of the precise form of dropsize spectrum) is that of determining how quickly water is released from the storm. The way in which the numerical model represents the evaporation of rain does not incorporate any dependence on dropsize; questions concerning the relation of evaporation to the size, number and availability of raindrops require further investigation. Nevertheless, the cooling of downdraught air in the model compares well with observed changes in surface temperature.

### Summary

The combination of observational analysis and numerical simulation has yielded a graphic and dynamically consistent model of a quasi-stationary severe cumulonimbus, which consisted of several convective cells exhibiting similar and consecutive life-cycles. The interaction between the downdraught outflow and the low-level ambient wind was responsible for the generation of new cumulonimbus cells, each of which produced rain a similar distance downwind.

CHAPTER VI : DISCUSSION AND GENERALIZATION OF THE HAMPSTEAD MODEL

In this chapter we shall discuss some of the dynamical points which have arisen from our description of the Hampstead storm, particularly the problem of 'impulsiveness' (which has implications for the efficiency of generation of precipitation as well as the propagation of the convective system), and the role of a vector wind shear (that is, a change of wind direction with height) in maintaining a regenerating cumulonimbus system. Further case studies help support several of the ideas presented here.

6.1 PRECIPITATION EFFICIENCY AND IMPULSIVENESS

In the introduction to this thesis we referred to the distinction between ordinary, impulsive cumulonimbus convection and the less common travelling severe storm, which is characterized by a quasi-steady configuration of updraught and downdraught with both branches of the circulation existing 'symbiotically' for periods up to several hours. The 'supercell' storm (as it was called by Browning, 1962) requires a comparatively rare combination of atmospheric parameters, but the weather associated with it is notably severe, often with violent squalls and large hail. However, the results of airflow and moisture budgets carried out by several workers in the USA indicate that the more severe storms have rather low precipitation efficiencies (defined in terms of the total rain at the surface and the moisture content of the updraught inflow). Auer and Marwitz (1968) estimated precipitation efficiencies of less than 35% for two hailstorms (which were severe enough to produce hailstones 5 cm in diameter); efficiencies were 55% and close to 100% for less severe storms which produced



moderate size hail and no hail respectively. In an intensive analysis of a Colorado hailstorm by radar, rawinsonde and aircraft, Foote and Fankhauser (1973) calculated a precipitation efficiency of only 15%. They also reviewed previous work by relating precipitation efficiencies to the vertical shear of the horizontal wind; for high values of shear (greater than about  $3 \times 10^{-3} \text{ sec}^{-1}$ ) there was a strong inverse dependence, while the data points were more scattered for low shear.

One explanation of the low efficiencies of supercell storms is that strong winds aloft tend to carry large quantities of water substance downwind in the anvil outflow; precipitation thus falls out of the cloud through an unsaturated environment, and much of it may evaporate completely before reaching the ground. Another reason may be the rather large size of the vault in supercell storms, as suggested by Browning and Foote (1976). (The vault was first identified by Browning and Ludlam (1962) as a region of updraught so strong that water vapour had insufficient time to condense in it.) Normally some cloud water is converted to precipitation near the edge of the vault in the process of accretion of supercooled cloud droplets by hail, but if the vault extends far enough upwards, cloud water freezes homogeneously before it has been converted to precipitation and may pass through the storm without falling out.

Evidently, less severe, more impulsive cumulonimbus are likely to be more efficient producers of rain than the supercell, since updraughts are not so strong and they do not produce such large anvil clouds. Since we have described the Hampstead storm as an impulsive cumulonimbus system, it would be interesting

to obtain some estimate of its precipitation efficiency. Such a computation is, however, hardly possible due to a lack of the necessary data; nevertheless a simple moisture budget obtained from the numerical simulation results might be expected to give further insight into the model's handling of the rain-producing mechanisms.

In figure 6.1 we have plotted cumulative values of the mass of water entering the cloud together with the total rainfall at the ground for 88 minutes of simulated convection. The flux of water substance into the cloud was obtained by integration of the grid point vertical velocities at the 750 mb level (chosen as the closest model surface to cloud base with well-defined updraughts) and assumed a mean water vapour mixing ratio for the inflowing low-level air. Figure 6.1 also shows the evolution of the precipitation efficiency, which is defined as the mass of rainwater reaching the surface divided by the total mass of water transported into the storm. We can see that the efficiency appears to reach a steady value near 20% by the time that the system of mature and decaying cumulonimbus has been established. In the context of the earlier discussion this is a much lower value than would have been expected of the real storm; in the rather low wind shear conditions of the Hampstead storm (compared to those of the supercells of the USA) it is likely that microphysical processes are of prime importance in determining the precipitation efficiency (as suggested by Foote and Fankhauser, 1973). The inference to be drawn, therefore, is that despite the adjustments made to the model in the transition from tropical to mid-latitude simulations, the microphysical parameterization scheme is still rather inefficient in releasing precipitation

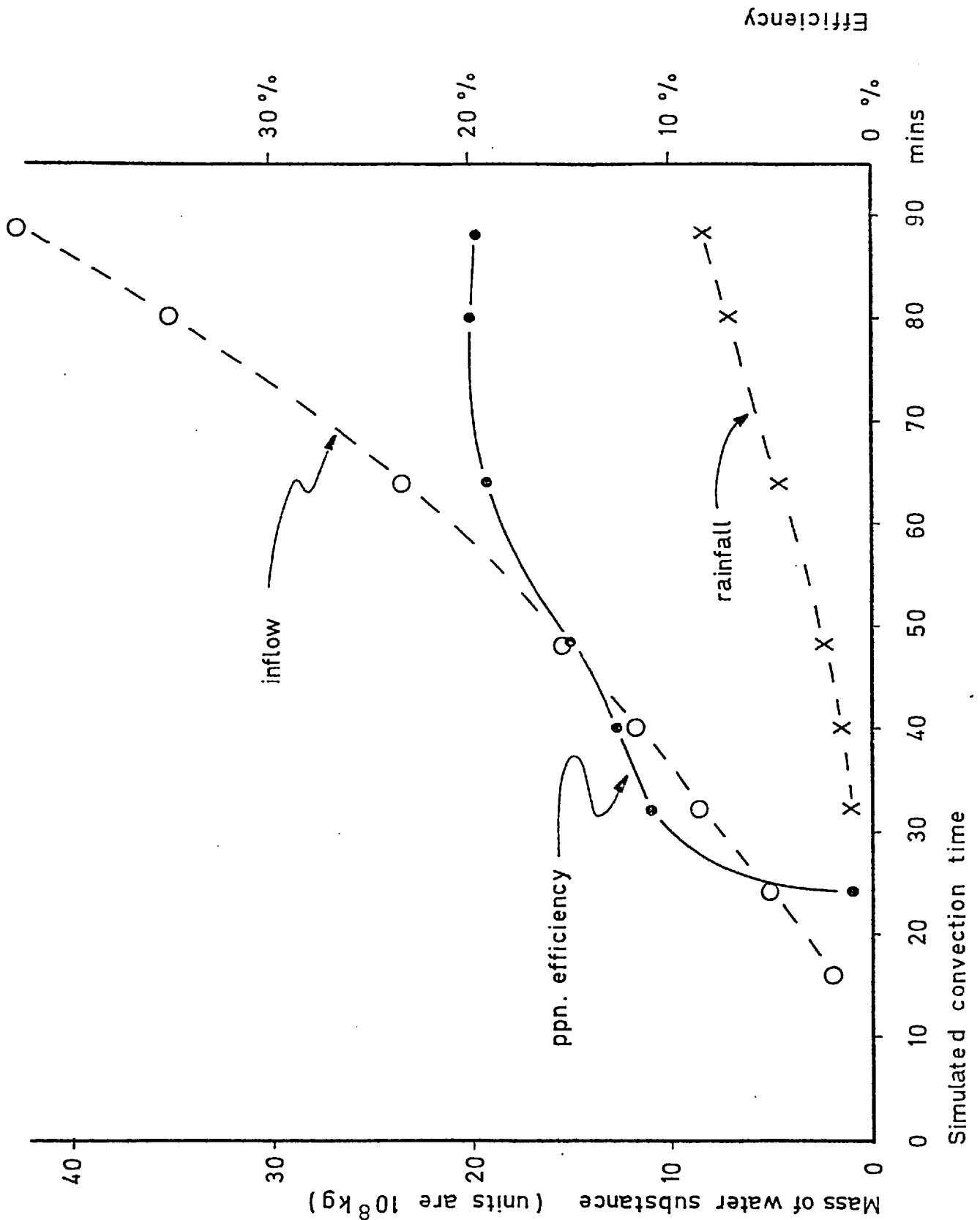


FIG. 6.1

Cumulative values of the mass of water entering the storm and the mass of water appearing as rain at the ground in the Hampstead simulation. Precipitation efficiency (right hand ordinate) is defined as the ratio of rainfall to inflow.

from the cloud, although in this case there was sufficient rainfall to reproduce the important dynamical features of the storm, particularly those which depend on the production of a strong downdraught. Further research is clearly necessary to determine whether the present parameterization can be generalized to the simulation of other mid-latitude storms, or whether a certain amount of 'tuning' is required in each situation.

#### Impulsiveness and cell movement

In their theoretical and numerical study of a tropical cumulonimbus, Moncrieff and Miller (1976) discussed the steadiness of the convective system and its relation to the downdraught outflow. In accordance with the observed characteristics of squall lines, a system which propagated relative to the ambient flow at all levels was sought; perturbation analysis showed that the development of such an amplifying wave required a finite amplitude mechanism. The initial perturbation in the numerical simulation produced a cumulonimbus, which, as it decayed, gave rise to a strong downdraught. On reaching the ground the cool air propagated as a density current, part of which moved relative to the winds at all levels, and the boundary layer convergence between the outflow and the wind near the surface initiated the 'second generation' cumulonimbus which comprised the squall line of the study.

Thus the authors recognized the essential cooperation between the updraught and downdraught branches of the circulation, and suggested that for a regime of steady convection to be maintained (in other words, a situation in which the airflow configuration is maintained for a period which is long compared to the time taken for individual 'parcels' of air to move

through the system) the propagation speeds of the cumulonimbus and the density current have to be equal. The speed of the cumulonimbus depends on the convective available potential energy, whereas that of the density current is a function of its depth and potential temperature deficit; thus a particular combination of parameters would be required in order to maintain a steady system. If the two speeds are not equal, the convection either becomes impulsive or ceases altogether, since the density current can advance far enough ahead of the convective system to cut off the supply of boundary layer air forming the updraught inflow (this was also suggested by observations reported by Zipser, 1969).

It is interesting to extend these ideas to the case of the Hampstead storm, where, as we have seen, the development of secondary cells depended on the low-level convergence between the cool downdraught and the ambient flow near the surface. There is clearly a difference in the propagation speed of the density current (which was almost stationary relative to the ground on the south-eastern flank of the storm) and the individual cells of which the storm was composed, which moved away from the edge of the downdraught front. (Examination of the numerical results shows that when the cells are mature they have a velocity of between 9 and 10 m sec<sup>-1</sup> from the south-west, close to that of the wind near the 550 mb level.) Each of the successive cumulonimbus cells was characterized by a growth time between its cumulus and mature stage, and because these times were similar for each cell, each one deposited rain the same distance downwind from the region of boundary layer forcing. As before, the speed of density current relative to the ground depends on its depth, temperature deficiency and the

ambient low-level winds; the equation given in chapter IV, section 3 may be used to suggest the combination of parameters which would give rise to a stationary gust front. It is possible to envisage a situation with weaker flow near the surface, in which the edge of the downdraught outflow would move away from the initial cumulonimbus cloud. Provided that the low-level convergence remained strong enough, we would expect the system to be more impulsive; moreover the rainfall patterns from individual cells would no longer be superimposed, since the position of the initiating mechanism would now be changing. In the extreme case of little or no surface wind, the downdraught outflow becomes symmetrical, and no further generation of convective cells takes place.

## 6.2 THE MILL HILL STORM

The task of intercomparison of the characteristic features of stationary storms is a difficult one; their comparative rarity and the consequent paucity of reliable observational data make it impossible to construct a composite model. The brief case study presented here, however, is of a storm which appeared to have some features similar to those identified in the Hampstead storm, namely an unusually large and localized rainfall, an impulsive, cellular structure and a relatively small directional shear of the environmental winds (see table 3.1) compared to the stationary 'mid-latitude' storm discussed in chapter III.

On the afternoon of 7th June 1963 a severe thunderstorm affected parts of north-west London. Rain fell for up to 2 hours in some areas, giving a total of nearly 100 mm near Mill Hill with a secondary maximum of 60 mm near Kensington

Palace (figure 6.2). An area of about 150 km<sup>2</sup> received more than 20 mm of rain; severe flooding occurred, particularly in the vicinity of Barnet, where the Dollis Brook rose by 3 ft.

#### The storm environment

The synoptic situation was changing only slowly during the first week of June 1963. Throughout the period from 00 on 6th to 00 on 8th Britain was under a relatively slack pressure gradient between an anticyclone off west Scandinavia and an Atlantic depression which was moving slowly eastwards. A surface and upper-level trough associated with the low pressure system extended eastwards towards Biscay, and a small thundery depression was almost stationary over central Europe. Figure 6.3 shows the surface and upper air analyses prior to the storm. Winds at the surface were generally light, from between north and east, and away from the coast temperatures were above average (reaching 26°C in London on 7th). From 6th to 13th June thunderstorms were reported from many parts of the country.

Figure 6.4 shows a time-height section based on aerological data from Crawley, covering the period 0000 on 6th to 1200 on 8th June. Changes in the stratification of the troposphere were rather slow; near the surface  $\theta_w$  increased gradually during most of the period, but at middle and upper levels  $\theta_s$  was also increasing. The most striking development was evidently in the wind structure, with the transition from south-easterlies at all levels (associated with the Atlantic low/Scandinavian high circulation) to a regime of lighter north-easterly winds as the depression over Europe became established.

Because of the rather large difference in the reported winds at 1200 and 1800 on 7th June, particularly near the

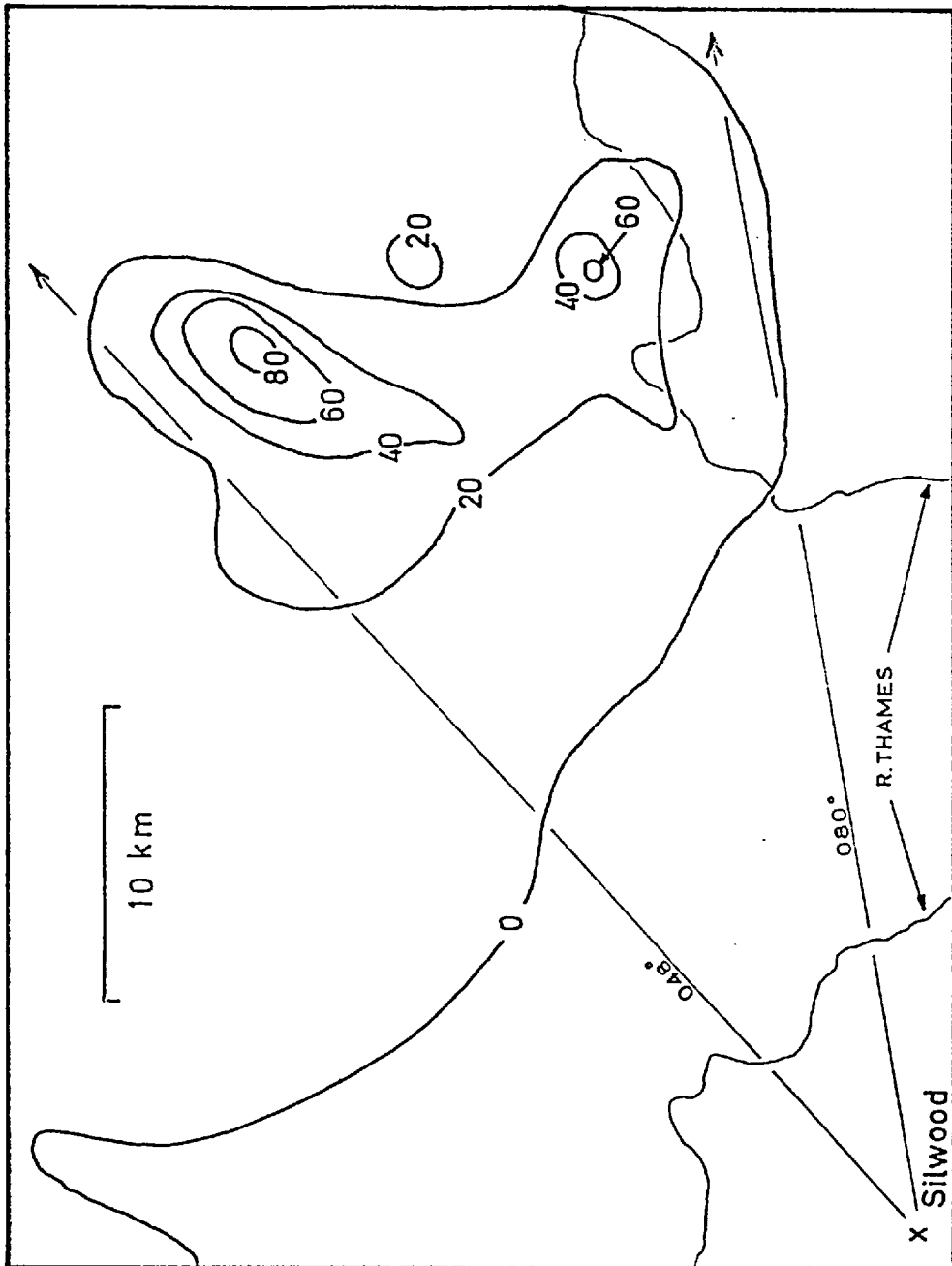
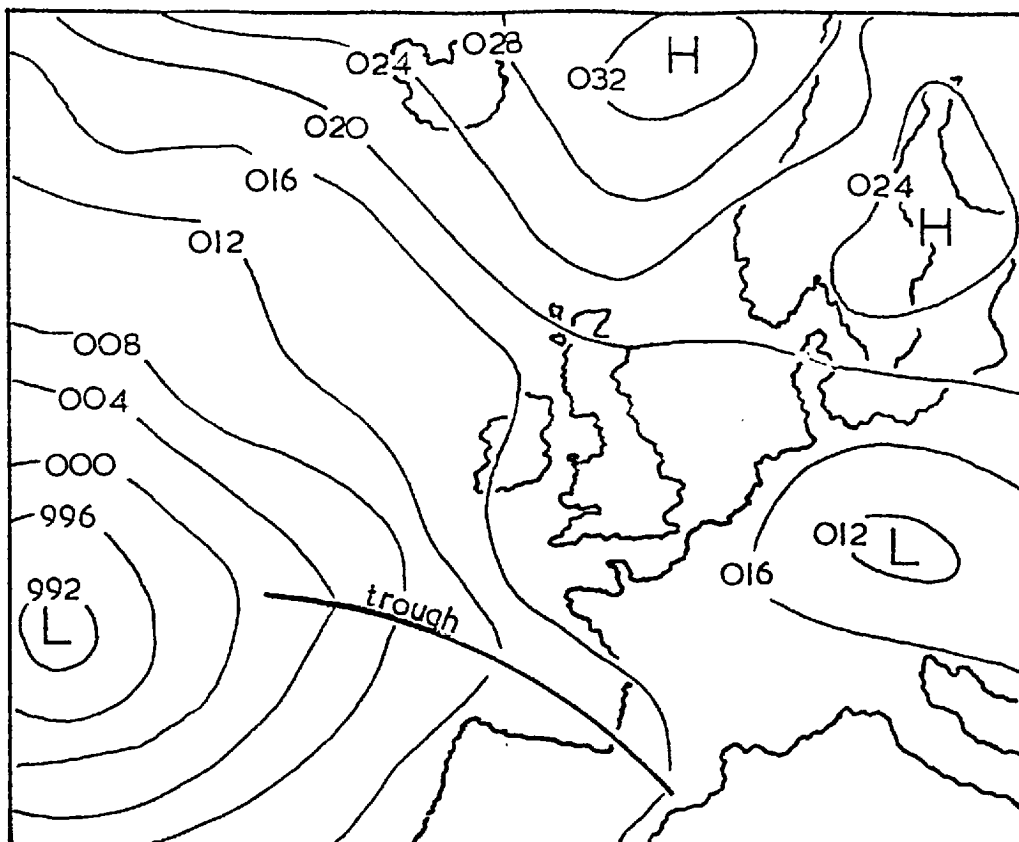


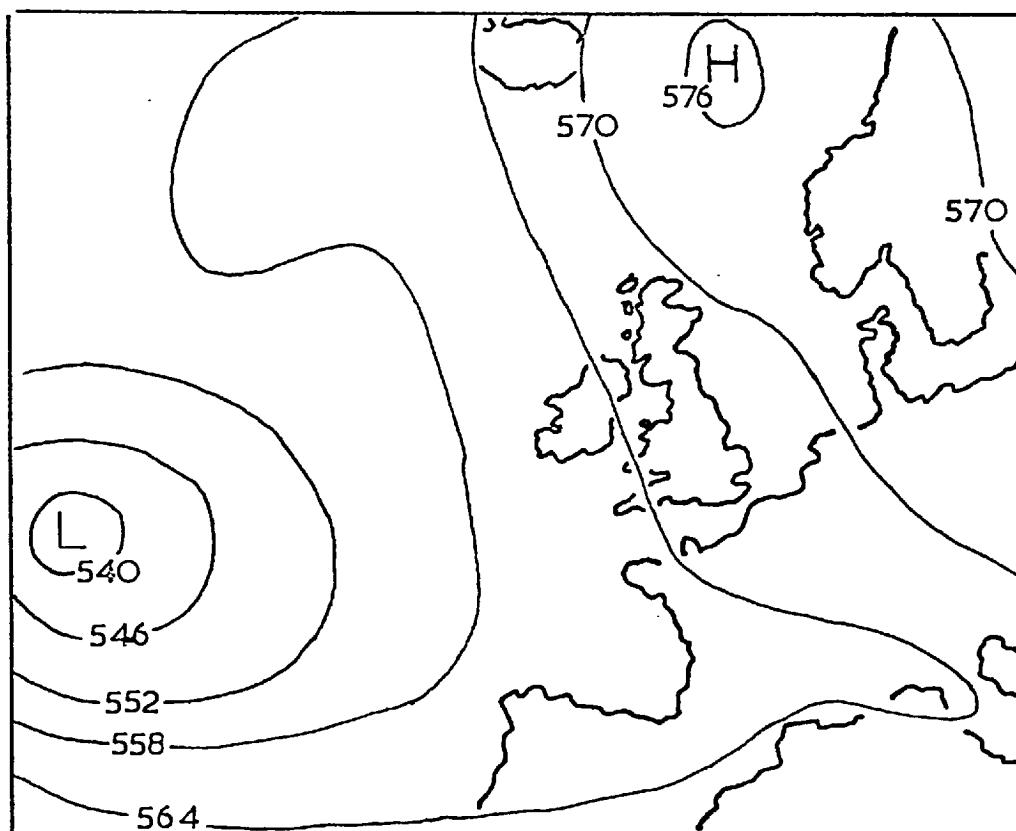
FIG. 6.2

Map showing total rainfall from 09 GMT 7th to 09 GMT 8th June 1963. Contour interval is 20 mm. The location of Silwood is shown, together with two bearings which mark the azimuthal field of view of the time-lapse photographic data.





Surface 12 GMT 7 June 1963



500 mb 00 GMT 7 June 1963

FIG. 6.3

Surface and upper air analyses prior to the storm near Mill Hill, with contour intervals of 4 mb and 6 gpm respectively.

Time-height section using aerological data from Crawley.  
 For clarity  $\theta_s$  near the surface and  $\theta_w$  aloft are not shown.

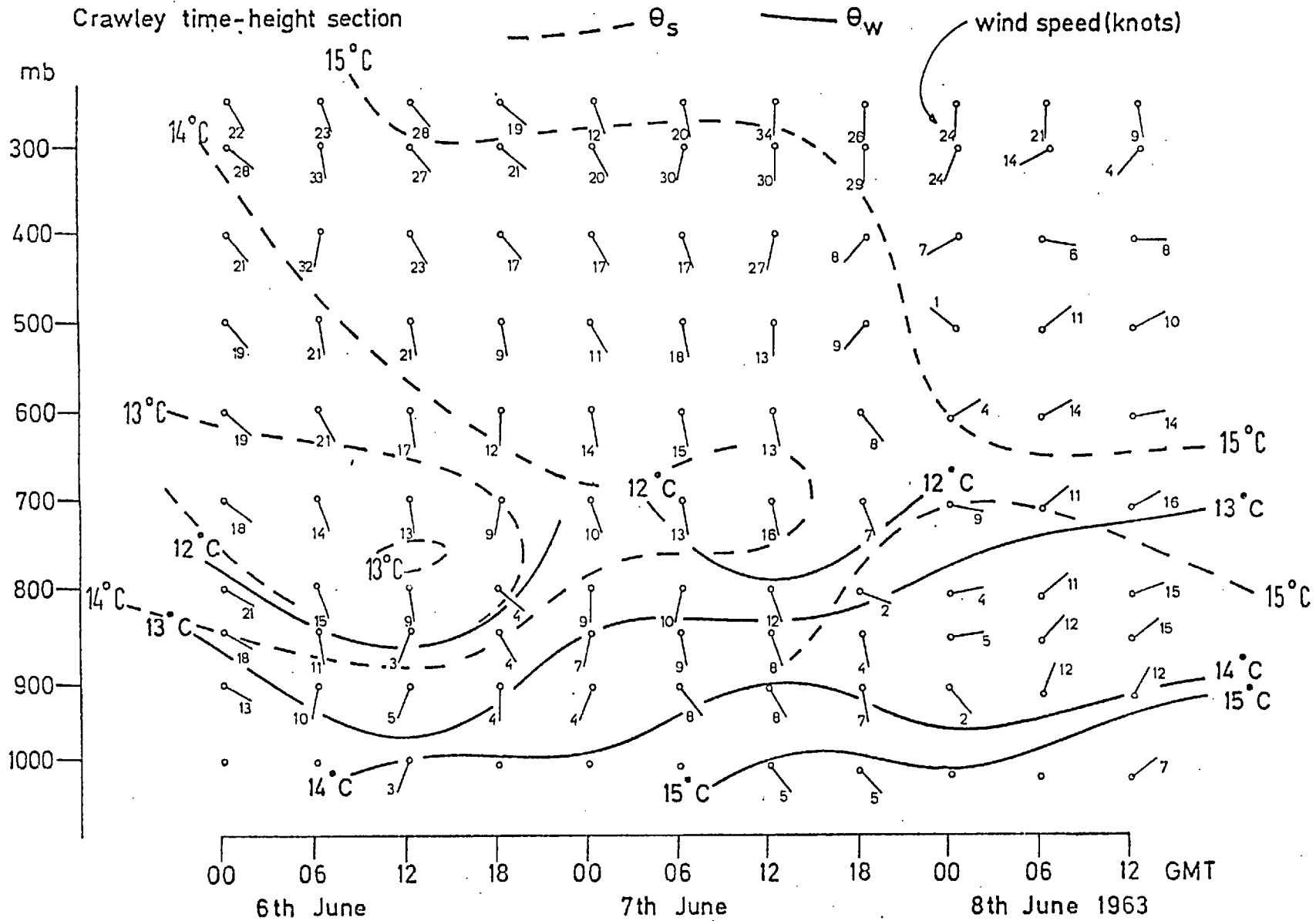


FIG. 6.4

400 and 500 mb levels, it is difficult to decide upon a representative sounding. However, by interpolating between the two soundings and including surface winds as reported from London we obtain the hodograph shown in figure 6.5. The similarities with the Hampstead storm environment are the veering of the wind through about  $90^\circ$  between the surface and upper levels, and the concentration of the shear in the middle and upper troposphere. Figure 6.5 also shows the Crawley temperature sounding for midday on 7th June. A well-defined adiabatic layer extends from the surface up to the 880 mb level, which is close to the cumulus cloud base height of 1500 m reported from Kew; above this level the lapse rate is close to the wet-adiabatic value. Low-level temperatures suggest a boundary layer value for  $\theta_w$  between  $15.5$  and  $16^\circ\text{C}$ ; because the lapse rate above cloud base is wet-adiabatic, the value of the positive area depends very sensitively on  $\theta_w$  and is about  $870$  and  $1200 \text{ J kg}^{-1}$  respectively.

#### The storm structure

In the case of the Mill Hill storm, observations do not permit any inference concerning the forcing role of a down-draught outflow. Other potentially useful data are available, however, including autographic rain records and radar and photographic information from Silwood, near Ascot. The reliability of these data is, as we shall see, uncertain, so that any conclusions drawn from them are necessarily tentative.

#### Rainfall data

At the time of the Mill Hill storm a number of recording raingauges were in operation, under the auspices of the Hydrology Section of the Greater London Council. A fairly

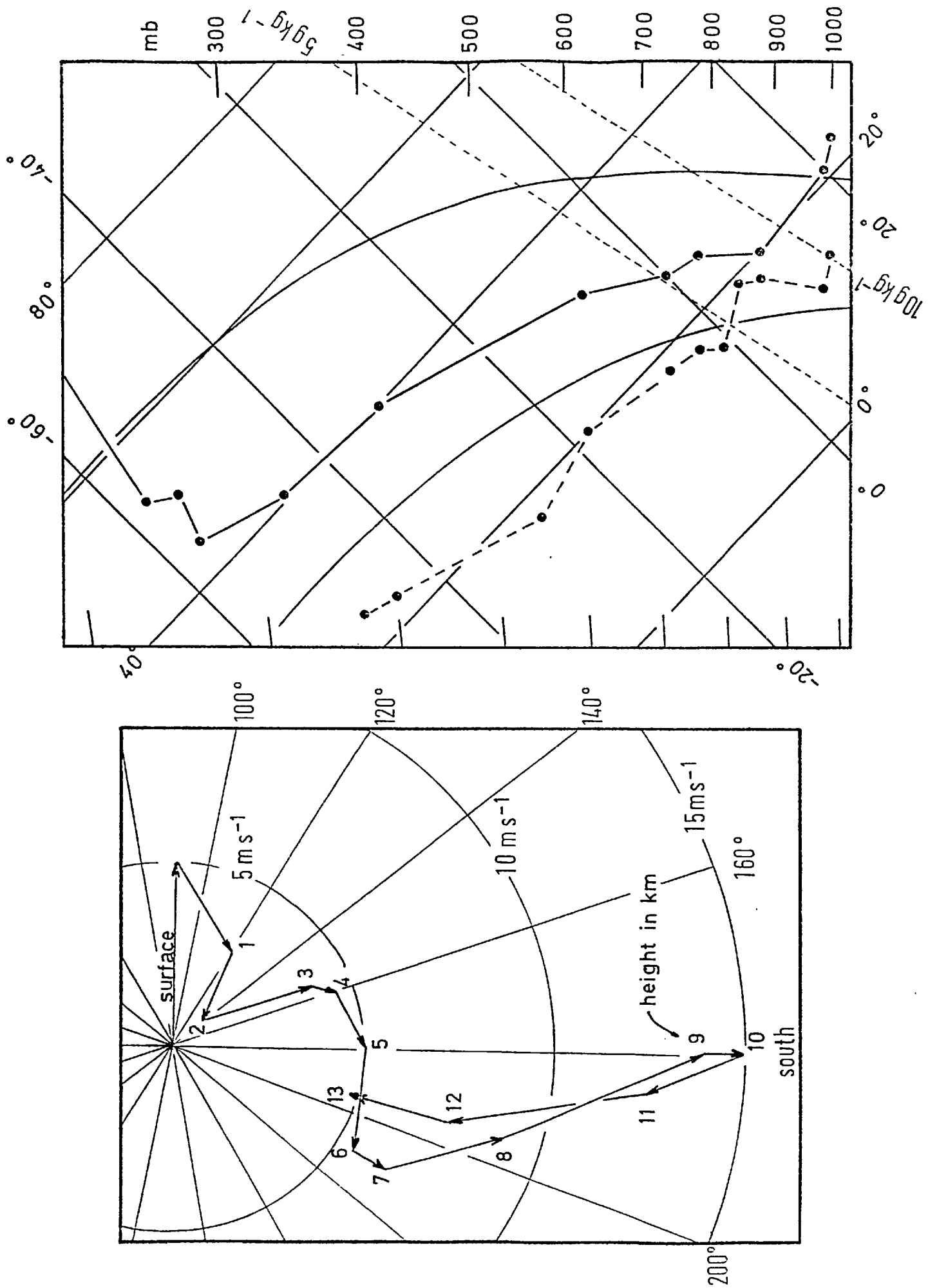


FIG. 6.5

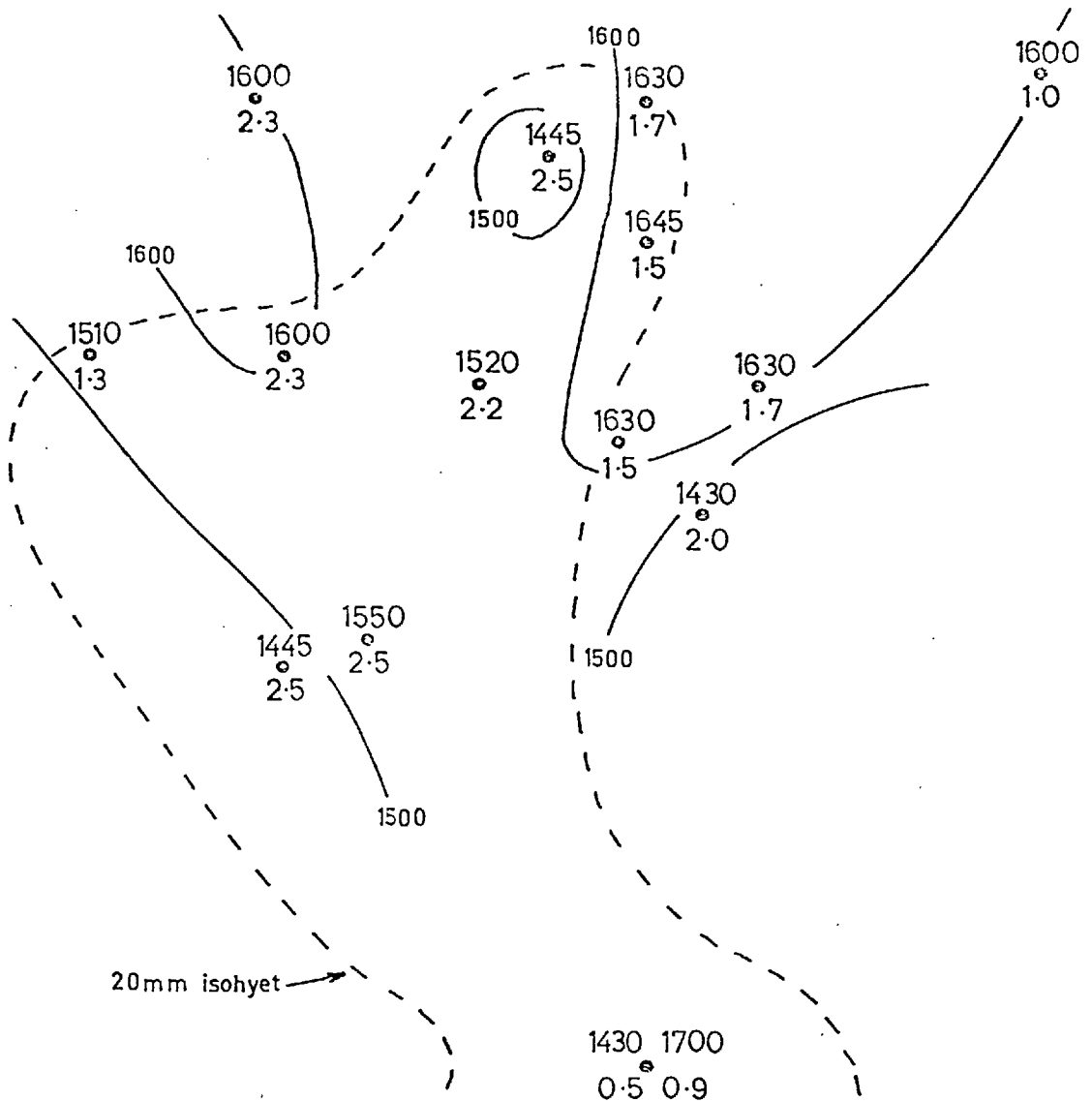
Crawley temperature sounding for midday, 7th June 1963 (above) and hodograph showing representative wind field over London.

dense network of gauges in north-west London reported the time of onset of precipitation and its duration as well as the total rainfall, and this data is presented in figure 6.6. The possible unreliability of these data was suggested by examination of some of the original autographic charts, which showed clear signs of funnel blockage (at St. James's, Westminster, rainwater was still draining through the gauge when the chart was changed the following morning). Where blockages did occur the duration of rainfall was estimated by an observer; because of the nature of the data no 'quality control' has been possible (many of the original charts and observations having been destroyed).

A rather complex picture emerges from consideration of figure 6.6. Although the general impression is clearly one of rain falling earlier in the south of the area than in the north, closer inspection suggests three areas (to the south-east, south-west and north) where rain was recorded before 1500. Within about  $\frac{1}{2}$  hour precipitation was falling in the centre of the region (where the highest totals were recorded) and after about 1600 the rain area had extended further to the north-west and north-east. The secondary rainfall maximum to the south (near Kensington Palace) resulted from a later storm between 1700 and 1800.

#### Radar data

Some aspects of the rainfall distribution are clarified by radar observations from Silwood; these are in the form of bearing, range and height of prominent echoes as noted by the operator. The radar set was an MPS-4 type, having a wavelength of 4.7 cm and horizontal and vertical beam widths of  $4.0^{\circ}$  and



Station Model

time of onset of ppn. (GMT)  
○  
duration of ppn. (hours)

Autographic rainfall data 7 June 1963

FIG. 6.6

The positions of recording stations are indicated by the 20 mm isohyet (see fig. 6.2). Isochrones of the time of onset of precipitation (GMT) are sketched.

0.8° respectively. The maximum display range was 140 miles. At a range of about 40 km the tangential resolution was therefore about ±1 km. Sequential observations are plotted in figure 6.7. The 1305 observation identifies a small echo, 2 to 3 km south of Kensington which may have been associated with the first of the two periods of rainfall recorded there. At 1600 and again at 1704 deep echoes were present to the north of Mill Hill. By 1704 a vigorous convective cell was noted to the south which soon deepened and moved northwards; at 1727 and 1742 two distinct echoes were reported which evidently declined by 1751. Between 1751 and 1811 a further cell developed on the eastern edge of the rainfall area. The radar data were supplemented by brief notes made by the observer; at 1758 he noted an "obvious decline" in the convective activity, to be followed by a "new tower" at 1811. At 1846 the report was "all cumulonimbus decayed to the east, but 4/8 cirrus over much of the sky". A further interesting feature is the persistence of tall cumulonimbus to the west and north (see also the rainfall map) for at least 1 hour after the decline of the storm over London; this contrasts with the day of the Hampstead storm when the convection was much more localized over the city.

In general the radar observations appear to be in accord with the autographic rain data. It seems that the first rain fell just to the north of Mill Hill, with subsequent convective cells forming further south.

#### Photographic data

A time-lapse film of the convective activity over London was taken from Silwood, and gives some insight into the cellular structure of the storm. The film ran from 1530 until

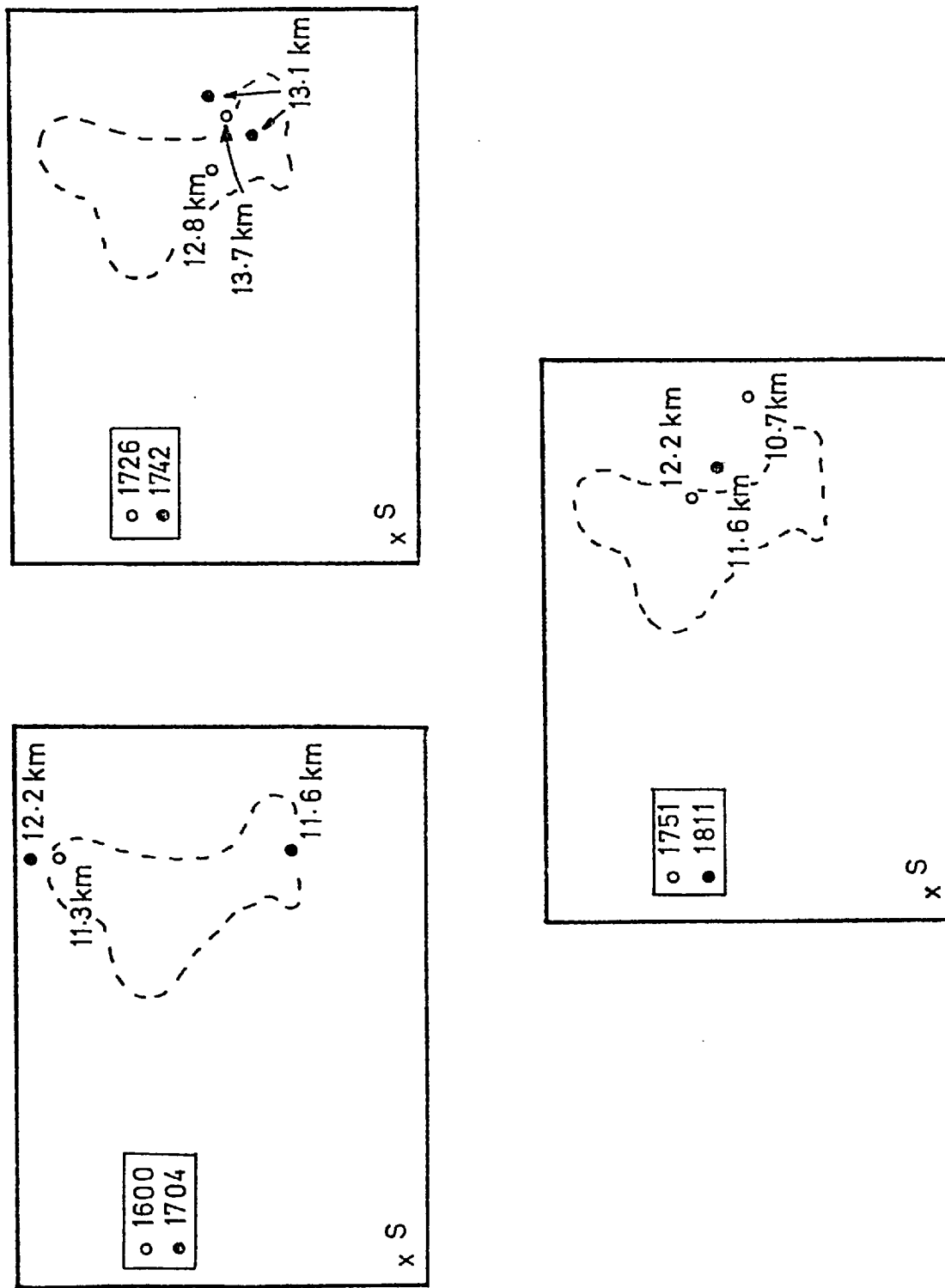


FIG. 6.7

Mill Hill storm radar observations from Silwood in the form of echo location and height at six times between 1600 and 1811 GMT. As in fig. 6.6 the 20 mm isohyet is included.



after the cessation of convection at 1840; the angular dimensions of the field of view are  $32^{\circ}$  azimuth (from  $048^{\circ}$  to  $080^{\circ}$ , as indicated in figure 6.2) and  $22^{\circ}$  elevation. Figure 6.8 is one of several photographs taken by a separate camera which enabled the time interval between successive frames of the time-lapse film to be determined. Enlargements were then made of each 20th frame, giving a sequence of prints at 2 minute intervals.

In figure 6.9 we have traced cloud outlines from successive prints which show the emergence and decay of eight principal cloud towers, and in figure 6.10 we have estimated the corresponding rates of change of azimuth and elevation as observed from Silwood. In order to convert these data to vertical and horizontal velocities a constant range of 38 km was assumed. Because the cloud towers did not necessarily move in a plane perpendicular to the camera axis, both horizontal and vertical velocities will be underestimated. If the 'true' plane and 'apparent' plane differ by about  $30^{\circ}$ , then calculated horizontal velocities will be up to 15% smaller than the actual values. Furthermore, during the lifetime of a typical cloud tower, its range may increase by up to 4 km; simple geometry shows that its vertical velocity may thus be underestimated by as much as  $3 \text{ m sec}^{-1}$ .

Consideration of the previous figures allows us to suggest the following pattern of convective activity. By about 1540 the first cumulonimbus cell was established to the north of the area (near Mill Hill) - this time is a little uncertain because of discontinuities near the beginning of the film. Major development of secondary cells began at about 1550 and

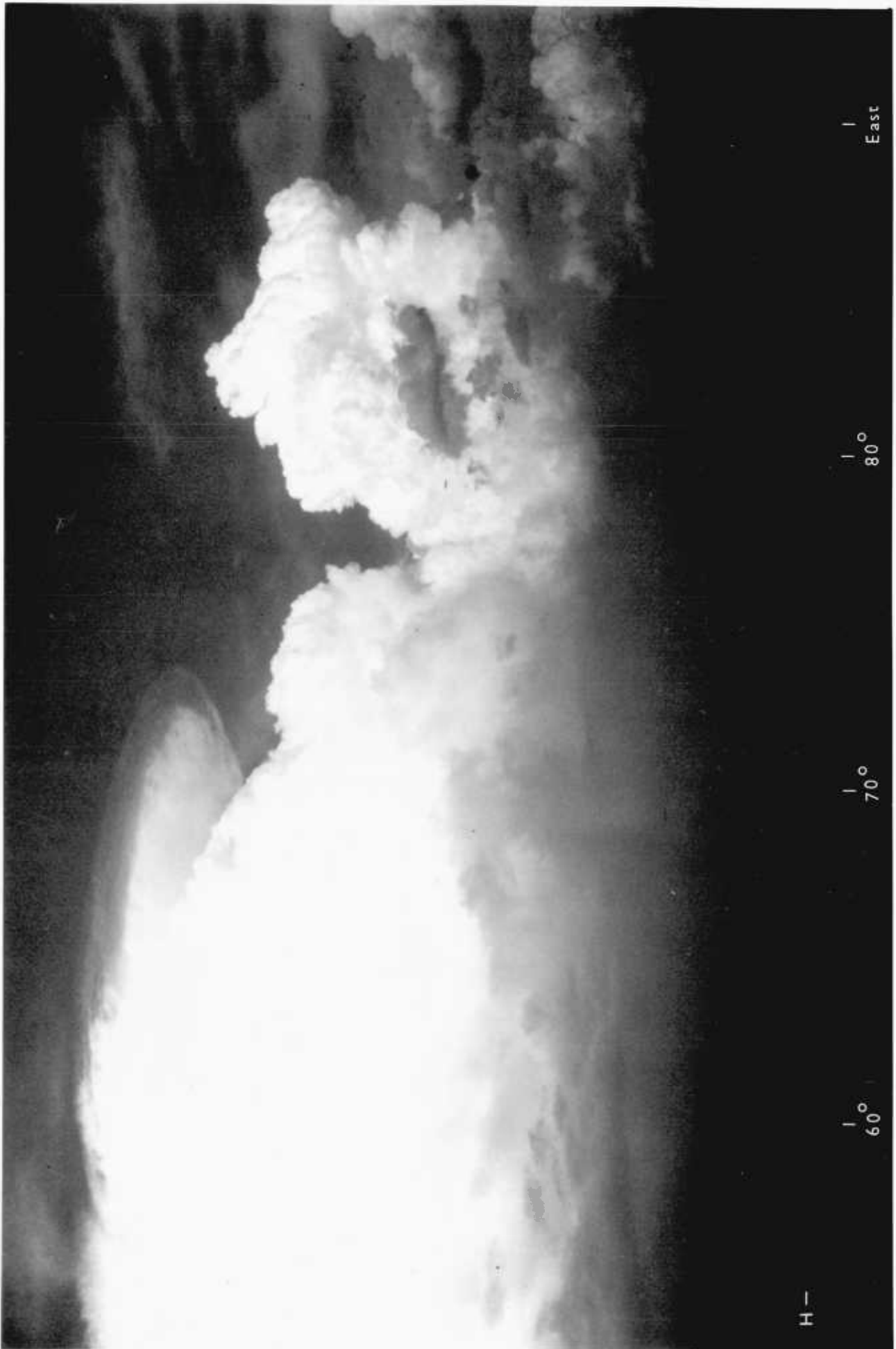
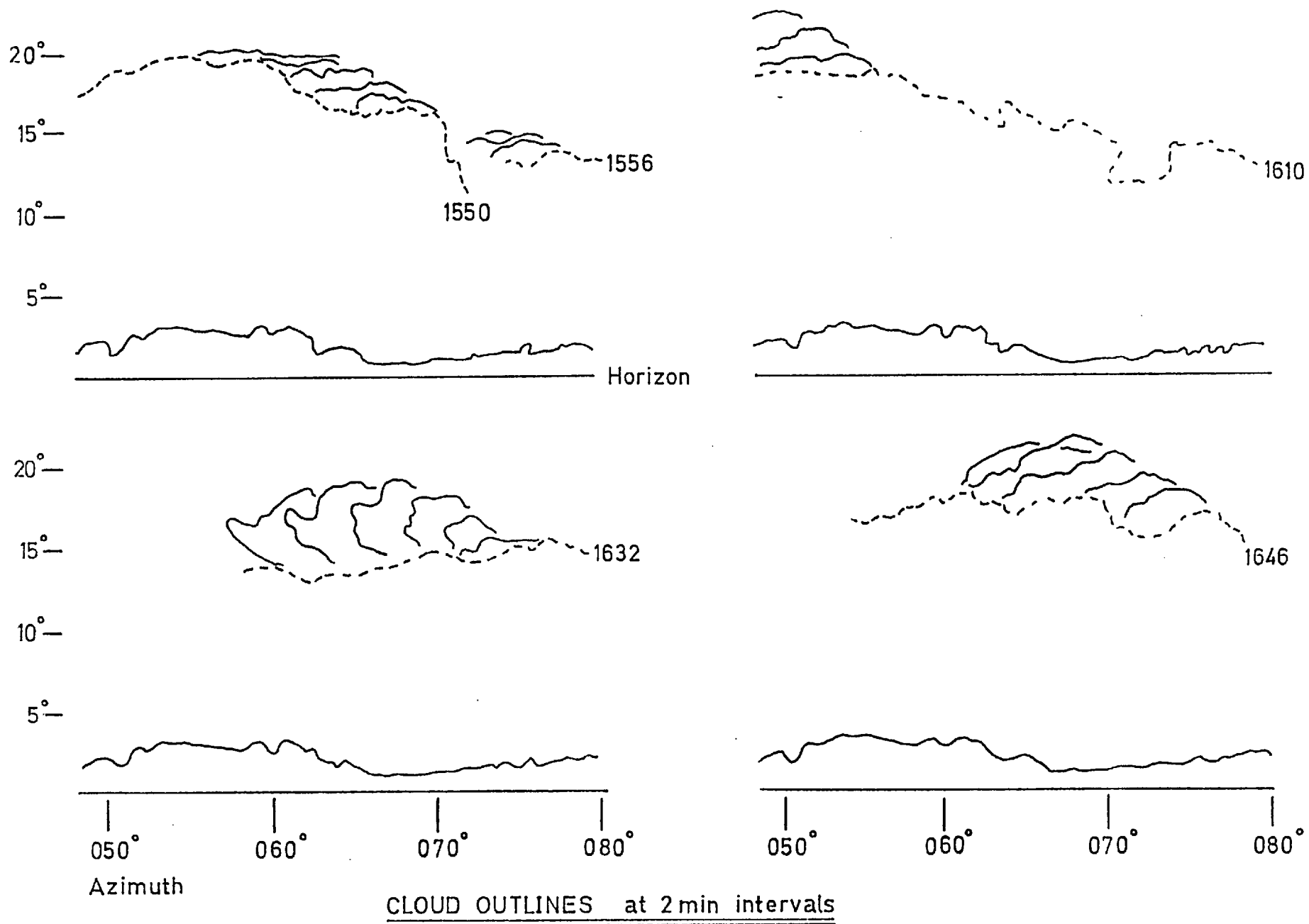


FIG. 6.8

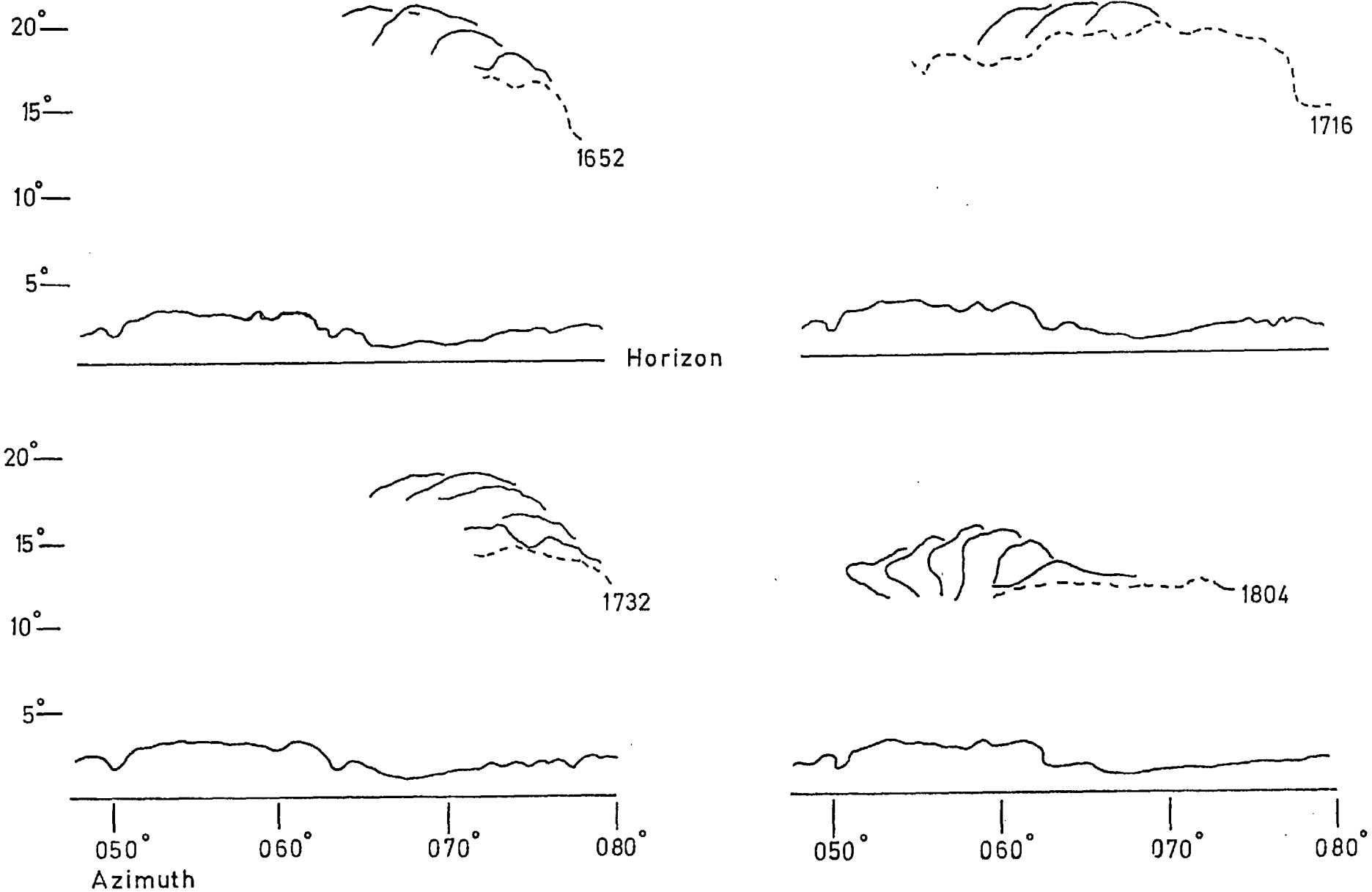
Photograph from Silwood of the Mill Hill storm system at 1704 GMT, 7 June 1963. Range between 30 and 35 km.

Cloud outlines traced from time-lapse photographs showing evolution of cloud towers. Pecked line gives initial outline at the time indicated.

FIG. 6.9(a)



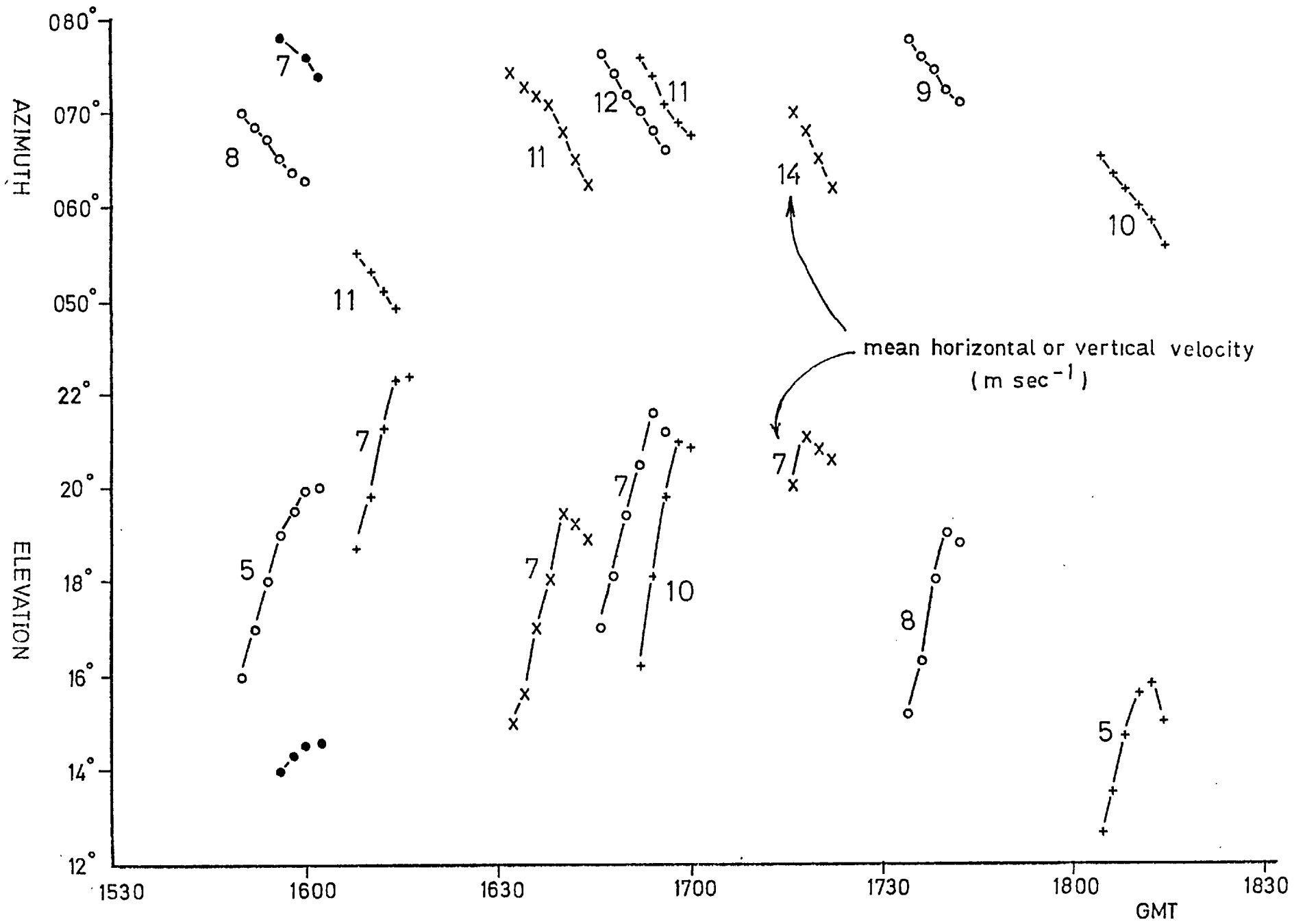
As FIG. 6.9(a).  
FIG. 6.9(b).



CLOUD OUTLINES (cont.)

Elevation and azimuth of cloud towers as a function of time,  
 derived from fig. 6.9.

FIG. 6.10



again at about 1630, with individual cloud towers having a separation of 10 minutes and an average lifetime of about 8 minutes. (The apparent gap in activity soon after 1700 is occupied by vigorous development further south just outside the range of the time-lapse camera. The striking photograph in figure 6.8 shows this development, with a large cell about to merge with the main storm system, of which the spreading anvil cloud can be identified.) It appears that cell growth occurred to the south of the area which received the maximum rainfall (bearing  $053^{\circ}$ ); as the cells grew they moved northwards to merge with a large cumulonimbus system situated over the area near Mill Hill. (Calculated horizontal velocities of individual cloud towers are close to the reported wind speeds at heights between 8 and 12 km (see figure 6.5); however, the measured elevation of cloud tops imply vertical extents of up to 15 km, and with a tropopause at between 10 and 11 km these are unacceptably high. It is possible that the position of the horizon was not identified correctly on the original photographs, but this error does not affect the estimation of vertical or horizontal speeds.)

As already stated, it is not possible to account for the regeneration of the storm in terms of low-level convergence, but the observations discussed here do suggest a cumulonimbus of an impulsive, cellular nature, with the large local rainfall arising from a succession of convective clouds. As in the case of the Hampstead storm, the environment was characterized by a directional wind shear of about  $90^{\circ}$  over the cumulonimbus layer; the significance of such a structure is discussed in the following section.

### 6.3 VECTOR WIND SHEAR

A common feature of the environments of both the Hampstead and the Mill Hill storms was the veering of the wind with height, by about  $90^{\circ}$  between the surface and the upper troposphere. Further examination of the numerical simulation results of chapter V suggested a mechanism by which the vector shear supports a regenerating cumulonimbus system.

In response to the wind shear in middle and upper levels, the initial cumulonimbus cell produced a region of rainfall which was elongated towards the north-east (see figure 5.4). At lower levels the evaporation of this rain resulted in cooling and an associated pressure increase at the surface (resulting from both hydrostatic and non-hydrostatic effects); in figure 5.2(c) this is apparent as an elongation of the surface deviation height field pattern, the orientation of which is determined by the wind at middle and upper levels. Between the surface and the 400 mb level the winds turn through about  $90^{\circ}$ , so that the surface 'meso-high' is elongated across the low-level flow and is thus ideally orientated to maximize the convergence of air approaching the storm. Subsequent cells, generated as a result of the low-level convergence, maintain the position of the 'meso-high' as can be seen in figure 5.2(d).

The significance of this mechanism was illustrated by a further run of the numerical model in which all thermodynamic parameters and wind speeds were unchanged, but with middle and upper level winds now blowing from the south-east, so that there was now no change of direction with height. In

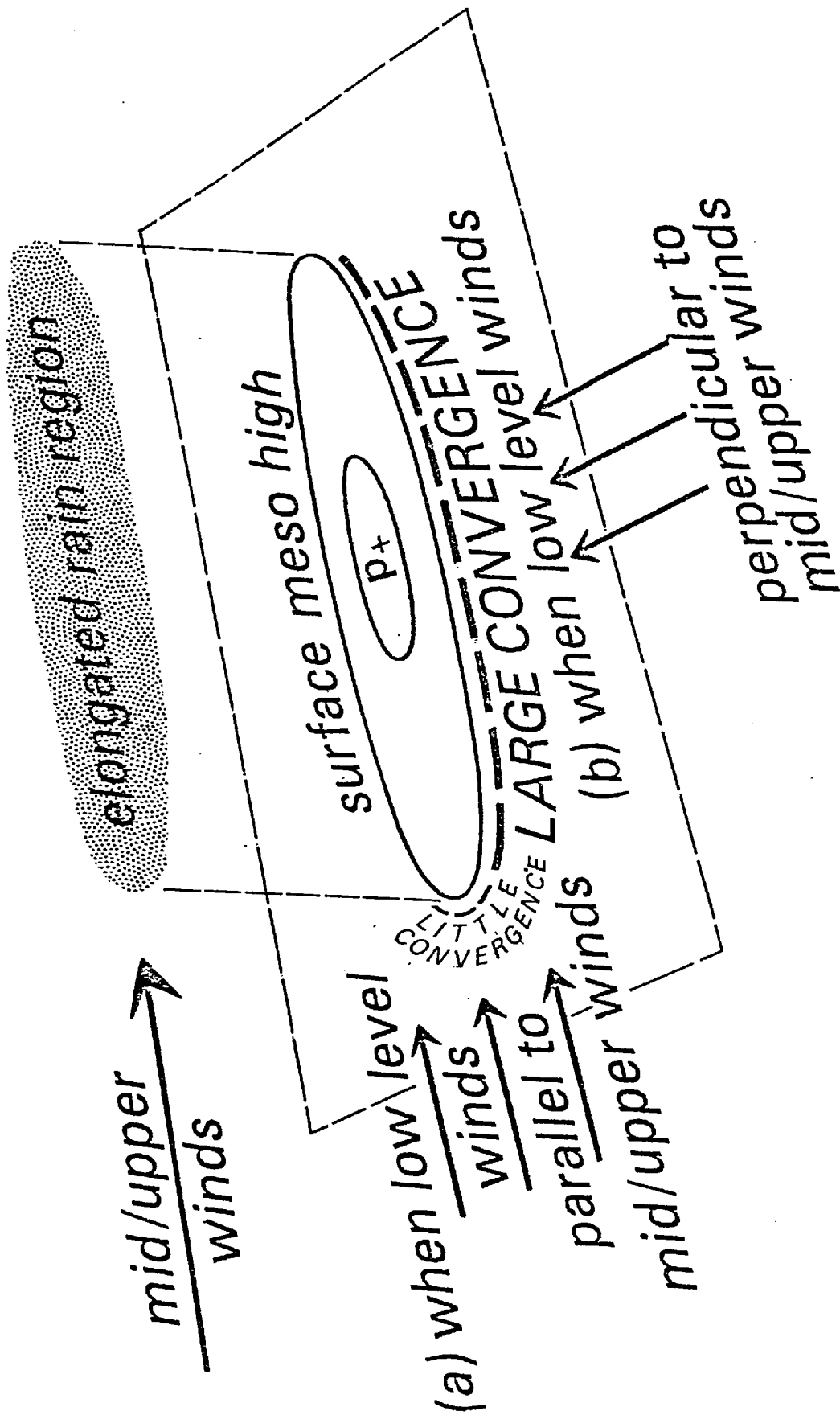


FIG. 6.11

A schematic diagram of the suggested mechanism whereby a vector wind shear assists the regeneration of convection by maximizing the low-level convergence.



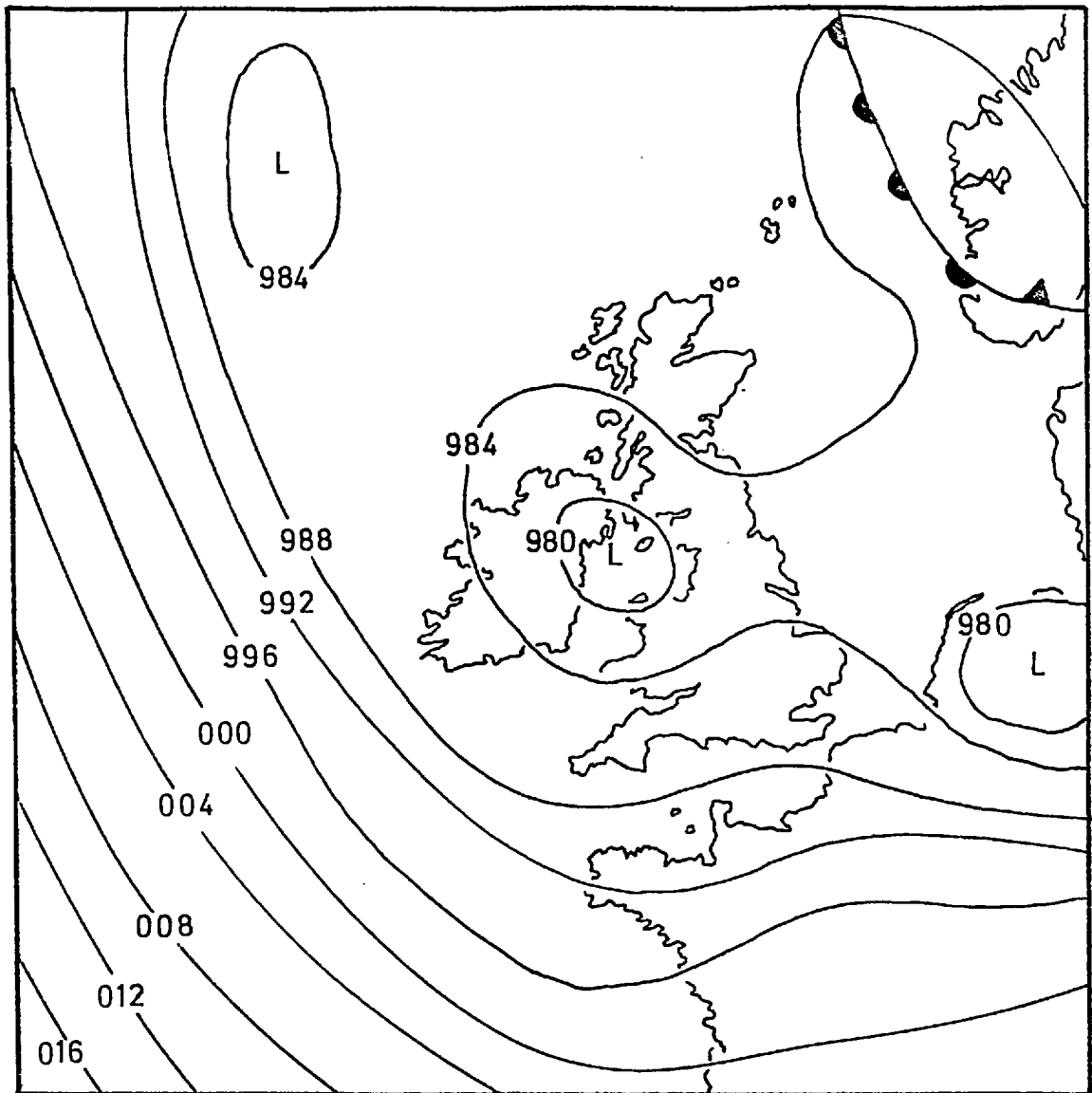
the simulation the rainfall area and low-level temperature and pressure patterns were once again elongated along the upper winds (towards the north-west), but this orientation was now along, not at right angles to, the lower winds. No significant new growth occurred on the south-eastern flank, and the stationary character of the storm was not evident. The schematic diagram in figure 6.11 attempts to summarize the importance of the relative orientation of upper and lower winds.

A further brief case study gives additional support to the proposed mechanism. The following description is of another storm which may have arisen from an urban heat source, but because of a different ambient wind field, moved away from its region of initiation.

#### Storm of 10th October 1964

On this occasion heavy showers with hail and thunder occurred over most of Britain, due to the presence of a low pressure area of deep polar maritime air (see figure 6.12). Over much of southern Britain winds were west-south-westerly, reaching  $10 \text{ m sec}^{-1}$  near the surface and increasing to about  $20 \text{ m sec}^{-1}$  near the rather low tropopause (at about 8 km). Figure 6.13 gives the Crawley aerological data; taking into account the surface temperatures and dewpoints reported from London, the adiabatic condensation level is at about the 900 mb level (which is close to the reported cloud bases of between 750 and 900 m) with a  $\theta_w$  of about  $9^\circ\text{C}$ . The available potential energy is readily calculated as  $440 \text{ J kg}^{-1}$ , which gives a mean Richardson number of about 3.5.

Towards late afternoon (a little after the time of maximum surface temperature, when competing non-urban heat sources may



SURFACE 10 October 1964 0600 GMT

FIG. 6.12

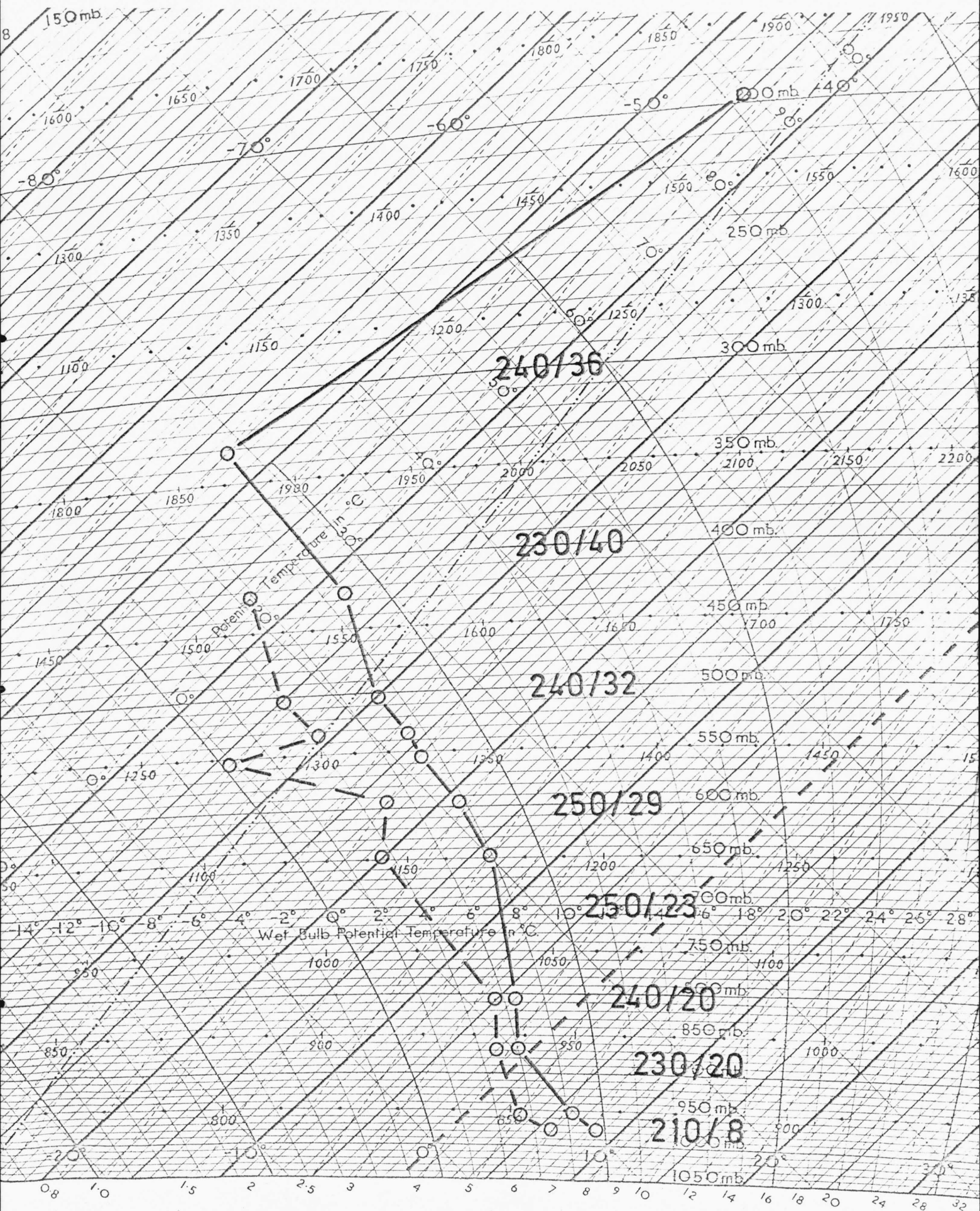


FIG. 6.13

Crawley upper-air data for midday, 10 October 1964.  
Wind direction in degrees and speed in knots.

have weakened) a cumulonimbus was observed (again from Silwood) to develop over south-west London, with cloud towers reaching cirrus level at or a little below the tropopause. Photographic data (see figure 6.14) show the cloud towers being successively renewed at the rear at intervals of about 6 minutes, but the region of formation (and hence the storm itself) moves away with a velocity of about  $255^{\circ}$ ,  $12 \text{ m sec}^{-1}$ . Inspection of the wind profile shows that this velocity corresponds to a steering level at about 3.5 km; if, as in chapter III, we apply Moncrieff and Green's (1972) theory, using  $(-R_i) = 3.5$  and  $H = 7.8 \text{ km}$ , we obtain a steering level only slightly higher at about 4 km.

The rainfall swath at the ground (shown in figure 6.15) confirms the motion of the storm, having an orientation along the line  $255^{\circ}/075^{\circ}$ . Point rainfall values were between 4 and 7 mm, which corresponds to a rainfall rate of up to  $40 \text{ mm hr}^{-1}$  if, as surface reports suggest, we assume a duration of about 10 minutes (implying a dimension of several km at the storm's mean speed of  $12 \text{ m sec}^{-1}$ ). The rainfall map also suggests that the initial source of the warm air may have been the suburban district to the south-west of London; a second swath of similar dimensions is also apparent further to the north, evidently originating over north-west London.

Returning to the occasion of the Mill Hill storm, it is instructive to examine the rainfall map for other parts of the country. Figure 6.16 shows the isohyetal analysis for central southern England, with only the 0 and 10 mm contours sketched. As mentioned before, this was a day of widespread showers, but it is clear that storms further west behaved in a manner quite different to that over London. Over the counties of Gloucestershire and parts of Wiltshire a number of long

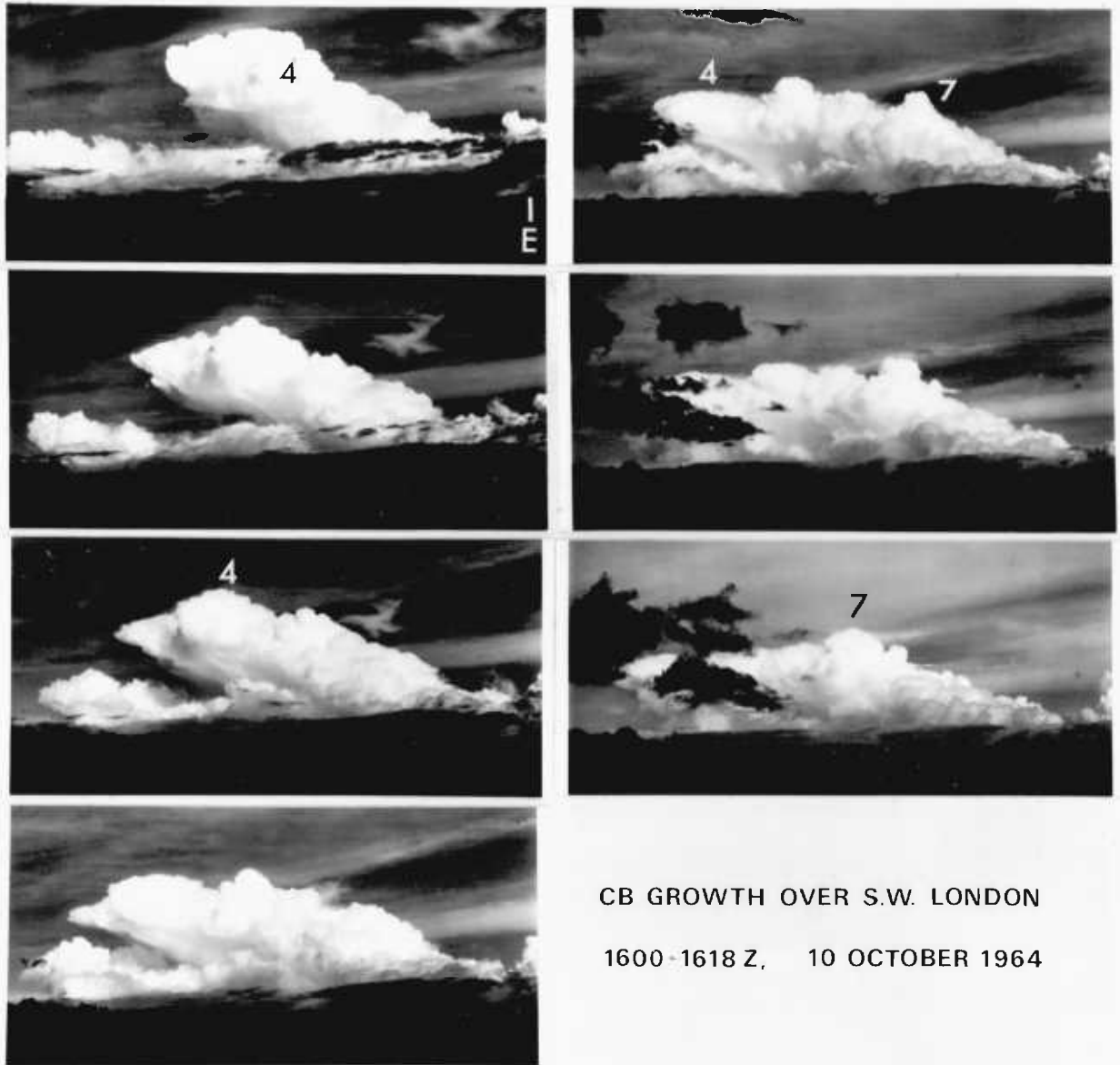
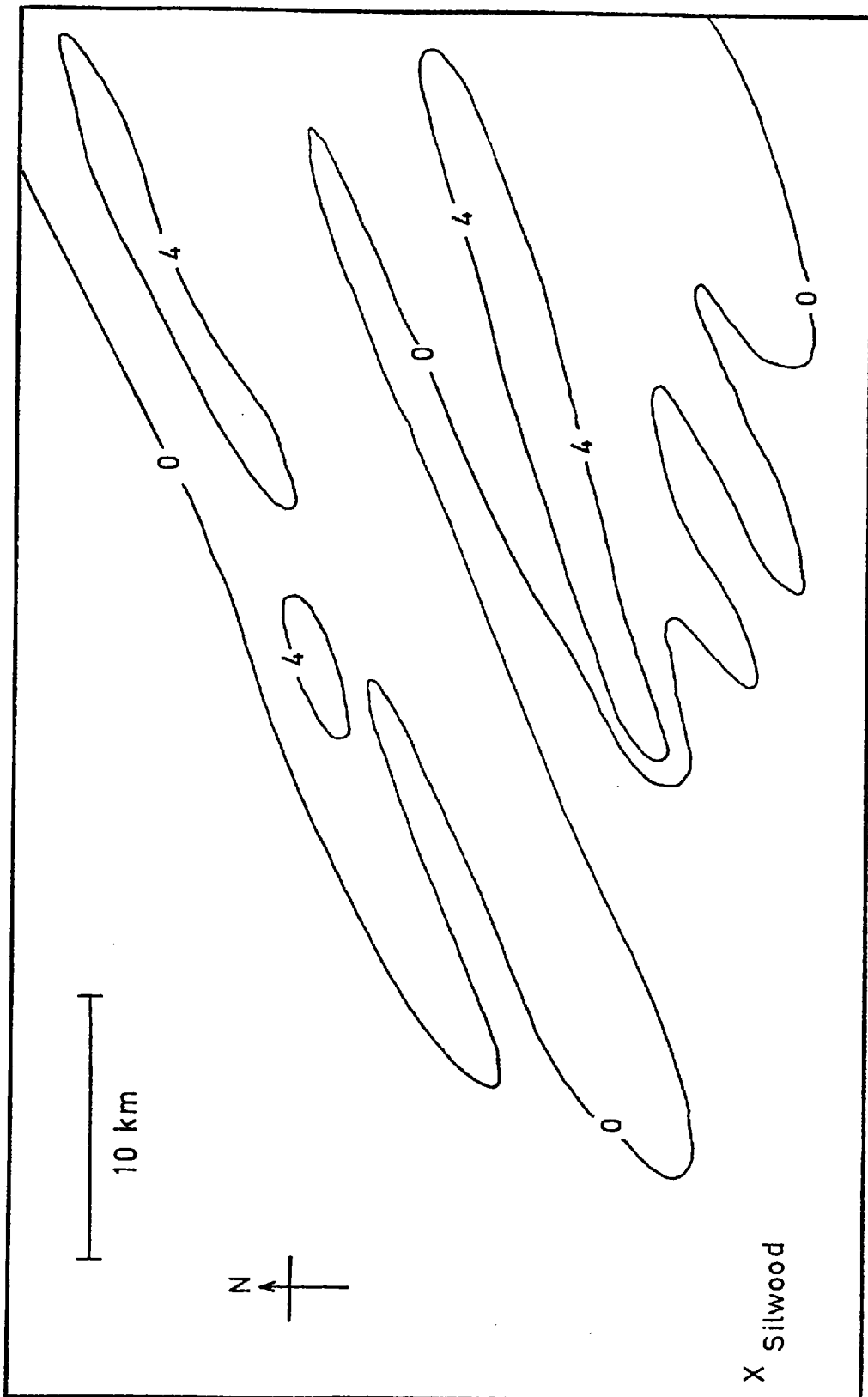


FIG. 6.14

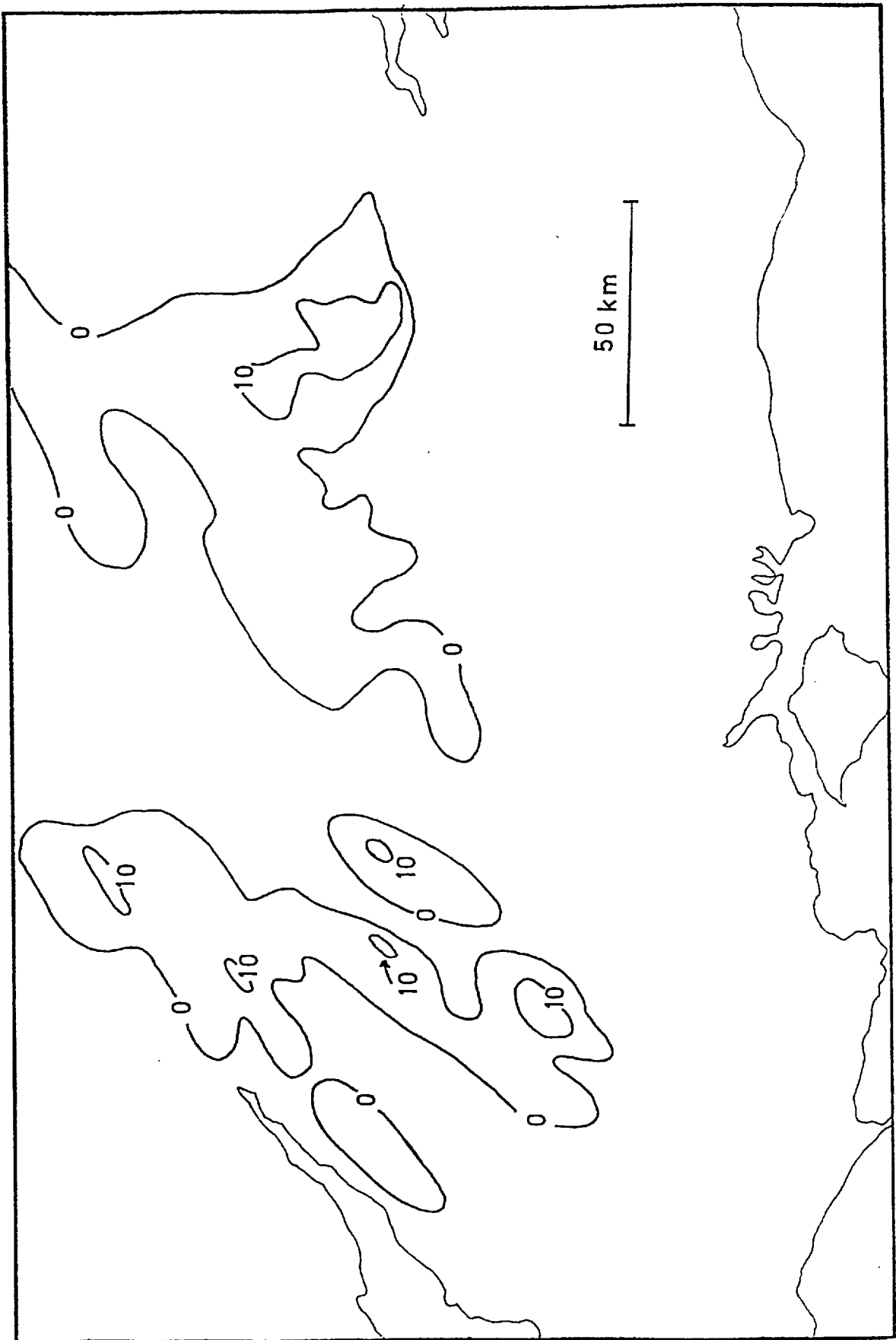
A sequence of photographs from Silwood at intervals of 3 min, showing the ascent into prominence of the fourth to the seventh of the major cloud towers. Their decreasing maximum elevation implies motion of their source away from the camera with a velocity of about  $255^{\circ} 23$  kt. (Details in the cirrus can be seen to move faster, with a stronger component from the south.)



0 and 4 mm isohyets    10 October 1964

FIG. 6.15

Rainfall map showing narrow swath produced by the storm over SW London on 10 October 1964.



0 and 10 mm isohyets 7 June 1963

FIG. 6.16

Rainfall map for southern England on the occasion of the Mill Hill storm.

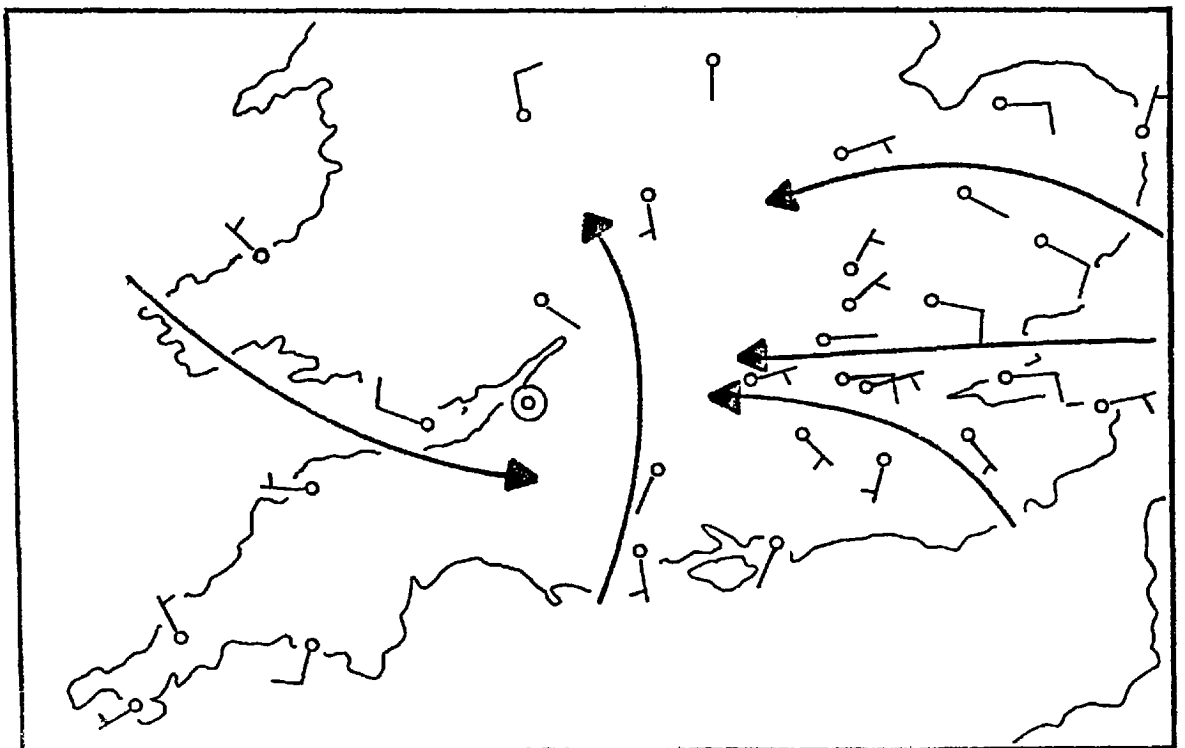
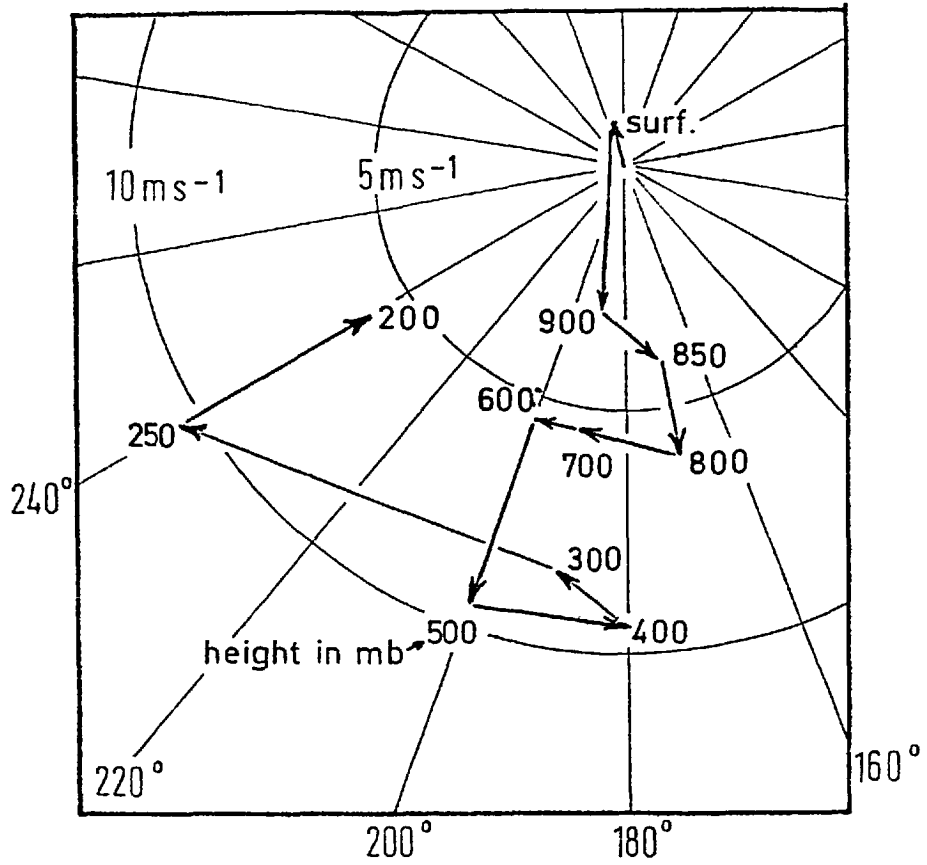
swaths of rainfall can be identified (some of them overlapping), and their orientation implies motion of individual cumulonimbus clouds from the south-west. In only a few locations did point rainfall totals exceed 10 mm, and there orographic features may have been important. Surface reports indicate that these showers occurred during the afternoon; if their speed was between 8 and 10 m sec<sup>-1</sup> (close to the mid-level wind speed) the length of the rainfall swaths imply a lifetime of about 50 minutes.

We wish to account for the contrasting behaviour of these showers (compared with the storm over London) in terms of the environmental wind field. Figure 6.17 shows surface streamlines for southern Britain and upper winds from Camborne for the afternoon of 7th June 1963. The presence of sea breezes probably complicates the pattern, and the representativeness of available data is uncertain, but there is an obvious distinction between the strong surface easterlies near London and the weaker flow from between south and west which affected most south-western areas. The upper air stations of Camborne and Crawley are almost equidistant from the region of interest, but the upper winds from the former indicate very little directional shear over the lowest 9 km, being almost southerly at all levels up to 300 mb.

The above evidence, based on both numerical results and observations, does not claim to be definitive or conclusive, but nevertheless lends support to the suggested importance of a vector wind shear in the maintenance of a stationary, regenerating storm system.



Camborne 18 GMT 7 June 1963



Surface streamlines 18 GMT 7 June 1963

FIG. 6.17

CHAPTER VII : SUMMARY AND CONCLUDING REMARKS

The complexity of atmospheric processes in general, and cumulonimbus convection in particular, is well known, and at first sight often overwhelming. In this thesis we have attempted to progress by making considerable simplifications in the hope of identifying some of the more important physical processes and parameters.

In chapter II we used various data to investigate the existence of a mean layer stratification accompanying shower rainfall. The results suggested that, at least over the ocean, a simple index incorporating the saturated or wet-bulb potential temperature at two routine levels can give a strong indication of the occurrence of 'showers' or 'no showers'. Over land the situation is more complicated, although interesting results were obtained by a simple inspection of surface and upper-level potential temperatures. An approach to the problem of large-scale shower rainfall was made by considering the mean daily rainfall total for a 100 km-square area over land (here we assumed that processes on the cloud scale would be unimportant, and that large-scale vertical motions might be expected to dominate). An encouraging degree of correlation was found between this mean areal rainfall and a vertical component of vorticity, which was used as an indicator of the large-scale vertical motion. While the findings of this chapter were based on rather crude hypotheses, it seems that they may be able to provide a basis for some simple forecasting techniques.

The remainder of the thesis has concentrated on a particular type of cumulonimbus cloud, the stationary or slow-moving severe storm. Although a comparatively rare phenomenon

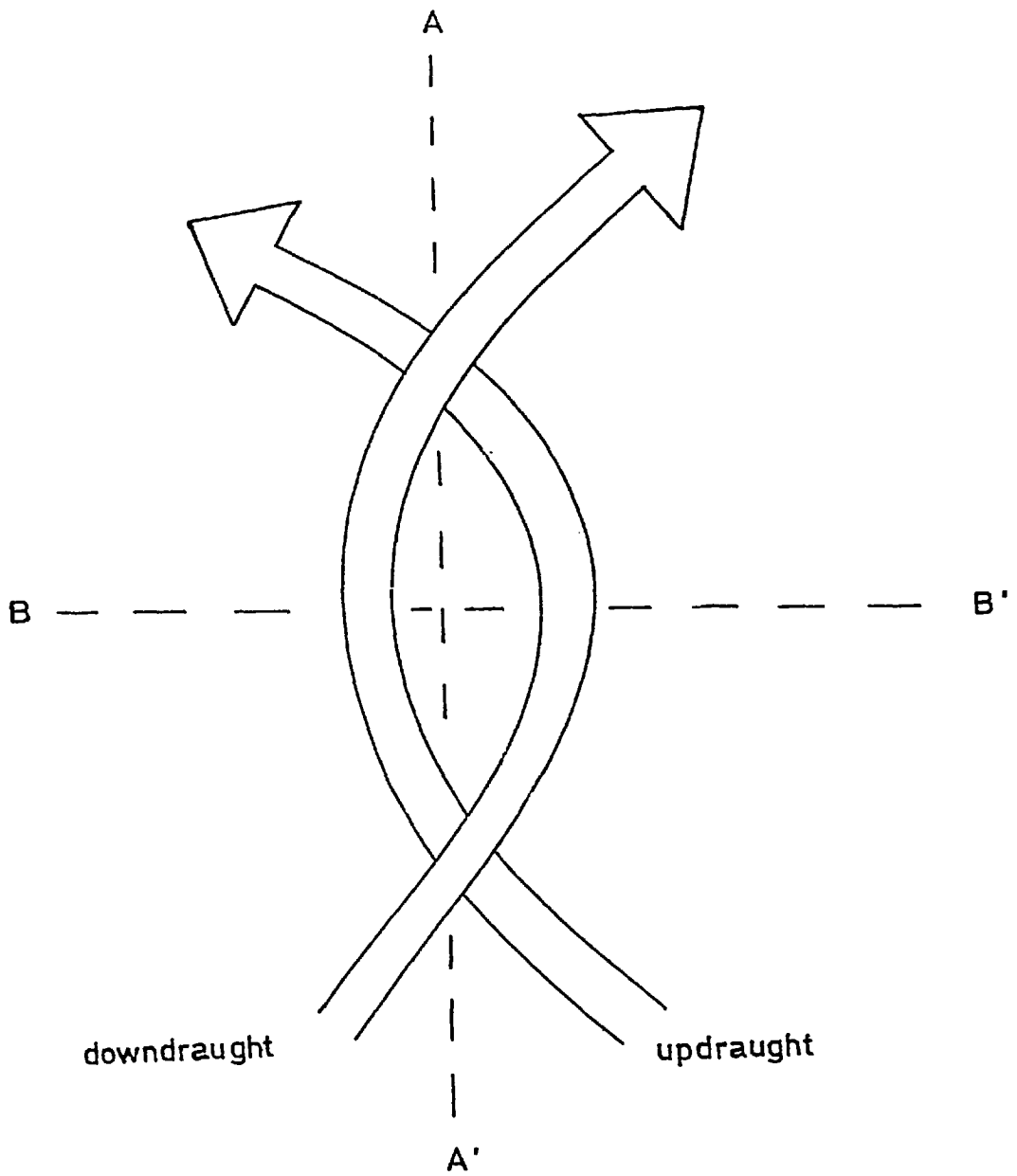
it is locally very damaging, and is therefore worthy of the meteorologist's attention. In chapter III we described a number of these storms, and showed that not all could be associated with a reversal of wind with height, as might be expected from a simple 'steering-level' model of persistent cumulonimbus.

Retrospective cumulonimbus studies (involving storms for which no special observational programme was prepared) are especially difficult if the phenomenon is confined to a small locality. In the case of the Hampstead storm the paucity of routine data was alleviated to some extent by appeal to voluntary observers; nevertheless the observational description in chapter IV cannot be regarded as definitive, even though it represents a plausible deduction from the available information. The model of the Hampstead storm was placed on a firmer physical basis by consideration of the numerical simulation results, as described in chapter V. The model reproduced satisfactorily, and in some cases emphasized, several observed features, namely the rainfall distribution, the asymmetric downdraught outflow and the impulsive, multicellular appearance of the storm.

In chapter VI some of these properties were considered further, and, in the case of the Hampstead storm, appeared to be important in determining the stationary character of the cumulonimbus system. In this chapter we also discussed an apparently similar storm; although some of the data were less reliable on this occasion, it was possible to isolate several common features, notably the turning with height of the environmental winds and the impulsive aspects of the storm system.

Some of the distinctive features observed in the Hampstead storm, most notably the updraught configuration and the evolution of successive cumulonimbus cells, are apparently also typical of a class of severe storm which is more common in the USA. An intensive analysis of a multicellular hailstorm near Raymer, Colorado, was undertaken as part of the National Hail Research Experiment; this is described in a series of five articles published in *Monthly Weather Review*, Volume 104, Number 5 (May 1976). Its motion was similar to that of Browning and Ludlam's (1960) model in that it was the result of two components; one due to the advection of individual cells along the direction of the middle level winds, and another due to the discrete propagation by new cells forming on the right forward flank of the storm. The most important distinction between the Hampstead and Raymer storms is that in the former case the successive individual cumulonimbus cells are generated in the same location relative to the ground, and thus contribute to a highly localized large rainfall.

Although this thesis has not attempted a theoretical description of stationary storms, it is hoped that the work described here may provide some foundation for the future. One of the most important aspects of severe storms to be recognized in recent years is their three-dimensionality, and this is a striking feature of the Hampstead storm. It seems likely that a three-dimensional generalization of the work of Moncrieff and Green (1972) and Moncrieff and Miller (1976) may be possible, along the following lines. In figure 7.1 we have sketched a plan view of the quasi-steady flow configuration of the Hampstead storm model. Along the plane



Components of flow along AA' :



along BB' :



FIG. 7.1

Schematic diagram of the flow configuration of the Hampstead storm model (in plan view), with components in orthogonal planes AA' and BB'.

AA<sup>1</sup> the components of the flow resemble that of the tropical cumulonimbus, with updraught and downdraught branches both entering and leaving on the same side of the storm; along BB<sup>1</sup> the components appear similar to a mid-latitude type of storm circulation. Because the two branches of the flow are 'interlocked', the projections onto each of these planes remain strictly three-dimensional, nevertheless the problem of determining the 'systems' propagation and transfer properties would become analytically tractable in each of the two planes. Another aspect which seems worthy of further attention is the interaction between the cool downdraught and the ambient flow near the surface which, as we have seen, played an important role, not only in this study, but also in the tropical cumulonimbus simulation work of Moncrieff and Miller.

Sophisticated computer models of clouds are playing an increasingly important role in the current understanding of cumulonimbus dynamics, and it is thought that the work described in this thesis represents a contribution to that progress. The fact that a certain amount of 'tuning' was required during the course of the experiments discussed here before a realistic simulation was obtained should itself prove beneficial in at least two ways; firstly by prompting closer consideration of the microphysical parameterization schemes employed, and secondly by questioning the mechanisms whereby the atmosphere provides and maintains an environment capable of sustaining cumulonimbus convection. There are, of course, limitations to this approach, and they are perhaps most apparent in the practical problem of hail suppression. This aspect of cumulonimbus dynamics requires an accurate description of the behaviour of cloud particles in three

dimensions, and such a task is well beyond the present capability of even the largest computers. In this field the most powerful tools seem to be sophisticated observational programmes, including doppler radar and instrumented aircraft. At the same time, however, there is a need for synthesis as well as analysis, and generalizations from existing data as well as the development of new measuring techniques. Progress in the understanding of cumulonimbus clouds will thus demand continued cooperation between the theoretician, the modeller and the observer.

REFERENCES

- Atkinson, B.W. 1968 A preliminary examination of the possible effect of London's urban area on the distribution of thunder rainfall, 1951-60. *Trans. Inst. Br. Geogr.*, 44, pp 97-118.
- 1969 A further examination of the urban maximum of thunder rainfall in London, 1951-60. *Ibid.*, 48, pp 97-120.
- 1970 The reality of the urban effect on precipitation - a case study approach. *W.M.O. Tech. Note*, 108, pp 342-360.
- 1971 The effect of an urban area on the precipitation from a moving thunderstorm. *J. Appl. Meteor.*, 10, pp 47-55.
- 1977 Urban effects on precipitation: an investigation of London's influence on the severe storm in August 1975. *Occasional Paper no. 8*, Dept. of Geography, Q.M.C., London. 31 pp.
- Auer, A.H. and 1968 Estimates of air and moisture flux Marwitz, J.D. into hailstorms. *J. Appl. Meteor.*, 7, pp 196-198.
- Barnes, F.A. 1960 The intense thunder rains of 1st July 1952, in the northern Midlands. *E. Mid. Geogr.*, 14, pp 11-26.
- Bergeron, T. 1935 On the physics of cloud and precipitation. *U.G.G.I. Memoir*, Lisbonne, Sept. 1933. 19 pp.
- Bleasdale, A. 1957 Rainfall at Camelford, Cornwall, on June 8, 1957. *Met. Mag.*, 86, pp 339-343.
- Bleasdale, A. and 1952 Storm over Exmoor on August 15, Douglas, C.K.M. 1952. *Ibid.*, 81, pp 353-367.
- Bleeker, W. and 1951 On the diurnal variation of precipitation, particularly over central USA, and its relation to large-scale orographic circulation systems. *Quart. J. Roy. Meteor. Soc.*, 77, pp 260-271.
- Bonacina, L.C.W. 1915 The severe thunderstorm of May 6th, 1915. *Met. Mag.*, 50, p 63.



- Booker, D.R. 1963 Modification of convective storms by lee waves. *Meteor. Monogr.*, 5, pp 129-140.
- Booth, R.E. 1956 Severe hailstorm at Tunbridge Wells on August 6, 1956. *Met. Mag.*, 85, pp 297-299.
- Borland, S.W. and Snyder, J.J. 1974 Effects of weather variables on the prices of Great Plains cropland. *Prepr. 4th Conf. on Weather Mod.*, Ft. Lauderdale, Fla. (Amer. Meteor. Soc., Boston.) pp 545-550.
- Braham, R. and Draginis, M. 1960 Roots of orographic cumuli. *J. Meteor.*, pp 214-226.
- Briggs, J. and Johns, J. 1960 Variation in shower activity. *Met. Mag.*, 89, pp 48-51.
- Browning, K.A. 1964 Airflow and precipitation trajectories within severe local storms which travel to the right of the winds. *J. Atmos. Sci.*, 21, pp 634-639.
- Browning, K.A. and Ludlam, F.H. 1960 Radar analysis of a hailstorm. *Tech. Note No. 5, Imp. Coll. of Sci. and Technology, London. Dept. of Meteorology.* 106 pp.
- 1962 Airflow in convective storms. *Quart. J. Roy. Meteor. Soc.*, 88, pp 117-135.
- Browning, K.A., Ludlam, F.H. and Macklin, W.C. 1963 The density and structure of hailstones. *Ibid.*, 89, pp 75-84.
- Browning, K.A. and Foote, G.B. 1976 Airflow and hail growth in supercell storms and some implications for hail suppression. *Ibid.*, 102, pp 499-533.
- Carlson, T.N. 1967 Isentropic upslope motion and an instance of heavy rain over southern Florida. *Mon. Weath. Rev.*, 95, pp 213-220.
- Carlson, T.N. and Ludlam, F.H. 1968 Conditions for the occurrence of severe local storms. *Tellus*, 20, pp 203-226.
- Chandler, T.J. 1965 "The Climate of London." Hutchinson, London. 292 pp.
- Chandler, T.J. and Gregory, S. (editors) 1976 "The Climate of the British Isles." Longmans, London. pp xvii + 390.
- Changnon, S.A. 1968 The La Porte weather anomaly - fact or fiction? *Bull. Amer. Meteor. Soc.*, 49, pp 4-11.

- Changnon, S.A. 1969a Urban-produced thunderstorms at St. Louis and Chicago. *Prepr. 6th Conf. on Severe Local Storms*, Chicago, Ill. (Amer. Meteor. Soc., Boston.) pp 95-99.
- 1969b Recent studies of urban effects on precipitation in the United States. *Bull. Amer. Meteor. Soc.*, 50, pp 411-421.
- Crutcher, H.L., 1950 Forecasting the heights of cumulus  
Hunter, J.C., cloud-tops on the Washington-  
Sanders, R.A. and Bermuda airways route. *Ibid.*, 31,  
Price, S. pp 1-7.
- Dennis, A.S., 1973 Meteorology of the Black Hills  
Schlensener, R.A., flood of 9 June 1972. *Prepr. 8th*  
Hirsch, J.H. and *Conf. on Severe Local Storms*, Oct.  
Koscielski, A. 1973. (Amer. Meteor. Soc., Boston.)
- Dightman, R.A. 1968 Central Montana rainstorms and  
floods - June 6-15, 1967. *Mon.*  
*Weath. Rev.*, 96, pp 813-823.
- Douglas, C.K.M. and 1946 Relation between wind direction in  
Moorhead, J.K. the middle troposphere and the  
incidence of thundery rainfall in  
England. *Quart. J. Roy. Meteor.*  
*Soc.*, 72, pp 207-216.
- Eastwood, E. and 1961 A radar observation of a sea-  
Rider, G.C. breeze front. *Nature*, 189,  
pp 978-980.
- Fairgrieve, J. 1914 The rain-fields of the thunder-  
storm of June 14th, 1914.  
*Br. Rainfall(1914)*, pt.I, pp 48-56.
- Fawbush, E.J. and 1954 Types of air masses in which  
Miller, R.C. N. American tornadoes form. *Bull.*  
*Amer. Meteor. Soc.*, 35, pp 154-165.
- Findlater, J. 1964 The sea-breeze and inland  
convection - an example of their  
interrelation. *Met. Mag.*, 93,  
pp 82-89.
- Foote, G.B. and 1973 Airflow and moisture budget beneath  
Fankhauser, J.C. a northeast Colorado hailstorm.  
*J. Appl. Meteor.*, 12, pp 1330-1353.
- Fujita, T. 1967 Mesoscale aspects of orographic  
influences on flow and precipi-  
tation patterns. *Proc. Symp. on*  
*Mountain Meteor.*, 26 June 1967, Ft.  
Collins, Colorado. pp 131-146.
- Garcia-Prieto, P.R., 1960 The possibility of artificially  
Ludlam, F.H. and increasing rainfall on Tenerife.  
Saunders, P.M. *Weather*, 15, pp 39-51.

- Goldie, A.H.R. 1931 Characteristics of rainfall distribution in homogeneous air currents and at surfaces of discontinuity. *Geophys. Mem. (Met. Office)*, 53, 19 pp.
- 1936 Rainfall at fronts of depressions. *Ibid.*, 69, 18 pp.
- Gunn, R. and Phillips, B. 1957 An experimental investigation of the effect of air pollution on the initiation of rain. *J. Meteor.*, 14, pp 272-280.
- Harnack, R.P. and Landsberg, H.E. 1975 Selected cases of convective precipitation caused by the metropolitan area of Washington, D.C. *J. Appl. Meteor.*, 14, pp 1050-1060.
- Hillaby, J. 1975 Strictly for the record. *New Scientist*, 67, pp 607-608.
- Hosler, C.L., Davis, L.G. and Booker, D.R. 1963 Modification of convective systems by terrain with local relief of several hundred metres. *J. Appl. Maths. and Phys. (ZAMP)*, 14, pp 410-419.
- Huff, F.A. and Changnon, S.A. 1964 A model 10-inch rainstorm. *J. Appl. Meteor.*, 3, pp 587-599.
- 1973 Precipitation modification by major urban areas. *Bull. Amer. Meteor. Soc.*, 54, pp 1220-1232.
- Jetton, E.V. and Woods, C.E. 1967 Heavy rains in southeastern New Mexico and southwestern Texas, August 21-23, 1966. *Mon. Weath. Rev.*, 95, pp 221-226.
- Keers, J.F. and Wescott, P. 1976 The Hampstead storm, 14th August 1975. *Weather*, 31, pp 2-10.
- Lautzenheizer, R.E. and Fay, R. 1966 Heavy rainfall at Island Falls, Maine, August 28th, 1959. *Mon. Weath. Rev.*, 94, pp 711-714.
- Lazarus, E.H. 1930 The great thunderstorm at St. Lunaire, near Dinard, France, 15-17 Sept. 1929. *Quart. J. Roy. Meteor. Soc.*, 56, pp 181-182.
- List, R. and Gillespie, J.R. 1976 Evolution of raindrop spectra with collision-breakup. *J. Atmos. Sci.*, 33, pp 2007-2013.
- Liu, J.Y. and Orville, H.D. 1969 Numerical modelling of precipitation and cloud-shadow effects on mountain-induced cumuli. *Ibid.*, 26, pp 1283-1298.

- Lowndes, C.A.S. 1965 The forecasting of shower activity in airstreams from the NW quarter over SE England in summertime. *Met. Mag.*, 94, pp 264-280.
- 1966a The forecasting of shower activity in airstreams from the NW quarter over SW England and S Wales in summertime. *Ibid.*, 95, pp 1-13.
- 1966b The forecasting of shower activity in NW airstreams over NW England in summertime. *Ibid.*, 95, pp 80-91.
- 1966c The forecasting of shower activity in airstreams from the NW quarter over SE England in October to April. *Ibid.*, 95, pp 248-252.
- 1967 The forecasting of rain in southerly airstreams over SE England in summertime. *Ibid.*, 96, pp 212-215.
- Ludlam, F.H. 1963 Severe local storms: a review. *Meteor. Monogr.*, 5, pp 1-30.
- 1976 Aspects of cumulonimbus study. *Bull. Amer. Meteor. Soc.*, 57, pp 774-779.
- Ludlam, F.H. and Saunders, P.M. 1956 Shower formation in large cumulus. *Tellus*, 8, pp 424-442.
- Ludlam, F.H. and Scorer, R.S. 1953 Convection in the atmosphere. *Quart. J. Roy. Meteor. Soc.*, 79, pp 317-341.
- Merritt, L.P., Wilk, K.E. and Weible, M.L. 1974 Severe rainstorm at Enid, Oklahoma, October 10, 1973. *NOAA Tech. Mem.*, ERL NSSL-73. National Severe Storms Lab., Norman, Oklahoma. 50 pp.
- Miller, M.J. 1972 Numerical modelling of moist convection in two and three space dimensions. Ph.D. Thesis, Univ. of London. 196 pp.
- Miller, M.J. and Pearce, R.P. 1974 A three-dimensional primitive equation model of cumulonimbus convection. *Quart. J. Roy. Meteor. Soc.*, 100, pp 133-154.
- Miller, M.J. and Betts, A.K. 1977 Travelling convective storms over Venezuela. *Accepted for pub. in Mon. Weath. Rev.*
- Miller, R.C. 1959 Tornado-producing synoptic patterns. *Bull. Amer. Meteor. Soc.*, 40, pp 465-472.
- Moncrieff, M.W. and Green, J.S.A. 1972 The propagation and transfer properties of steady convective overturning in shear. *Quart. J. Roy. Meteor. Soc.* 98, pp 336-352.

- Moncrieff, M.W. and Miller, M.J. 1976 The dynamics and simulation of tropical cumulonimbus and squall lines. *Ibid.*, 102, pp 373-394.
- McAuliffe, J.P. 1921 Excessive rainfall and flood at Taylor, Tex. *Mon. Weath. Rev.*, 49, pp 496-497.
- McIlveen, J.F.R. 1966 Isentropic analysis of large-scale tropospheric motion systems. Ph.D. Thesis, Univ. of London. 130 pp.
- Natural Environment Research Council (NERC) 1975 Flood Studies Report vol. II: Meteorological Studies. 81 pp.
- Neumann, J. 1951 Land breezes and nocturnal thunderstorms. *J. Meteor.*, 8, pp 60-67.
- Orville, H.D. 1965 A numerical study of the initiation of cumulus clouds over mountainous terrain. *J. Atmos. Sci.*, 22, pp 684-709.
- Parry, M. 1956 An 'urban rainstorm' in the Reading area. *Weather*, 11, pp 41-48.
- Petterssen, S., Knighting, E., James, R.W. and Herlofson, N. 1945 Convection in theory and practice. *Geofys. Pub. (Oslo)*, vol. 16, no. 10. 41 pp.
- Pielke, R. 1974 A three-dimensional numerical model of the sea breezes over south Florida. *Mon. Weath. Rev.*, 102, pp 115-139.
- Richardson, E.A., Peck, E.L. and Green, S.D. 1964 Heavy precipitation storm in northern Utah, January 29 to February 2, 1963. *Ibid.*, 92, pp 317-325.
- Robb, A.D. 1959 Severe hail, Selden, Kansas, June 3, 1959. *Ibid.*, 87, pp 301-303.
- Rosby, C.-G. and collaborators 1937 Isentropic analysis. *Bull. Amer. Meteor. Soc.*, 18, pp 201-209.
- Saunders, W.E. 1966 Tests of thunderstorm forecasting techniques. *Met. Mag.*, 95, pp 204-210.
- 1967 Further tests of thunderstorm forecasting techniques. *Ibid.*, 96, pp 85-89.
- Sayers-Duran, P. and Braham, R.R. 1965 An intensive rainstorm at Fremont, Missouri, July 28-29, 1964. *Mon. Weath. Rev.*, 93, pp 387-391.
- Schmauss, A. 1927 Großstädte und Niederschlag. *Meteor. z.*, 44, pp 339-341.

- Scorer, R.S. 1953a Theory of airflow over mountains: II - The flow over a ridge. *Quart. J. Roy. Meteor. Soc.*, 79, pp 70-83.
- 1953b The spreading out of downdraughts. *Weather*, 8, pp 198-201.
- Shaw, E.M. 1962 An analysis of the origins of precipitation in northern England, 1956-1960. *Quart. J. Roy. Meteor. Soc.*, 88, pp 539-547.
- Shearman, R.J. and 1975 An objective rainfall interpolation and mapping technique. *Hydrol. Sci. Bull.*, 10, pp 356-363.
- Salter, P.M.
- Simpson, J.E., 1976 Gravity current heads observed in a steady state. Unpublished MS.
- Mansfield, D.A. and
- Milford, J.R.
- 1977 Inland penetration of sea-breeze fronts. *Quart. J. Roy. Meteor. Soc.*, 103, pp 47-76.
- Sims, F.P. 1960 The annual and diurnal variation of shower frequency at St. Eval and St. Mawgan. *Met. Mag.*, 89, pp 293-297.
- Sourbeer, R.H. and 1961 Rainstorm in southern Florida, 21 January, 1957. *Mon. Weath. Rev.*, 89, pp 9-16.
- Gentry, R.C.
- Squires, P. and 1957 Some measurements in the orographic cloud of the island of Hawaii and in trade wind cumuli. *Tellus*, 9, pp 475-494.
- Warner, J.
- Summersby, W.D. 1967 Variation of shower frequency at sea. *Met. Mag.*, 96, pp 41-49.
- Tucker, G.B. 1961 Precipitation over the North Atlantic Ocean. *Quart. J. Roy. Meteor. Soc.*, 87, pp 147-158.
- Wickham, P.G. 1974 Some examples of the rainfall forecasts produced by the fine-mesh version of the 10-level model. *Met. Mag.*, 103, pp 209-224.
- Zipser, E.J. 1974 The role of unsaturated convective downdraughts in the structure and rapid decay of an equatorial disturbance. *J. Appl. Meteor.*, 8, pp 799-814.

ACKNOWLEDGEMENTS

The work described in this thesis was supervised by the late Professor F.H. Ludlam, whose death in June 1977 represented a great loss to the science of Meteorology.

I am very grateful to Dr. M.J. Miller for interesting collaboration (and for many fine games of squash), and to Mr. J.R. Probert-Jones, who kindly assumed the role of supervisor.

The immaculate typing in this thesis was the work of my wife, Penny, who also provided generous amounts of patience and encouragement.